1-1-1992

Microtuble [i.e. Microtubule] dynamics in interphase and mitotic cells

Eric A. Shelden
University of Massachusetts Amherst

MICROTUBLE DYNAMICS IN INTERPHASE AND MITOTIC CELLS

A Dissertation Presented

by

ERIC A. SHELDEN

Submitted to the Graduate School of the
University of Massachusetts in partial fulfillment
of the degree requirements for the degree of

DOCTOR OF PHILOSOPHY

September 1992

Department of Biology

MICROTUBLE DYNAMICS IN INTERPHASE

AND MITOTIC CELLS

A Dissertation Presented

by

ERIC A. SHELDEN

Approved as to style and content by:

Patricia Wadsworth, Chair

Christopher L. Woodcock, Member

Lawrence M. Schwartz, Member

David J. Gross, Member

Rachel Fink, Member

Mindaugas S. Kaulenas, Department Head
Department of Biology

To Ronald and Lotti Shelden,
Dennis Shelden
Mary and Seth Tyler
Patricia Wadsworth
and
Kristine Brenc

for believing.

ACKNOWLEDGEMENTS

As is always the case with any major endeavor, the successful completion of this doctoral thesis represents the efforts and skill of many individuals not mentioned on the title page of this work. Indeed it is sometimes hard for me to tell where their contributions end and mine begins. In addition to the professional assistance and advice of my colleagues and co-workers, friends and family members have supported me during the difficult periods and shared my achievements when it all worked out. I have singled out the following people for particular mention; the list is neither complete, nor is its organization intended to indicate the relative importance of anyone to the completion of this dissertation work.

Thanks to C. L. Woodcock for his vision and dedication to imaging and microscopy at the University of Massachusetts, as well as Peter Hepler, Dave Gross and Rachel Fink for inspiration, advice and consultation. Thanks to Larry Schwartz and Randal Phillis for scintillating conversation, unflagging humor and humanity in the face of their responsibilities and sharing of computer goodies. Speaking of computers, thanks to Elizabeth Conner for helping to launch my Mac career.

Thanks to George Drake for being an inseparable part of all of this work. George has patiently taught me as much as I could absorb on any number of occasions, and put aside more pressing tasks to make whatever new idea I happened to have into a reality. I could not have done this without him.

Thanks to Clark Honneywell for sharing fishing hot-spots and bug-bites, and to Clifford Carpenter and Clark Honeywell for making beautiful music with me. My life here would be poor indeed without you.

Thanks to my parents, Ronald and Lotti Shelden, and to my wife, companion and friend, Kristine Brenc, for their support and encouragement, and John Keller, Dawn Hamil and Jerry Shwerin for their friendship through good times and bad.

Lastly, I'd like to thank Patricia Wadsworth. We have shared a small window-less workplace for the last 5 years. She has been confidant, mentor, evaluator and friend; I am her first graduate student. I think neither of us are unchanged by the experience. I'd like to thank her for her patience and support while I figured out what I was doing, and more recently, for guiding me through the work which this thesis represents. I have been fortunate to work with Dr. Wadsworth while she built and balanced both a successful scientific career and a family, and I hope that I have learned enough from her to do the same.

Portions of chapter 2 have been reprinted with permission from The Company of Biologists Limited, London England (see Shelden and Wadsworth, 1990. J. Cell Sci. 97:273-281), and portions of chapter 3 has been reprinted with permission from The Rockafellar Press, NY, NY (see Shelden and Wadsworth, 1992. J. Cell Biol. 116:1409-1420).

ABSTRACT

MICROTUBULE DYNAMICS IN INTERPHASE
AND MITOTIC CELLS

SEPTEMBER 1992

ERIC A. SHELDEN, B.S., UNIVERSITY OF MAINE
M.S., UNIVERSITY OF MASSACHUSETTS
Ph.D., UNIVERSITY OF MASSACHUSETTS
Directed by: Professor Patricia Wadsworth

Microtubules are dynamic polymers which play important roles in mitosis, cell locomotion, and the determination and maintenance of cell polarity. To understand the role of microtubule assembly and disassembly in these processes I have localized sites of microtubule growth by injecting labeled tubulin subunits into cells during spindle elongation (anaphase B) and chromosome separation (anaphase A). The behavior of microtubules in interphase cells was also examined by injection of fluorescent tubulin subunits, and observation of the resulting fluorescent microtubules using low light level fluorescence microscopy.

These experiments demonstrate that rapid assembly of interzonal microtubules occurs concomitantly with the maximal rate of spindle elongation. Furthermore, the rate of interzonal microtubule elongation is greater than the rate of spindle pole separation, and the pattern of microtubule assembly is most consistent with the dynamic instability model of microtubule behavior. These observations demonstrate that interzonal microtubule assembly is not directly coupled to spindle elongation in these cells and place constraints on existing models of spindle pole separation.

Electron microscopic and confocal fluorescence observations of cells injected during anaphase A reveal that injection of biotin-tubulin can induce the assembly of kinetochore microtubules at their plus-ends - normally the site of microtubule disassembly at this stage - in a concentration dependent manner. The elongation of kinetochore microtubules is accompanied by the reversal of chromosome-to-pole motion. Thus, anaphase onset does not prevent addition of tubulin subunits at the plus-end of kinetochore microtubules, and some aspects of mitosis can be regulated by the concentration of free tubulin in vivo.

Finally, fluorescent microtubules in living CHO fibroblasts and PtK_1 epithelial cells have been examined using a 2 second observation interval. These observations confirm results of earlier studies which demonstrate that microtubules turn over more rapidly in fibroblasts than in epithelial cells. Surprisingly, quantitative analysis of individual microtubule behavior reveals that microtubules in epithelial cells undergo depolymerization more frequently than microtubules in fibroblasts. However, microtubules undergoing disassembly are rapidly rescued in epithelial cells but not fibroblasts. These results demonstrate that microtubule behavior is regulated in a cell type specific manner and suggest that epithelial cells contain regulatory factors not found in fibroblasts.

TABLE OF CONTENTS

LIST OF TABLES

LIST OF FIGURES

Figure Page

CHAPTER 1

GENERAL INTRODUCTION

Microtubules are ubiquitous cytoskeletal components of eukaryotic cells which are required for the directed motion of intracellular organelles and mitotic chromosomes and play important roles in the determination and maintenance of polarized cell morphology and directed cell motion. In addition, microtubules are highly labile structures under many conditions, and thus their involvement in normal cell function requires the assembly, selective stabilization and disassembly of microtubules in an organized and coordinated manner.

Microtubule Structure and Polarity

Microtubules are formed by the polymerization of alpha-beta tubulin heterodimers (Luduena et al., 1977), into tubules generally 25 nm in diameter and 13 subunits in circumference (for review, see Amos et al., 1976). Tubulin dimers (subunits) are oriented in the same direction within a microtubule (Amos and Klug, 1974), thus, microtubules poses two morphologically distinct ends, one with exposed beta tubulin, the other with exposed alpha tubulin. In vitro experiments demonstrate that the two ends of a microtubule are functionally as well as morphologically distinct; the rate of microtubule polymerization at one end of a microtubule, termed the plus or fast growing end, is greater than that at the opposite minus or slow growing end (Allen and Borisy, 1974; Dentler et al., 1974; Bergen and Borisy, 1980), and the affinity of the plus end for tubulin subunits is higher than that of the minus end (Margolis and Wilson, 1978). Various methods can be used to determine the structural polarity of intact microtubules. For example, microtubules placed in conditions which promote polymerization increase in length more rapidly at the plus end.

This method has been used to reveal the polarity of microtubule arrays found in cilia and flagella (Allen and Borisy, 1974; Binder and Rosenbaum,1978) as well as of single microtubules (Summers and Kirschner, 1979). Dynein, a microtubule motor protein, binds to microtubules at an angle with respect to the microtubule axis. The orientation of attached dynein reveals the polarity of microtubules in the same way that the polarity of actin filaments is revealed by the attachment of heavy meromyosin (Haimo et al., 1979). Finally, under some conditions microtubules can provide a substrate for the polymerization of new incomplete microtubules along the length of the original "seed" microtubule (Burton and Himes, 1978). In cross sections, these incomplete microtubules appear as curved hooks, and the direction of curvature indicates the orientation of the seed microtubule with respect to the observer (Mandelkow and Mandelkow, 1979). This technique has been used to demonstrated that the vast majority of microtubules found in living cells have free plus ends, while the minus ends are embedded in or attached to intracellular structures (Allen and Borisy, 1974; Heidemann and McIntosh, 1980; Euteneuer and McIntosh, 1980,1981). Although the orientation of the alpha-beta dimers within microtubules is not known, kinetic arguments suggest that beta tubulin is exposed at the plus or fast growing end, while alpha tubulin is exposed at the minus end (Mandelkow and Mandelkow, 1989).

Microtubule Assembly Requires GTP

Each member of an alpha-beta dimer is capable of binding a molecule of GTP (Weisenberg et al., 1968; Bryan, 1972). Alpha tubulin binds GTP tightly, and exchange of GTP at this site (the N site) is slow. In contrast, GTP bound to beta tubulin (the E site) is capable of both rapid exchange and hydrolysis (Zeeberg and Caplow, 1979). Tubulin-GTP must be present for microtubule assembly, and assembly is accompanied by the rapid hydrolysis of bound GTP to form tubulin-GDP (Carlier, 1982). Once formed, GDP remains associated with tubulin subunits until the subunits depolymerize. Because addition

and loss of tubulin subunits in vivo occurs almost exclusively at the plus end of a microtubule (Geuens et al., 1989; Mitchison et al., 1986; Schulze and Kirschner, 1986), the plus end of an elongating microtubule contains a high proportion of tubulin-GTP subunits, while the remaining microtubule polymer is comprised of dimers in which GTP has been hydrolyzed. It has been suggested that under physiological conditions a microtubule is "protected" from disassembly by the presence of a "cap" of tubulin-GTP subunits at its plus end (Carlier and Panteloni, 1981; for review, see Bayley, 1990). Although the presence of a GTP cap has not been directly demonstrated, numerous experiments have both provided strong evidence in favor of this "GTP-cap" model of microtubule assembly, and suggested that this cap may be as small as a few dimers in length (Walker et al., 1991).

Dynamic Instability Model of Microtubule Assembly

In the presence of high concentrations of tubulin-GTP, the loss of a microtubule's GTP "cap", and the subsequent conversion of the microtubule from growing to shrinking is an infrequent event (Walker et al., 1988). In the presence of more limited concentrations of tubulin-GTP, however, random diffusion of tubulin-GTP subunits, coupled with microtubule polymerization, may result in local depletion of free tubulin-GTP subunits at a microtubule's plus-end, and a decrease in the rate of tubulin-GTP addition. Under these conditions, formation of tubulin-GDP within the microtubule lattice may proceed as far as the exposed microtubule end and result in disassembly of the microtubule. Because the rate of tubulin-GDP disassembly is higher than the rate of tubulin-GTP assembly, such random depolymerization events result in populations of microtubules in which both slow growing and rapidly shrinking microtubules are present (Mitchison and Kirschner, 1984a). This behavior of microtubule populations, termed dynamic instability (Mitchison and Kirschner, 1984a), has now been directly observed both in vitro (Horio and Hotani, 1986; Walker et

al., 1988) and in vivo (Cassimeris et al., 1988; Sammak and Borisy, 1988; Schulze and Kirschner 1988), and may be an underlying principle in the formation and function of all microtubule containing structures.

Treadmilling Model of Microtubule Assembly

Because the plus and minus ends of a microtubule have different affinities for tubulin subunits, under some conditions subunits can add to a microtubule at its plus end while being lost at its minus end. If addition and loss of tubulin subunits are balanced, turnover or "treadmilling" of the microtubule lattice can occur without net change in the total length of the microtubule polymer (Margolis and Wilson, 1978). It has been suggested that if an end of such a microtubule were held stationary, translocation of the microtubule lattice, and of attached organelles or chromosomes, would occur from the plus end toward the minus end (Mitchison, 1989a; Nicklas, 1987a). Although few examples of treadmilling behavior in vivo exist, net translocation or "flux" of microtubule polymer toward the minus end of both kinetochore (Mitchison, 1989a) and non-kinetochore microtubules has recently been demonstrated. The role of this mechanism in the in vivo function of the mitotic spindle apparatus has yet to be determined.

Regulation of Microtubule Assembly

Microtubules in vivo exhibit a much greater range of behaviors than microtubules in vitro. For example, microtubules observed in vitro are rarely seen to pause, while microtubules in vivo can remain in a meta-stable state, during which neither elongation or shortening can be detected, for extended periods of time (Schulze and Kirschner, 1976,1987). Experiments conducted in mitotic cells at the level of microtubule populations (Salmon et al., 1984) and direct observation of individual microtubules in living interphase

cells (Cassimeris et al., 1988; Sammak and Borisy, 1988; Schulze and Kirschner, 1988) have further revealed that microtubules in vivo can convert from growing to shrinking states (catastrophe) and from shrinking to growing states (rescue) much more frequently than microtubules in vitro (Walker et al., 1988). In addition, although tubulin in vitro is capable of self assembly in solution, most microtubules in living cells are nucleated from microtubule organizing centers (MTOCs). Finally, microtubules undergoing depolymerization in interphase cells are often rescued before they depolymerize completely. This behavior, termed "tempered" dynamic instability (Sammak and Borisy, 1988b), results in microtubule arrays where exchange between polymerized and free tubulin subunits (microtubule turnover) occurs most rapidly at microtubule plus ends, while the remaining microtubule polymer undergoes turnover more slowly.

Microtubule Associated Proteins

Some of the first microtubule regulatory factors to be isolated were microtubule associated proteins (MAPs; Sloboda et al., 1975). MAPs are a diverse group of proteins which bind tightly to, and are thus co-purified stoichiometrically with, microtubules. Some, such as dynein, are microtubule-based motor proteins (Gibbons, 1965), while others lack motile functions but affect the assembly behavior of microtubules. Experiments conducted at the level of microtubule populations demonstrate that the presence of MAPs stimulates the in vitro and in vivo assembly of microtubules (Cleveland et al., 1977; Drubin and Kirschner, 1986; Herzog and Weber, 1978; Sloboda and Rosenbaum, 1979), and increases the resistance of microtubules to microtubule destabilizing agents (for review, see Purich and Kristofferson, 1984). Examination of individual microtubules in vitro further reveals that MAPs increase the growth rate of individual microtubules, and can both decrease the frequency of catastrophe events and increase the frequency of rescue events (Bre and Karsenti, 1990; Pryer, 1989). Although MAPs were first isolated from sources of highly stable microtubules, such as cilia and nerve tissues (Gibbons, 1965; Olmsted and

Borisy, 1973) MAPs have now been found in association with microtubules in a wide variety of cell types during both interphase and mitosis (for reviews, see Bloom and Vallee, 1989: Olmsted, 1986; Wiche et al., 1991). Finally, the binding of MAPs to microtubules in vitro is strongly affected by both phosphorylation of MAPs (Jameson and Caplow, 1981; Murphy and Flavin, 1983; Sloboda et al., 1975) and the interaction of MAPs with calmodulin (Lee and Wolff, 1984) indicating that the regulation of microtubule dynamic behavior by MAPs is under cellular control.

Calcium and Magnesium

The concentration of various cations, particularly calcium and magnesium, has also been demonstrated to affect the in vitro and in vivo behavior of microtubules. Magnesium is required in small amounts for microtubule polymerization in vitro (Weisenberg, 1972) while even low concentrations of calcium ions prevents the in vitro assembly of microtubules (Weisenberg, 1972), and causes the disassembly of intact microtubules (Kiehart, 1981; Salmon and Segall, 1980; Zhang et al., 1992). Although the mechanism whereby calcium ions inhibits microtubule polymerization is still poorly understood, this effect is now known to be mediated by the calcium binding protein calmodulin. Both calmodulin and calcium sequestering membrane systems have been found in association with subsets of cellular microtubules (De Mey et al., 1980; Hepler, 1980,1989; Petzelt, 1984; Welsh et al., 1978) strongly suggesting that local changes in calcium ion concentration may be involved in the in vivo regulation of microtubule assembly and disassembly. In addition, experiments using calcium ions or calcium chelating agents have demonstrated that the onset of kinetochore microtubule disassembly during anaphase chromosome-to-pole motion (Izant, 1983), the integrity of the mitotic spindle (Izant, 1983; Kiehart, 1981; Salmon and Segall, 1980) and the rate of anaphase chromosome-to-pole motion (Cande, 1981; Zhang et al., 1990) can be experimentally regulated by changes in the concentration of calcium ions. Furthermore, observations using calcium indicator dyes

have revealed that elevation of intracellular calcium concentration (Hepler and Callaham, 1987) or calcium transients (Poenie et al., 1986; Ratan et al., 1986) can occur in vivo as cells initiate the motion of chromosomes toward the poles during mitosis.

Post-translational Modification

Dynamically distinct groups of microtubules found in living cells are often characterized by the post-translational acetylation or detyrosination of alpha tubulin subunits or the phosphorylation of beta tubulin subunits (for review, see Greer and Rosenbaum, 1989). Microtubules comprised of such post-translationally modified tubulin are generally less dynamic and more resistant to depolymerization than microtubules comprised of non-modified tubulin. For example, microtubules found in cilia and flagella (Gunderson and Bulinski, 1986a; Schneider et al., 1987), neurite cell processes (Black and Keyser, 1987; Wehland and Weber, 1987), centrioles (Gunderson et al., 1984), and some stable microtubules found in the interior regions of cultured animal cells (Schulze and Kirschner, 1986; Schulze et al., 1987) react strongly with antibodies to detyrosinated or acetylated tubulin. Other studies have demonstrated increases in the in vivo phosphorylation of microtubules during differentiation of neuroblastoma cells (Gard and Kirschner, 1985), and have indicated that the level of tubulin acetylation and detyrosination varies in both a cell cycle dependent and developmentally regulated manner (Cambray-Deakin and Burgoyne, 1987; Gunderson and Bulinski, 1986b; Sherwin et al., 1987). However, experimental detyrosination of cytoplasmic microtubules has no effect on the dynamic behavior of these microtubules as shown by photobleaching studies of fluorescent microtubules (Webster et al., 1990). Furthermore, in vitro assays fail to detect differences in the assembly or disassembly behavior of modified and unmodified tubulin subunits (Raybin and Flavin, 1977; Maruta et al., 1986), and immunofluorescent and immunogold staining using antibodies to tyrosinated and detyrosinated tubulin has revealed that some individual microtubules contain both modified and unmodified tubulin (Gunderson et al.,

1984, Geuens et al., 1986). Thus, the role of post-translational modification in generating dynamically distinct microtubule arrays remains to be resolved.

Microtubule Drugs

In addition to binding GTP, tubulin dimers can bind several drug molecules which dramatically alter the behavior of microtubules. Some, such as colchicine, colcemid, vinblastine and nocodazole cause the rapid disassembly of microtubules (Bergen and Borisy, 1983; Jordan et al., 1986; Margolis and Wilson, 1977; Snyder et al., 1982), while others such as taxol, promote microtubule assembly and stability (Bajer et al., 1982; Schiff and Horwitz, 1980; Vallee, 1982). These drugs have become indispensable experimental tools in the study of microtubule function and microtubule based motility in vivo (for reviews, see Dustin, 1984; Schliwa, 1986). In addition, although endogeneous compounds related to these drugs have yet to be discovered, the presence of microtubule drug binding sites suggest that functional analogues of microtubule poisons may be used by cells to regulate some aspects of microtubule behavior.

Tubulin Concentration

Finally, it should be noted that the concentration of tubulin subunits is itself a potent regulator of microtubule behavior in vitro. The concentration of tubulin-GTP has been shown to increase the stability of microtubules in vitro by increasing the frequency of rescue events and decreasing the frequency of catastrophe events in a concentration dependent manner (Walker et al., 1988). Experimental increases in the intracellular concentration of tubulin have also been shown to increase the rate of microtubule growth in vivo (Schulze and Kirschner, 1986), and induce the reversal of anaphase A chromosome-to-pole motion (Shelden and Wadsworth, 1992). Furthermore, recent direct observations of microtubules in vitro have demonstrated that the integrity of intact microtubule walls is dependent upon a sufficient concentration of free tubulin subunits (Dye and Williams,

1991). Finally, the intracellular concentration of tubulin has been shown to be autoregulated at the level of tubulin mRNA translation (Yen et al., 1988). Such observations strongly suggest that the behavior of microtubules in vivo is regulated by changes in tubulin subunit concentration.

Organization and Function of Microtubules in Interphase Cells

Microtubules in interphase cells provide a substrate for the organization and movement of intracellular organelles and are involved in the generation and maintenance of polarized cell morphology. The polarized morphology of interphase microtubule arrays is largely determined by the presence of a single microtubule organizing center (MTOC) (Pickett-Heaps, 1969) associated with the nucleus, to which the majority of interphase microtubules are attached by their minus end. This creates a microtubule array with microtubule plus ends distal and minus ends proximal to the MTOC. Microtubule based motor proteins frequently translocate along microtubules in a unidirectional manner (Vale et al., 1985a). For example, the motor protein dynein translocates toward the minus end of a microtubule (retrograde motion) (Paschal and Vallee, 1987), while kinesin generally moves along microtubules toward the plus-end (anterograde direction) (Vale et al., 1985b). Thus, organelles and vesicles which bind selectively to these microtubule motor proteins can be directed toward or away from the cell center.

MTOCs may also play a role in regulating the number and behavior of microtubules. For example, in vitro experiments reveal that MTOCs nucleate microtubules at tubulin concentrations well below the concentration necessary for tubulin self-assembly (Mitchison and Kirschner, 1984b). Other observations reveal that the number of microtubules attached to centrosomes varies in a cell-cycle dependent manner (Snyder and McIntosh, 1975; Kuriyama and Borisy, 1981). More recently, in vitro experiments have demonstrated that the nucleation capacity of centrosomes can be increased by the

phosphorylation of centrosomal proteins (Verde et al., 1990,1991). Because cells contain a limited amount of tubulin, changes in the number of centrosomal microtubules may have additional effects on the intracellular concentration of free tubulin.

In mammalian cells, MTOCs are characterized by a central pair of barrel shaped microtubule arrays, the centriole pair, and a surrounding cloud of electron dense pericentriolar material. Microtubules are found embedded in the pericentriolar material but do not generally appear to interact with the centrioles. In addition, a variety of experimental evidence indicates that the pericentriolar material, not the centriole pair, is necessary and sufficient for the generation of interphase microtubule arrays (Gould and Borisy, 1977) and separation of chromosomes during anaphase (Berns and Richardson, 1977). Although the biochemical composition of MTOCs is still poorly defined, a third form of tubulin subunit (gamma-tubulin) has recently been found in association with MTOCs (Joshi et al., 1992) and has been shown to mediate microtubule nucleation. Gamma tubulin may thus play a crucial role in the determining the over-all organization of microtubule arrays.

A variety of experimental evidence indicates that interphase microtubules are also involved in maintaining and possibly determining the direction of cell motion. For example, cells treated with microtubule destabilizing drugs lose the ability to undergo directed locomotion, although random motion can still occur (reviewed in Vasiliev and Gelfand, 1976; see also Euteneuer and Schliwa, 1984 for an alternate view). In addition, other experiments indicate that the orientation of the MTOC can be correlated with the direction of cell motion (Gotlieb et al., 1981) and that destruction of the centrosome or centriole pair results in loss of a cell's ability to display directed cell motion (Koonce et al., 1984; Albrect-Buehler, 1979). Other experimental evidence indicates that the presence of modified microtubule subpopulations can be correlated with the direction of cell motion (Gunderson and Bulinski, 1988), and that the bending of microtubules in living neurons during growth cone movements predicts changes in the direction of motion (Tanaka and Kirschner, 1991). Finally, it should be noted that microtubules arrays are more dynamic in

motile fibroblasts than in more stationary epithelial cells (Pepperkok et al., 1990; Wadsworth and McGrail, 1990), indicating that microtubule dynamic behavior may be required for or correlated with cell locomotion.

Organization and Function of Microtubules in Mitotic Cells

The ability of eukaryotic cells to regulate the dynamic behavior of microtubules is perhaps most dramatically displayed during mitosis, the process of cell division. The onset of mitosis is accompanied by the disappearance of interphase microtubules and the appearance of a highly dynamic array of microtubules, the mitotic spindle. Mitotic spindles are bipolar structures containing three functionally distinct populations of microtubules: the kinetochore microtubules (KMTs), interzonal microtubules, and astral microtubules. The regulated assembly and disassembly of these microtubules plays a crucial role in affecting the various motions of mitosis (Salmon, 1989). However, although microtubules were recognized in the mitotic spindle apparatus as early as 1950 (for review, see McDonald, 1989), and the dynamic nature of spindle microtubules in living cells was recognized almost 30 years ago (Inoue, 1964; Inoue and Sato, 1967), the manner in which microtubules-containing structures are generated and regulated during mitosis remain important and unresolved issues.

Interphase/Mitosis Transition

During the initial stages of mitosis, the interphase array of microtubules is rapidly disassembled. Little is known about the mechanism of this disassembly, however, many cells which contain highly stabilized microtubules arrays are terminally differentiated and do not divide. This suggests that the disassembly of interphase microtubule arrays may occur through the random disassembly of microtubules predicted by the dynamic instability model of microtubule behavior. Alternatively, a variety of experimental evidence indicates

that interphase microtubules may be actively disassembled as cells enter mitosis through the action of agents which increase the frequency of microtubule catastrophe events (Belmont et al., 1990), reduce the frequency of rescue events (Cassimeris et al., 1988), or break microtubules into fragments (Vale, 1991). Finally, some evidence suggests that interphase microtubules may be released from the centrosome during the entry into mitosis (Belmont et al., 1990; McBeath and Fujiwara, 1990).

Kinetochore Microtubules

Kinetochore microtubules form a bundle of several to hundreds of microtubules which attach the spindle pole regions to specialized areas found at the primary constriction of each chromosome pair, termed the kinetochore (for review, see Rieder, 1982). Although kinetochores have been shown to nucleate the growth of microtubules in vitro (Bergen et al., 1980; Gould and Borisy, 1978; Snyder and McIntosh, 1975) it is now thought that KMTs are nucleated by the centrosomes, or mitotic poles, and are captured at their plus end through chance interaction with kinetochore regions (Rieder, 1982). Lateral association of the kinetochore region with microtubules has been well documented and may play an important role in the initial formation of kinetochore fibers (Rieder and Alexander, 1990; Roos, 1973), however, ultrastructural analysis of the interaction between the kinetochore and KMTs reveals that the majority of KMTs attached to the kinetochore are attached with their plus ends in contact with, and possibly inserted into, the kinetochore region (for reviews see Brinkley et al., 1989; Rieder, 1982). A wide range of experiments in which cells are treated with microtubule destabilizing agents further demonstrate that the interaction of KMT plus-ends with the kinetochore alters the dynamic behavior of KMTs by greatly increasing the stability of attached kinetochore microtubules (Cassimeris et al., 1990; Huitorel and Kirschner,1988). However, slow turnover of kinetochore microtubules has been demonstrated during both metaphase (Gorbsky and Borisy, 1989) and early anaphase (Wadsworth et al., 1989). In addition, in vitro evidence further suggests that

kinetochores may also decrease the stability of attached microtubules under some conditions (Hyman and Mitchison, 1990). Rieder (Rieder, 1982) notes that MTs found within the kinetochore fiber display increased stability regardless of whether they are attached directly to the kinetochore. The increased stability of KMTs may therefore be due in part to lateral interactions of KMTs with each other or with MAPs found within the kinetochore fiber rather than to the actual attachment of KMTs to the kinetochore (Rieder, 1982).

During prometaphase and metaphase, chromosomes become aligned at the spindle equator, or metaphase plate, a process termed chromosome congression. During congression, linked sister chromatids move back and forth (oscillate) across the spindle equator; these oscillations become reduced in in extent and frequency as anaphase onset approaches. Recent experimental evidence reveals that such oscillations require the coordinated assembly and disassembly of KMTs attached to opposing kinetochores (Mitchison et al., 1986; Wise et al., 1991, for review see Mitchison, 1988). These experiments further reveal that the majority of KMT assembly and disassembly during chromosome oscillations occurs at the kinetochore proximal or plus ends of the KMTs (Mitchison et al., 1986; Wise et al., 1991), although some disassembly at KMT minus ends may contribute to the overall changes in KMT length at this stage (Mitchison, 1989a). Although it is clear that the alignment of chromosomes at the metaphase plate requires a balance of opposing forces applied to the kinetochores of sister chromatids, the nature of these forces remains unknown. It has been postulated that the assembly and disassembly of KMTs could generate the force required for motion of chromosomes at this stage (for discussion, see McIntosh et al., 1989). However, other experimental evidence suggests that congression results from a balance of pulling forces generated at the kinetochore (Hays et al., 1982).

During anaphase, the attachment between KMTs and kinetochores continues to provide a mechanical link between the chromosomes and poles. Both <u>in vitro</u> and <u>in vivo</u>

experiments have demonstrated that the kinetochore is the site of microtubule disassembly during anaphase chromosome-to-pole motion (Gorbsky et al., 1988; Koshland et al., 1988; Nicklas, 1987b). However, the manner in which the attachment between the kinetochore and KMTs is maintained during chromosome motion and disassembly of the kinetochore microtubules, and the manner in which the force used to move chromosomes is generated, remain unresolved issues. The observation that chromosome motion and the disassembly of KMTs are tightly coupled, and the exothermic nature of microtubule disassembly, led Inoue and others (Hill, 1981; Inoue, 1976; Inoue and Sato, 1967) to suggest that the the disassembly of KMTs is itself responsible for the movement of chromosomes. Some support for this hypothesis has come from recent experiments which have demonstrated that isolated kinetochores can remain attached to microtubules which are undergoing disassembly in response to a decreased tubulin subunit concentration (Koshland et al., 1988) and that microtubules undergoing depolymerization in vitro in response to a reduction in tubulin concentration can promote the minus end directed motion of chromosomes and chromosome fragments (Coue et al., 1991). Further evidence in support of this hypothesis has been provided by ultrastructural analysis which reveals that microtubule ends become splayed during disassembly, giving the end of a microtubule a frayed appearance (Mandelkow et al., 1991). It has been suggested that if this conformational change is accompanied by the generation of force, the kinetochore, acting as a sliding collar, could be driven down kinetochore microtubules ahead of the region of microtubule splaying (Koshland et al., 1988; Mitchison, 1988).

Some evidence for an alternative hypothesis has been obtained from in vitro observation of stable microtubules attached to isolated kinetochores, which reveal that kinetochores can generate motion of microtubules in an ATP dependant manner (Hyman and Mitchison, 1991; Mitchison and Kirschner, 1985b). Further observations reveal that this motion can be produced in both a plus end and a minus end directed manner (Hyman and Mitchison, 1991), suggesting that either two motors which move along microtubules in

opposite directions are present at the kinetochore, or that the direction of motion can be regulated in some manner. Recently, both direct observation of the motion of chromosomes in vivo (Rieder and Alexander, 1990) and immunological studies (Pfarr et al., 1990; Steuer et al., 1990; Wordeman et al., 1991) have provided strong evidence for the presence of dynein, a minus-end directed microtubule motor, at the kinetochore.

Interzonal Microtubules

Although chromosome separation in many cells occurs largely through the motion of chromosomes toward the spindle poles (anaphase A) most cells also undergo some degree of pole-pole separation (anaphase B). In some organisms anaphase B plays only a minor role in the separation of chromosomes, while in others anaphase B may replace chromosome-to-pole motion as the mechanism of chromosome separation. There is general agreement that spindle pole separation involves the interaction and elongation of microtubules from opposite spindle poles (for reviews, see McIntosh, 1989; Cande et al., 1989). It remains unclear, however, if interzonal microtubules generate, regulate or convey the forces required for spindle elongation. In vitro studies conducted using isolated diatom spindles have provided strong evidence for the presence of a motor protein in the mid-region of these spindles which generates sliding of the overlapping anti-parallel interzonal microtubules (Cande and McDonald, 1985; Masuda and Cande, 1987,1988; for review see Cande et al., 1989). In these cells, interzonal microtubules may therefore convey force generated in the interzone to the spindle poles. It should be noted, however, that the diatom spindle is somewhat unusual in that it is made up largely of a bundle of overlapping interzonal microtubules arranged in a paracrystalline array (for review, see Pickett-Heaps, 1991). In addition, these organisms exhibit very little anaphase A chromosome-to-pole motion and the chromosomes are divided to the two daughter cells largely through the process of spindle pole separation. Alternatively, experiments conducted during anaphase B in Fusarium (Aist and Bayles, 1988,1992) and in PtK_1 epithelial cells (Kronebusch and

Borisy, 1981), in which interzonal microtubules are severed using a highly focused laser beam or micromanipulation produce substantial increases in the rate of spindle pole separation. Such experiments suggest that in these organisms the interaction of interzonal microtubules from opposite poles serves to regulate rather than generate the force used to separate the spindle poles. Finally, it should be noted that the dynamic instability behavior of microtubule populations can generate "polar ejection forces" (Rieder et al., 1986; Salmon, 1989) capable of moving objects as large as chromosomes away from the pole, and that interzonal microtubules are most dynamic in mammalian epithelial cells, as measured by the incorporation of labeled tubulin subunits, when the rate of anaphase B spindle elongation is greatest (Shelden and Wadsworth, 1989). Together these observations provide evidence that microtubule assembly may itself generate the force required for spindle pole separation.

Astral Microtubules

Finally, the astral microtubules are those microtubules emanating from the spindle poles which do not interact with either a kinetochore or with microtubules from the opposite pole. Although the role of these microtubules in the process of mitosis is still largely unresolved, several investigators have proposed that these microtubules may generate forces required for the alignment of chromosomes at the metaphase plate during prometaphase and metaphase (for discussion, see Salmon, 1989), or convey pulling forces during separation of the spindle poles in anaphase B spindle elongation (Aist and Bayles, 1988,1992; Kronebusch and Borisy, 1981). Other experiments suggest that these microtubules may play an important role in the positioning of the spindle pole during unequal cleavage common to many embryonic cells (Salmon, 1976; Schatten, 1981), and indicate that astral microtubules are required for pronuclear migration during fertilization in several marine organisms (Hamaguchi and Hiramoto, 1986; Schatten, 1981). Finally, a variety of experimental evidence indicates that astral microtubules are required for the

organization of the contractile ring prior to the onset of cytokinesis (for reviews, see Mabuchi, 1986; Rappaport, 1986).

Research Objectives

To further characterize the in vivo behavior of microtubules, I have undertaken a three part study of microtubule dynamics at the level of individual microtubules. First, I have extended the observations of individual microtubule assembly during mitosis to include anaphase A and B. Briefly, biotin labelled tubulin subunits were injected into living cells at different stages of mitosis. After allowing the cells to incorporate injected subunits for varying amounts of time, the cells were lysed, fixed and immunostained with antibodies to tubulin and biotin to reveal both the sites and extent of subunit incorporation. Using this technique, I have documented that interzonal microtubule arrays remain dynamic while the cell utilizes them to perform mechanical work during anaphase B spindle elongation. Using quantitative methods, I have further determined that interzonal microtubules are most dynamic during the period of anaphase B when the spindle poles separate most rapidly. The results of this work therefore contrast with that conducted in isolated diatom spindles (Cande and McDonald, 1985; Masuda and Cande, 1988). Incorporation of biotin tubulin into interzonal microtubules was significantly reduced after the completion of spindle separation, when interzonal microtubules are much less dynamic (Saxton and McIntosh, 1987) and form tightly packed bundles. The assembly of mitotic microtubule populations has been shown to exert a pushing force capable of moving particles as large as mitotic chromosomes (Bajer, 1982; Rieder et al., 1986; Salmon, 1989). Therefore, the elevated levels of incorporation into interzonal microtubules detected during spindle pole separation suggest a new model of spindle elongation in which microtubule assembly itself produces the force for anaphase B spindle elongation.

Second, I have examined the relationship between microtubule dynamics and chromosome motion in anaphase cells by experimentally inducing the assembly of kinetochore microtubules during anaphase A. As chromosomes move toward the poles, kinetochore fibers must shorten to maintain the attachment between kinetochores and the spindle pole. Recent experiments have provided strong evidence that this disassembly occurs preferentially at the plus ends (Euteneuer and McIntosh, 1980) of the kinetochore microtubules, proximal to the kinetochore (Mitchison et al., 1986; Gorbsky et al., 1988; Nicklas, 1989). Surprisingly, the plus-ends of kinetochore microtubules appear to be highly competent to assemble subunits at this stage. The elevation of intracellular tubulin concentration induced by the microinjection of labeled tubulin subunits into anaphase cells resulted in rapid assembly of tubulin subunits at the kinetochore plus ends -- the presumed site of KMT disassembly. Furthermore, this assembly was accompanied by a temporary reversal of chromosome-to-pole motion. Together these results suggest that the direction and possibly the rate of anaphase chromosome motion are tightly linked to the assembly and disassembly competence of kinetochore fiber microtubules, and provide the first demonstration that tubulin subunit concentration can regulate some aspects of anaphase chromosome motion in vivo.

Finally, microtubules in motile fibroblasts are more dynamic than those found in more stationary epithelial cells (Pepperkok et al., 1990; Wadsworth and McGrail, 1990), suggesting that the dynamic behavior of microtubules is intimately involved in the locomotion of interphase cells. However, the mechanisms involved in generating cell type-specific differences in microtubule dynamics were not examined in these previous studies. In the third part of my thesis research, I have addressed this issues by examining individual microtubules in living epithelial cells and fibroblasts, and quantifying the parameters of microtubule dynamic behavior in each cell type. Examination of individual microtubule behavior in these two cell types confirms that microtubules are more dynamic in fibroblasts than in epithelial cells as measured by the amount of time an individual

microtubule remains within an equivalent area of the cell lamella. Quantification of the dynamic behavior of microtubules in these cells further reveals that both the rate of growth and depolymerization are higher in fibroblasts than in epithelial cells, and that microtubules pause less frequently in fibroblasts than epithelial cells. Surprisingly, this analysis also reveals that the frequency of microtubule transitions is higher in epithelial cells than fibroblasts. However, microtubules in epithelial cells are characterized by growth and shrinking excursions of short duration and extent, while microtubules in fibroblasts undergo less frequent, but more extensive length changes. A small number of more stable microtubules are also detected in fibroblasts. The results of these experiments have increased the understanding of microtubule dynamics and its regulation in interphase cells, and by extension, suggest regulatory mechanisms involved in the formation and function of mitotic microtubule arrays.

CHAPTER 2

INTERZONAL MICROTUBULES ARE DYNAMIC DURING SPINDLE ELONGATION

Abstract

The pattern and extent of microtubule assembly during spindle elongation has been examined in PtK_1 cells by microinjection of biotin-tubulin and immunolocalization of biotin-tubulin containing microtubules using antibodies to biotin. PtK_1 cells were microinjected at 30^{o} C, incubated for various intervals to allow incorporation of biotin-tubulin into microtubules, then lysed, fixed and stained for biotin-tubulin and total tubulin. When mid- to late anaphase cells are examined at short times post-injection using conventional fluorescence light microscopy, rapid incorporation of biotin-tubulin is detected throughout the interzonal region, between the separating chromosomes, and in the spindle asters. Using confocal fluorescence microscopy, the segments of biotin labeled microtubules detected in the interzonal region are found to be continuous with the distal, or plus-ends, of unlabeled microtubules. When telophase cells are examined, a marked decline in the extent of incorporation is apparent.

Quantitative analysis of the total length of biotin-labeled polymer in the interzonal region of cells from mid-anaphase through telophase further reveals that the extent of incorporation is greatest during late anaphase, and decreases during telophase. The measured rate of interzonal microtubule growth remains relatively constant during this period. These results provide direct evidence for plus-end elongation of interzonal microtubules during spindle elongation and further reveal that interzonal microtubules are highly dynamic during late anaphase spindle elongation. The implications of these results for the mechanism of anaphase B are discussed.

Introduction

Anaphase chromosome motion consists of both chromosome-to-pole motion, anaphase A, and the separation of the poles, anaphase B. In cultured animal cells, pole-pole separation begins after chromosome-to-pole motion is nearly complete and continues for several minutes, depending on cellular morphology. The rate of pole separation is slower than the rate of chromosome-to-pole motion (Brinkley and Cartwright, 1971).

Structural analysis of the arrangement of spindle microtubules throughout mitosis has indicated that those spindle microtubules which overlap at the equator lengthen during spindle elongation, or anaphase B (McIntosh, 1985). These interzonal microtubules are composed of microtubules extending from each pole and thus are of opposite polarity, plus-ends distal to the pole from which they originated (Euteneuer and McIntosh, 1980). Recent experiments in which fluorescent tubulin has been microinjected into living cells suggest that these interzonal microtubules elongate by addition of subunits to their distal or plus-ends during spindle elongation, although individual microtubules could not be resolved in these experiments (Saxton and McIntosh, 1987). Further analysis of pattern photobleaches in the interzone of late anaphase/telophase cells (a stage which corresponds to telophase cells in this study) reveal that fluorescence recovery is slow and that the two half-spindles slide apart (Saxton and McIntosh, 1987). However, the rate of sliding in these cells is very limited (approximately 0.09 μm/min).

Additional information concerning the mechanism of anaphase B comes from analysis of elongation of the diatom central spindle. In these cells, the central spindle consists of a very regular, interdigitated array of overlapping microtubules which slide apart during elongation, reducing the extent of overlap (Cande and McDonald, 1985; McIntosh et al., 1979). These central spindles can be isolated and reactivated in buffers containing ATP and exogenous tubulin (Masuda and Cande, 1987,1988). When labeled tubulin is present in the reactivation solution, microtubule elongation at the ends of the

region of overlap is observed; as the spindle elongates, the zones of new microtubule growth approach each other. When central spindle reactivation is prevented by omitting ATP, microtubule polymerization continues, but the spindles do not elongate (Masuda and Cande, 1988). Thus, ATP dependent force generation within the overlapping array of microtubules contributes to spindle elongation; microtubule assembly increases both the rate and extent of spindle elongation in vitro (Masuda and Cande, 1988).

In the experiments presented here, the pattern and extent of microtubule polymerization during spindle elongation in cultured cells has been examined by microinjection of biotin-labeled tubulin (Mitchison et al., 1986; Wadsworth et al., 1989). At various intervals post-injection, cells were lysed, fixed and prepared for immuno-localization of both biotin-tubulin and total tubulin using either conventional or confocal fluorescence microscopy. These experiments demonstrate that microtubules remain highly dynamic during late anaphase as evidenced by the rapid incorporation of labeled tubulin subunits. This study further documents elongation of individual interzonal microtubules during anaphase B. Finally, quantitative measurements reveal time dependent changes in the amount of total polymer assembled in the interzonal region from mid-anaphase through telophase. The greatest extent of incorporation occurs during late anaphase, coincident with the maximal rate of anaphase B pole-pole separation in these cells.

Materials and Methods

Preparation of Biotin Tubulin

Biotin-tubulin was prepared as described (Mitchison et al., 1986; Wadsworth et al., 1989). Small aliquots were stored at -70^{o}C in injection buffer (20 mM sodium glutamate, 1 mM EGTA and 0.5 mM MgSO4, pH 7.2). The protein solution was adjusted to 1 mM GTP concentration and centrifuged for 10 min at maximum speed in an Eppendorf microcentrifuge before use. Biotin-tubulin was used at a concentration of 3-4 mg/ml in the

injection pipette as determined by a modification (Schacterle and Pollack, 1973) of the method of Lowry (Lowry et al., 1951).

Cell Culture and Microinjection

PtK_1 cells were grown at 37°C in Ham's F-12 medium supplemented with 10% fetal bovine serum, 10 mM HEPES and antibiotics. Cells were plated on glass coverslips and allowed to grow for 36-48 hours before use. Coverslips were then mounted in a laboratory constructed microinjection chamber (Wadsworth et al., 1989) and mounted on the stage of a Zeiss IM-35 microscope. In this chamber, individual cells could be readily observed, injected and relocated following staining. Temperature was maintained at 30° C using an Opti-Quip Red Beam Incubator calibrated with a YSI Telethermister. Microinjection was performed using a Narishige micromanipulator and an Eppendorf model 5242 microinjector. Needles were pulled to a final tip diameter of approximately 0.5 μm on a Sutter Instruments P-80 Brown-Flaming micropipette puller, using Microdot capillaries. Pipettes were back loaded with approximately 0.5 μl of biotin-tubulin using a Hamilton syringe. Chromosome position in injected cells was recorded photographically on thirty-five millimeter film. Cells incubated less than thirty seconds post-injection were photographed just after injection and again just after lysis. For some experiments in which cells were incubated longer than thirty seconds, the living cell was photographed after injection and just before lysis, to record any change in chromosome position.

Immunofluorescence

Following microinjection, cells shown in Figures 2.1 and 2.2, and control cells used for quantification (see Quantitative Methods), were lysed for approximately 50 sec in lysis buffer containing 80 mM PIPES, 5 mM EGTA, 1 mM $MgSO_4$ and 0.5% Triton X-100, pH 6.8 (Cassimeris et al., 1986). Cells shown in Figures 2.3-2.5, and cells quantified for Figure 2.6, were lysed as described above, then rinsed an additional 50 sec

in saline at room temperature before fixation. The saline rinse reduced the number of spindle microtubules, allowing a more precise determination of the extent and pattern of the remaining biotin-labeled microtubule segments (see Discussion). Cells were fixed for 25 minutes in 2% paraformaldehyde and 0.1% glutaraldehyde in PBS, pH 7.3 and rinsed in PBS containing 0.1% Tween and 0.02% azide (PBS-Tw-Az) and for 5 min in 1% sodium borohydride. Antibody incubations were performed in humid chambers at room temperature. Cells were incubated first with rabbit anti-biotin antibodies (Enzo Biochemicals, N.Y.) at a dilution of 1:50 in PBS-Tw-Az containing 1% BSA for 30 min, rinsed in PBS-Tw-Az and incubated with fluorescein goat anti-rabbit and then fluorescein rabbit anti-goat antibodies. Cells were then incubated in a mouse monoclonal anti-tubulin antibody (generous gift of Dr. J.R. McIntosh) for up to 3 hours followed by rhodamine goat anti-mouse antibodies. All fluorescent secondary antibodies were purchased from Cappel Laboratories and used at a final dilution of 1:50 in PBS-Tw-Az containing 1% BSA, for 30 minutes at room temperature. Stained cells were mounted in 0.1% n-phenyldiamine in glycerol and sealed with nail polish.

Analysis of Chromosome Motion

Recordings of chromosome motion were made using a Dage Newvicon camera (Model 67M) and a Gyyr 1/2" time lapse tape recorder (model TLC 1400). The rate of chromosome motion was determined from traces of chromosome position made onto sheets of clear acetate.

Microscopy

For standard immunofluorescence observations, a Zeiss IM-35 microscope equipped with a 63X 1.4 NA lens and filters for rhodamine and fluorescein excitation was used. Cells were photographed using TMAX 400 film, developed in HC 110 dilution B. For confocal microscopy, a BioRad MRC500 laser scanning head mounted on a Nikon

optiphot microscope equipped with a 60X 1.4 NA objective lens was used. The confocal microscope was operated with the pinhole set for a section thickness of approximately 0.9 μm. Section thickness was determined by imaging 10 μm diameter glass beads using back-scattered light. A step size for the stage motor which gave discernible difference in each sequential image in a through-focus series (Z-series) through the bead was used. The diameter was then measured at the widest point, and section thickness estimated by dividing the diameter by the number of images collected. A Z-series of images through the specimen was collected for both the rhodamine and fluorescein channels. Kalman averaging was used to increase the signal to noise ratio of confocal images, and images were further processed by application of a 9 X 9 crisping convolution matrix and contrast enhancement. Image overlays (merged images) were made in a similar manner, but the contrast and brightness of individual images were increased as required to balance the resulting image, and pairs of images were then simultaneously projected on the monitor. Finally, images were photographed using Kodak color slide film.

Quantitative Methods

Quantitative measurements of biotin-tubulin incorporation were made using a Masscomp computer. Biotin-labeled microtubule segments in each optical section through the cell were traced using a mouse driven cursor. Traces generated from each optical section were assigned different grey-scale values and a color look-up table was used to color code each optical section. Labeled microtubule segments could then be followed through successive image planes by adding traces to the monitor. When a complete trace was generated, the final length of a labeled microtubule segment was measured using the mouse, and the trace was then removed from the screen using a mouse driven "eraser" function. This technique ensured that microtubule segments were not traced more than once and facilitated tracing in regions dense in microtubules. No attempt was made to adjust the final calculated length of each microtubule segment for the number of image

planes through which it extended. Interzonal microtubules generally did not extend through more than two optical sections, as this region of the cell remains relatively flat during anaphase B. For cells rinsed in saline prior to fixation, successive trials gave a counting error of ±7.2%. Microtubules in cells placed in fixation buffer immediately after lysis (controls) were also quantified. Microtubules in these control cells were much more difficult to trace with accuracy; successive trials gave an error of ±27%. However, the pattern of incorporation, as well as the average growth rate of individual microtubules, were similar in cells prepared by both methods (for example, compare Figures 2.2 and 2.4). Half of the cells analyzed for Figure 2.6, and one third of the control cells, were quantified more than once to estimate the accuracy of the quantitative methods. Computer measurements were calibrated using an objective micrometer as a test object. Rates of microtubule elongation were calculated by dividing the average length of biotin-tubulin incorporation by the injection interval in each experiment.

Results

Microtubule Assembly During Spindle Elongation

To examine the pattern of microtubule polymerization during spindle elongation, PtK_1 cells were microinjected with biotin labeled tubulin (biotin-tubulin) (Mitchison et al., 1986; Wadsworth et al., 1989) and doubled-labeled to visualize both biotin-tubulin containing microtubules and the total microtubule staining pattern. For these experiments, cells were incubated at 30° C to reduce the number of microtubules (Wadsworth et al., 1989) and then lysed and stained as described in Methods. Three criteria were used to select mid-anaphase cells: (1) chromosome-to-pole motion was not yet complete, as evidenced by the presence of kinetochore fibers, (2) little change in the pole-to-pole spindle length had occurred and (3) the chromosomes maintained a characteristic "V" shape. A cell which was injected in mid-anaphase and fixed 60 sec post injection is shown in Figure 2.1.

Short segments of biotin labeled microtubules are detected in the interzonal region of this cell, between the separating chromosomes (Figure 2.1). Biotin-tubulin fluorescence is also detected in the region between the chromosomes and the pole, but is much less intense than the total tubulin staining pattern of this region of the cell. Astral microtubules also incorporate biotin-tubulin (out of the plane of focus in Figure 2.1); many of these astral microtubules appear to be labeled along their entire length.

The pattern of tubulin incorporation in late anaphase cells has also been examined. Cells were judged to be in late-anaphase on the basis the following criteria: (1) chromosome-to-pole motion was complete; chromosomes were no longer stretched in a "V" shaped toward the poles, (2) only very short kinetochore fiber microtubules were detected using immunofluorescence observations of total microtubule polymer, and (3) telophase events characterized by chromosome decondensation, nuclear reformation and the initiation of cytokinesis had not occurred. A pair of optical sections from a cell injected in late anaphase and lysed 30 seconds later is shown in Figure 2.2(a-d). These cells have been imaged using a confocal fluorescence microscope (see Methods) to improve the ability to detect labeled microtubules (compare Figures 2.1 and 2.2). Using this method, short microtubule segments containing biotin-tubulin, continuous with the distal, or plus end, interzonal microtubules are readily detected. In some cases, the entire length of a microtubule appears to be biotin-labeled (Figure 2.2(c, d)).

When late anaphase cells are incubated for longer intervals following injection, the total tubulin and biotin labeled tubulin staining patterns are nearly indistinguishable using the confocal fluorescence microscope. A pair of optical sections from a cell which was injected during late anaphase and lysed 67 seconds later is shown in Figure 2.2(e, h). Comparison of the total tubulin staining (Figure 2.2(g)) with the biotin staining pattern (Figure 2.2(h)) reveals that incorporation of biotin-tubulin into spindle microtubules is nearly complete within 67 seconds. Phase micrographs of the injected cells (Figures 2.2(a,b) and 2.2(e,f)) reveal that little or no pole separation has occurred during these

incubation intervals; thus both cells shown in Figure 2.2 contain labeled segments which are much longer than the extent of pole separation during the incubation interval. This is especially noticeable in Figure 2.2(e-h) where the majority of interzonal microtubules, including those in microtubule bundles, appear to have fully incorporated biotin-labeled subunits. The rapid incorporation of biotin-labeled tubulin into individual interzonal microtubules during anaphase B elongation is therefore not directly coupled to pole separation in these cells.

Microtubule Assembly During Telophase

Microtubule assembly during midbody formation has also been investigated by injecting cells with biotin-tubulin during telophase. Telophase cells were defined by the following criteria: (1) chromosome-to-pole motion is complete, as judged by the lack of kinetochore fibers, (2) bundles of microtubules are present in the interzone, and (3) cytokinesis and chromosome decondensation had begun. Figure 2.3 illustrates a telophase cell which was lysed 55 sec post injection and examined using confocal microscopy. Short segments of biotin containing microtubules are observed in the center of the interzone/forming midbody; longer labeled segments are also present. However, incorporation in this telophase cell is much less extensive than in late anaphase cells incubated for similar post-injection intervals (compare Figure 2.2(g,h) with Figure 2.3). Astral microtubules are also labeled, frequently along their entire length (Figure 2.3).

When telophase cells are examined following somewhat longer post-injection incubation intervals, nearly complete labeling of astral microtubules is observed and increased incorporation into the midbody is detected. In Figure 2.4 a cell which was lysed 82 sec post-injection is shown; the total tubulin staining pattern shows intense staining of the forming midbody, and of astral microtubules extending from each pole. When the anti-biotin staining is observed, nearly all the astral microtubules are labeled along their entire length. Thus, within the 82 second incubation period, nearly complete turnover of the

entire astral array occurred. Biotin-tubulin is also detected in the forming midbody, but in contrast to the astral microtubules, the staining is much less intense than the corresponding total tubulin fluorescence. In this instance, because of the density of midbody microtubules, staining of individual microtubules is not apparent using conventional fluorescence optics. It is clear, however, that complete turnover of interzonal microtubules did not occur during this post-incubation interval, although astral microtubules in the same cell appear to have fully incorporated labeled subunits.

Telophase cells, injected and incubated for 1.5 to 2 minute intervals, have also been examined using confocal microscopy. Heterogenous incorporation of labeled tubulin into the bundles of interzonal microtubules is observed: some bundles are unlabeled while other are labeled to various extents (data not shown). With progressively longer incubations (3-5 minutes), nearly all of the bundles of interzonal microtubules become labeled. Because of the close proximity of microtubules in these bundles, it is not possible to determine whether all the microtubules in a bundle incorporate biotin-tubulin at these longer time points.

Quantitative Analysis of Interzonal Microtubule Assembly

The results described above indicated that time-dependent changes in the assembly of microtubules in the interzone occur during spindle elongation. To further examine these changes, the extent of biotin-tubulin incorporation has been quantified from complete Z-series of images through each cell, acquired using confocal microscopy (see Methods). Using this technique, individual fluorescent fibers can be detected in interzonal regions. Many of these fibers are judged to be single microtubules based on their similarity to fluorescent fibers in adjacent interphase cells (Osborn et al., 1978); other fibers are stained more intensely, and probably represent microtubules which were sufficiently close to each other that they could not be detected as two (see Sammak and Borisy, 1988). Anti-biotin stained segments appear thicker than the rhodamine staining of total microtubule polymer, due to the use of additional secondary antibodies (see Methods) and are continuous with

thinner rhodamine labeled microtubules. Because microtubule ends are distributed throughout the interzonal region during these cell stages, and because these cells have been analyzed at very short times post-injection, most biotin segments occupy a unique location at the end of rhodamine-labeled microtubule segment, and therefore are considered to represent individual microtubules. Only cells which were lysed within 65 seconds of injection have been used for this quantification, as microtubules in cells incubated for longer periods are difficult to distinguish accurately. In cells which were fixed before lysis or fixed and lysed simultaneously (Geuens et al., 1989), individual microtubules and segments of biotin labeled microtubules are much more difficult to detect, even in the confocal microscope, due to the superimposition of the more numerous microtubules and the higher background staining.

The extent of new microtubule polymerization from mid-anaphase through late telophase has been quantified by measuring the length of all biotin-labeled polymer in the interzone per cell; these measurements have been normalized with respect to the post-injection incubation interval. Cells were lysed and rinsed in saline before fixation as described in Methods. Two examples of late anaphase PtK1 cells injected with biotin-tubulin, lysed and examined by confocal microscopy are shown in Figure 2.5. Merged images in which anti-tubulin staining appears in dark grey and anti-biotin fluorescence in white or light grey are shown. Short segments of biotin-tubulin containing microtubules, which are continuous with non-biotin containing microtubules, are seen in the interzonal region. Measurements of the total biotin-labeled microtubule polymer per cell demonstrate that incorporation of biotin-tubulin into interzonal microtubules increases from mid- to late anaphase and decreases sharply as cells progress into telophase (Figure 2.6). Approximately 5 times more labeled polymer is present in the interzone in late anaphase cells than in telophase cells (Figure 2.6). When the number of labeled microtubules/cell are examined a similar pattern is found, with the maximal number of labeled microtubules present in late anaphase cells (data not shown). These quantitative data support the

qualitative observations of injected cells and demonstrate that maximal incorporation into interzonal microtubules occurs during late anaphase.

Because the lysis conditions used in these experiments remove labile microtubules, the extent of total biotin-tubulin incorporation into interzonal microtubules has also been quantified for cells lysed more gently (control cells, see Methods). In these cells, the total length of biotin-labeled polymer is greater than in cells lysed and rinsed in saline for mid-anaphase, late anaphase and telophase cells. However, both the pattern of biotin-tubulin incorporation (compare Figure 2.1 and 2.2 with Figure 2.5) and the changes in extent of incorporation throughout anaphase (data not shown) are very similar for cells lysed by both methods. Examination of microtubule length histograms further reveals a very similar distribution of microtubule lengths in cells lysed by either method (Figure 2.7, late anaphase) and for all other stages examined (data not shown). However, quantitative measurements are more reproducible in cells both lysed and saline rinsed because of the decreased density of microtubules which facilitates the tracking of labeled segments through successive optical sections.

The average rate of interzonal microtubule polymerization has also been measured from mid-anaphase through telophase for the cells quantified for Figure 2.6 (see Methods). The average, measured rates of microtubule growth are 3.1 ± 0.4, 3.9 ± 0.9 and 2.8 ± 0.5 μm/min for cells in mid-anaphase, late anaphase and telophase, respectively. Similar rates are obtained for cells fixed immediately after lysis (data not shown). Because the measured rate of microtubule growth does not vary for interzonal microtubules from mid-anaphase through telophase, it is likely that the extent of microtubule polymerization is regulated independently of the rate of microtubule growth in these cells.

The measured rate of microtubule growth has also been examined as a function of post-injection incubation interval. The average microtubule growth rate is greatest when cells are examined just after injection. Average rates of up to 5.5 μm/min are measured at the earliest time points examined; values reported here correspond to rates measured

following an average post-injection incubation interval of 43 sec. These values are likely to underestimate the actual rate of microtubule elongation because the average behavior of the population of microtubules is measured. Thus, although some individual microtubules could elongate for the entire post-injection interval, others could elongate for only a portion of this interval or could begin rapid shortening, both of which would decrease the average measured elongation rate (Mitchison and Kirschner, 1984). None the less, it is important to note that the average microtubule polymerization rate measured here is greater than the rate of pole-pole separation in these cells (3.9 μm/min vs 0.9 μm/min, respectively).

Discussion

The results of these experiments provide the first direct visualization of plus-end elongation of individual interzonal microtubules in PtK_1 cells during spindle elongation. Biotin-labeled segments are located at the distal or plus-ends (Euteneuer and McIntosh, 1980) of unlabeled microtubules in the interzonal region. Plus-end dependant incorporation is observed from mid-anaphase through telophase, at short times after injection. With longer post-injection incubations the growth of individual microtubules becomes increasingly difficult to detect and microtubules found in the interzonal region are uniformly labeled, at the resolution of the light microscope.

The rapid incorporation of biotin-tubulin into interzonal microtubules could occur by de novo nucleation of new interzonal microtubules, by treadmilling or poleward flux along existing microtubules, by dynamic instability, or by some combination of these methods. Examination of Figure 2.2(c-d) shows that at early times post-injection, many unlabeled interzonal microtubules are present in the interzone. At slightly later times nearly all spindle microtubules have incorporated biotin-tubulin (Figure 2.2(g-h)). De novo nucleation of interzonal microtubules cannot account for the conversion of existing unlabeled microtubules to labeled as microtubules seen in Figure 2.2.

Treadmilling and/or poleward flux along existing microtubules could account for the conversion of unlabeled microtubules to labeled microtubules shown in Figure 2.2. However, no evidence of a uniform wave of incorporation, as might be produced by synchronous treadmilling of spindle microtubules was detected. Examination of the pattern of incorporation at short time points post-injection reveals unlabeled, partially labeled, and fully labeled microtubules in the interzonal region and reveals that the junctions between labeled and unlabeled microtubule segments are dispersed throughout the interzone. In addition, measurement of the extent of biotin-tubulin incorporation at the plus-ends of individual microtubules indicate that interzonal microtubules elongate at an average rate of approximately 3 μm/min, and clearly demonstrate that these microtubules can incorporate labeled subunits at rates up to 10 μm/min (see Figure 2.2(d)). These values are in contrast to the much slower rates observed for poleward flux in vivo (0.6 μm/min; Mitchison, 1989) and the rates of treadmilling observed in vitro for MAP rich and MAP depleted microtubules (0.01 and 0.9 μm/min, respectively; Farrel et al., 1987). Therefore, microtubule behavior in the interzone during anaphase B elongation is greatly different from previous observations of microtubules undergoing subunit flux or treadmilling.

The rapid incorporation of biotin-tubulin detected throughout the interzonal region could occur by microtubule dynamic instability behavior (Mitchison and Kirschner, 1984). In this model, most microtubules continually elongate, while a subset rapidly or catastrophically disassembles. Microtubules can be rescued from the rapid shortening phase, or if disassembly is complete, can be renucleated from the centrosome (Mitchison and Kirschner, 1984). Thus, a population of microtubules will contain both growing and shortening microtubules. Dynamic instability behavior has been directly observed in living interphase (Cassimeris et al. 1988; Sammak and Borisy, 1988; Schulze and Kirschner, 1988), and mitotic prometaphase newt lung cells (C.L. Rieder, personal communication). Measurements of dynamic instability in vivo further reveal that microtubules are capable of rapid assembly and disassembly (average rates of 7.2 ± 0.3 and 17.3 ± 0.7 μm/min,

respectively Cassimeris etal., 1988). Therefore, dynamic instability of microtubules provides the best explanation for the rapid and heterogenous incorporation of labeled tubulin and the conversion of unlabeled to fully labeled microtubules seen in the experiments presented here.

Biotin-tubulin incorporation is also detected in the asters of injected cells. Both elongation of existing astral microtubules and nucleation of new microtubules from the centrosome are observed. The extent of astral microtubule labeling has not been quantified due to the difficulty in measuring the highly three dimensional astral microtubule array. However, qualitative comparison of the extent of incorporation into astral and interzonal microtubule arrays during telophase demonstrates that astral microtubules are more dynamic than interzonal microtubules at this time. Finally, little label is detected in the region of the kinetochore fibers of late anaphase cells, consistent with previous observations that kinetochore fiber microtubules become refractory to turnover as anaphase progresses (Wadsworth et al., 1989).

Quantitative measurements of the incorporation of biotin-tubulin reveal that incorporation increases from mid- to late anaphase, and diminishes as cells progress into telophase. Several factors could contribute to the increase in incorporation from mid- to late anaphase. The disassembly of KMTs during anaphase could cause an increase in free tubulin concentration and stimulate microtubule assembly. Alternatively, more microtubule plus ends may become available for polymerization in this region, perhaps due to the movement of the chromosomes out of the interzone and/or local changes in cellular physiology which might stimulate microtubule growth. It should be noted that the increase in incorporation may not be the result of an increase in the total number of interzonal microtubules, as previous electron microscopy studies have measured a gradual decline in the number of interzonal microtubules from early anaphase through telophase (McIntosh et al., 1975).

The decreased biotin-tubulin incorporation observed as cells enter telophase may be due to the increase in microtubule bundling. Interactions between microtubules, mediated by microtubule associated proteins (MAPs), may suppress microtubule dynamic behavior and thereby decrease the extent of incorporation of labeled subunits. The observation that MAPs decrease microtubule dynamics in vitro (Pryer, 1989) supports this possibility. An alternative explanation is that the injected labeled tubulin is somehow excluded from microtubule bundles. While this possibility cannot be formally ruled out, it should be noted that the injected labeled tubulin and secondary antibodies are not excluded from the central region of the midbody of telophase cells in the experiments described here (Figures 2.3, 2.4), as has been previously observed for cells at later stages of mid-body formation. In addition, other experiments, using fluorescent tubulin and photobleaching methods (Saxton and McIntosh, 1987) in living cells, provide evidence that interzonal microtubule turnover is reduced when microtubules are bundled. In these previous experiments, cells were injected with labeled tubulin prior to anaphase and allowed to equilibrate; thus all the microtubules became uniformly labeled before microtubule bundling had occurred (Saxton and McIntosh, 1987). These photobleaching results and the data presented in the current study strongly suggest that microtubule dynamics are greatly reduced within the midbody of telophase cells.

It is unlikely that the time dependent changes in incorporation revealed by the experiments presented in this study are due to perturbation caused by the injection of exogenous tubulin (Schulze and Kirschner, 1986). If incorporation of biotin-tubulin is due to a perturbation, then all cells would be expected to incorporate similar amounts of biotin-tubulin into all classes of microtubules. Instead, stage specific changes in the extent of incorporation into the interzone are observed, and different classes of microtubules in the same cell show different extents of incorporation (Figures 2.3 and 2.4; Saxton and McIntosh, 1987). Furthermore, the rate of anaphase B motion is not altered by injection,

providing additional evidence that cells are not perturbed by the injection of biotin-tubulin during these experiments.

In order to quantify the incorporation of biotin-tubulin into interzonal microtubules in these cells, it was necessary to briefly rinse cells in saline following lysis in a detergent containing solution. The quantitative methods used in the present study are therefore valid only if the loss of microtubules during the saline rinse is random and relatively constant from mid-anaphase through telophase. To examine this possibility, the extent of incorporation of biotin-tubulin into microtubules in cells lysed and rinsed in saline and cells lysed but not saline rinsed (see Methods) have been compared. In both cases, similar patterns of tubulin incorporation (compare Figures 2.2(d) and 2.5), rates of microtubule elongation and microtubule length distributions are observed. If the loss of microtubules in the more highly extracted cells is due to a gradual shortening of all the microtubules during lysis, then one would expect a marked shift in the microtubule length distribution and growth rate as compared with more gently lysed cells. Since this is not observed (Figure 2.7), loss of microtubules under these conditions is likely to be random. Lysis might also select for more stable microtubules, however, biotin-tubulin incorporation into spindle microtubules at long time points post-injection is complete or nearly complete in both highly extracted and more gently lysed late anaphase cells (data not shown). Therefore, no sub-class of stable microtubules refractory to tubulin incorporation is seen in late anaphase by either method.

Although it is not possible to directly determine if the number of interzonal microtubules lost during lysis is influenced by the stage of mitosis, it should be noted that microtubules become bundled and are more resistant to depolymerization during lysis as anaphase progresses. The quantitative results presented here reveal a decrease in biotin-tubulin incorporation in telophase cells, even though a greater fraction of the endogenous microtubules may potentially be preserved in these cells. This suggests that changes in the

extent of incorporation seen in these experiments are not simply due to variations in the number of microtubules present in the interzone at different stages of the cell cycle.

The results of this study have several implications for the mechanism of anaphase B. Observations on the diatom central spindle and telophase PtK_1 spindles have led to a model for anaphase B in which interdigitated microtubules from opposite half-spindles slide apart, presumably due to mechanochemical motors acting within the interzone (Masuda and Cande, 1987; Saxton and McIntosh, 1987). The rapid turnover of interzonal microtubules during spindle elongation revealed by the experiments reported here places constraints on sliding models and further suggests a new role for microtubule polymerization in pole-pole separation.

Recent observations indicate that a dynamic population of astral microtubules can exert "polar ejection forces", which may contribute to chromosome orientation during prometaphase and exclude material from the spindle pole (Bajer, 1982; Rieder et al., 1986; Salmon, 1989). It is possible that dynamic arrays of astral microtubules at opposing poles could push each other apart during spindle elongation. This model predicts that inhibition of microtubule dynamics will prevent spindle elongation and suggests that some microtubule-microtubule interactions in the interzone may govern, rather than produce, pole separation (Aist and Berns, 1981; Kronebusch and Borisy, 1982).

Previous photobleaching experiments on telophase cells have revealed antiparallel sliding of interzonal microtubules. However, most pole-pole separation has already occurred in telophase cells and the contribution of sliding at earlier stages remains to be measured. The data presented in this study indicate that microtubules are most dynamic, as measured by the ability to incorporate labeled tubulin, during late anaphase, when rapid pole-pole separation occurs. As interzonal microtubules become more bundled in telophase, microtubules become less dynamic, as evidenced by the decrease in incorporation of labeled tubulin and the slow rate of FRAP (Saxton and McIntosh, 1987). The decrease in dynamics occurs coordinately with a ten fold change in the average rate of

pole-pole separation in these cells (0.9 μm/min for late anaphase cells (this report) and 0.09 μm/min for telophase cells (Saxton and McIntosh, 1987)). Thus, if sliding interactions produce pole-pole separation in late anaphase, either the interactions must be of short duration, or a small subset of stable interzonal microtubules, which are not detected in the present study, are responsible for force generation. It is possible that a cell must rapidly and continually nucleate microtubules from each pole to create a few antiparallel microtubule interactions which produce sliding, much as many microtubules are nucleated from the centrosome to ensure kinetochore fiber formation. Interestingly, the decrease in rate of pole-pole separation seen as microtubule bundling occurs during telophase suggests that pole separation and microtubule bundling are antagonistic processes and may therefore involve different MAPs.

Conclusion

In summary, these experiments reveal plus-end elongation of individual interzonal microtubules, and nucleation and growth of astral microtubules, during spindle elongation in PtK_1 cells. The results of these experiments reveal that interzonal microtubules are highly dynamic during spindle elongation. Quantitative measurements of the extent of incorporation demonstrate time-dependent changes in the incorporation of labeled tubulin during spindle elongation, with maximal incorporation of tubulin detected during anaphase B spindle elongation.

Figure 2.1.

A mid-anaphase PtK_1 cell which was injected with biotin-tubulin and processed for immunocytochemistry using anti-tubulin (a) and anti-biotin (b) antibodies. The cell was injected in mid-anaphase and incubated for 60 sec prior to lysis. The total tubulin staining (a) reveals fluorescence of the astral, interzonal and kinetochore fiber microtubules. In the biotin stained image (b) labeling is detected in the interzonal region and in the aster. Bar = 10 μm.

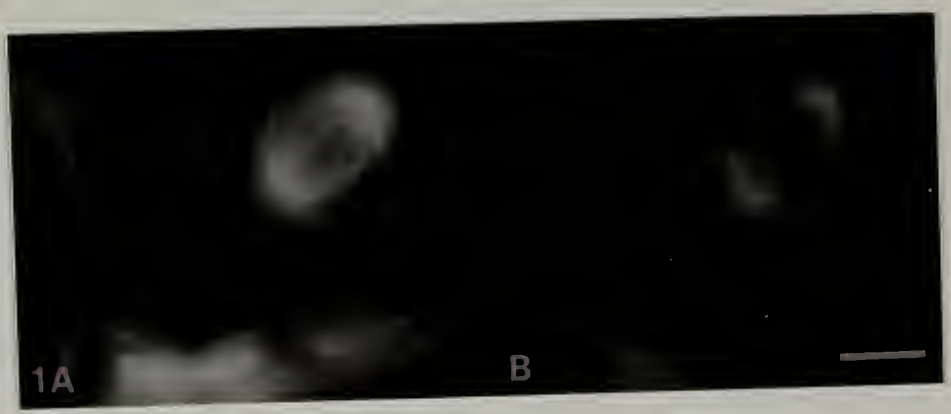
1A
B

Figure 2.2.

Phase and confocal micrographs of late anaphase PtK_1 cells injected with biotin-tubulin. Cells were incubated for 30 (a-d) and 67 (e-h) sec prior to lysis. Anti-tubulin staining is shown in (c,g); the corresponding anti-biotin is shown in (d,h). For the cell shown in (a-d), phase micrographs were taken just after injection (a) and just after lysis (b), using a 32x phase objective lense. The cell shown in (c,g) was photographed just after injection (e) and just before lysis (f). Bar = 5 μm.

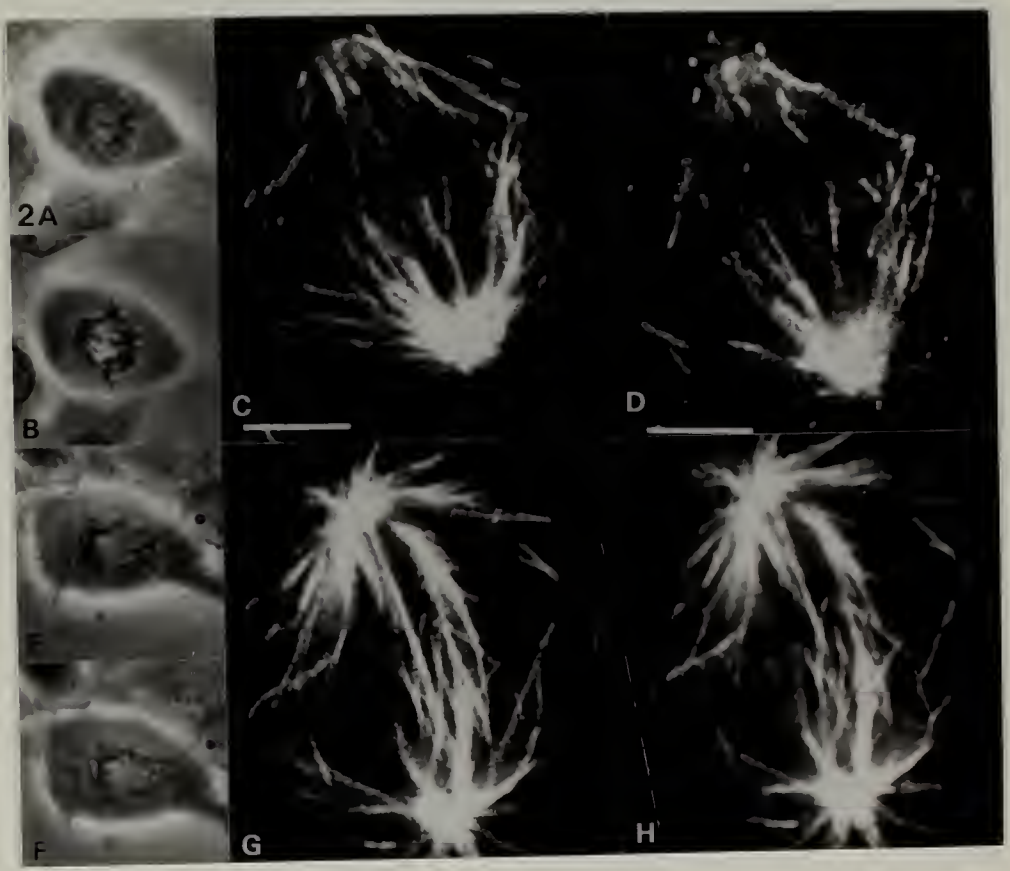
2A
B
C
D
E
F
G
H

Figure 2.3.

Confocal micrograph of a telophase cell injected with biotin-tubulin, incubated for 55 sec prior to lysis and stained with anti-biotin antibodies. A single optical section through the cell is shown. Biotin-tubulin has incorporated into the central region of the mid-body and into the asters (not in focus in this optical section).

Figure 2.4.

A telophase PtK_1 cell injected with biotin-tubulin and incubated for 82 sec prior to lysis; two different focal planes from the conventional fluorescence microscope are shown. (a,c) Anti-tubulin, (b,d) anti-biotin. Nearly all the astral microtubules have completely incorporated biotin-tubulin (compare a and b). Some biotin-tubulin fluorescence is also detected within the midbody (d) but is less intense than the total tubulin staining pattern (c). Bar = 10 μm.

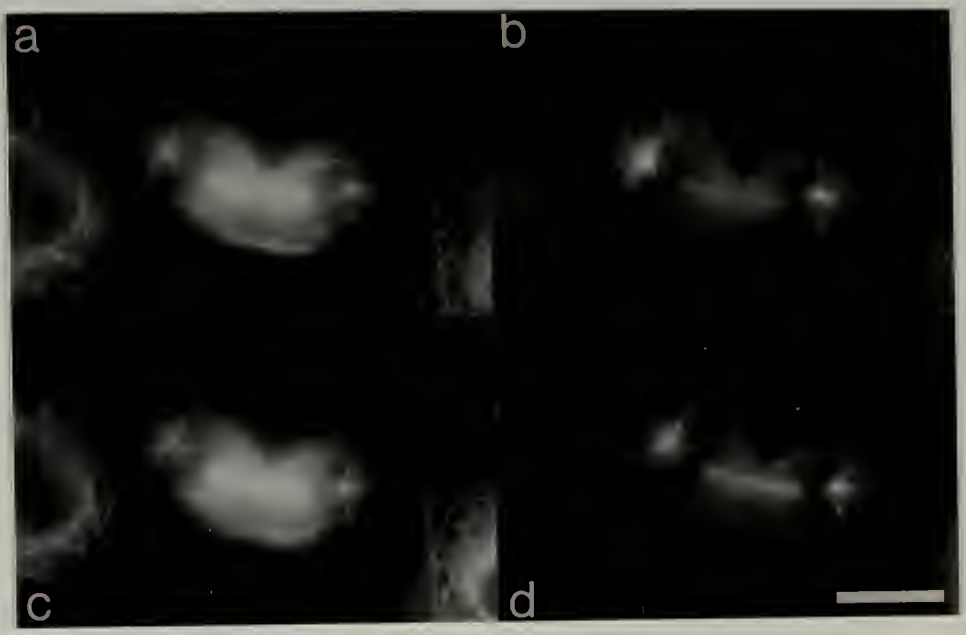
a
b
c
d

Figure 2.5.

Confocal micrographs of late anaphase PtK_1 cells injected with biotin-tubulin. Merged images of anti-tubulin staining (dark grey) and anti-biotin staining (white/light grey) are shown. The cells were incubated for 53 (a) and 58 (b) sec prior to lysis. In (a) a single section through the cell is shown, in (b) all the optical sections of the cell are shown simultaneously to reveal the total biotin labeling pattern. Biotin-tubulin incorporation at the ends of interzonal microtubules is detected. Bars = 10 μm.

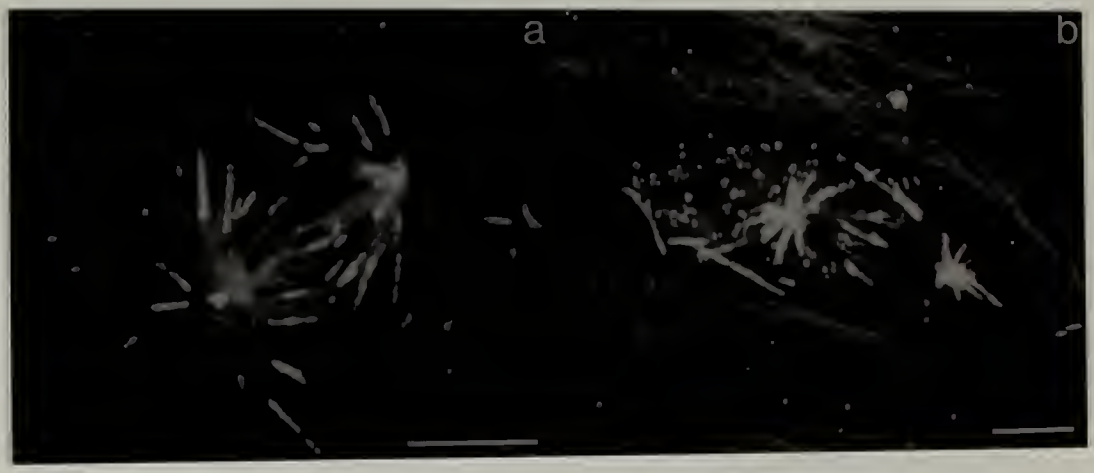
a
b

Figure 2.6.

Total labeled interzonal polymer/cell/min. The total labeled polymer (μm) was determined by measuring the total length of all biotin-labeled segments in the interzonal region for each cell; these values were normalized with respect to the injection interval. The stage of mitosis was determined from the cellular and chromosomal morphology.

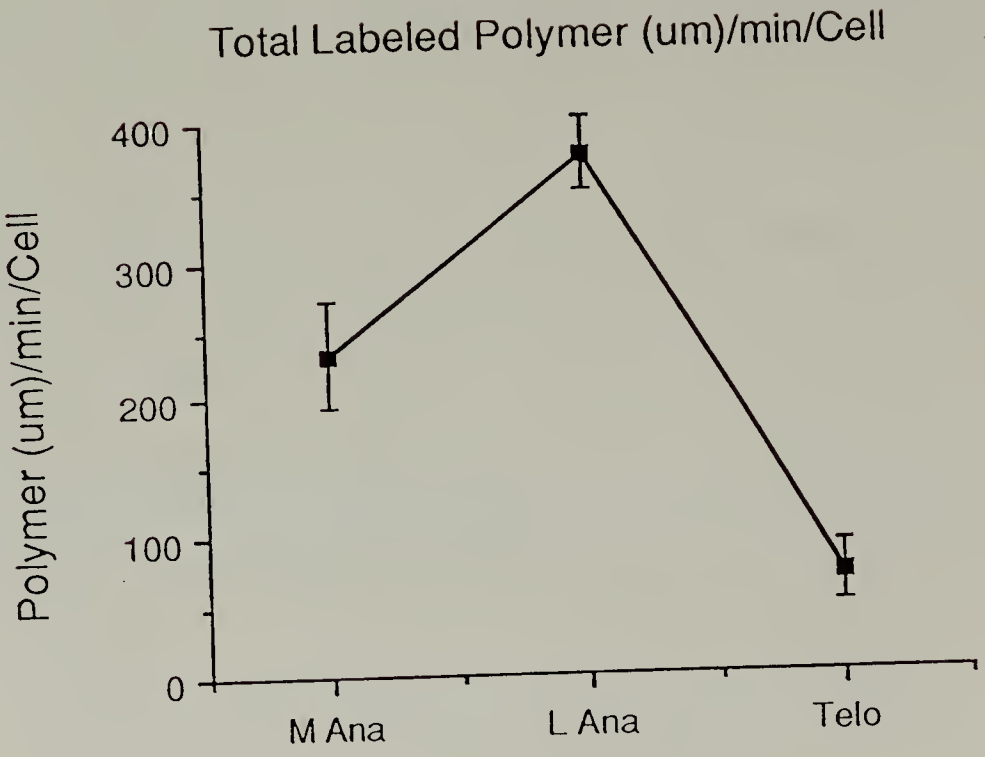
Total Labeled Polymer (um)/min/Cell
Polymer (um)/min/Cell
400
300
200
100
0
M Ana
L Ana
Telo

Figure 2.7.

Microtubule length histograms for cells lysed with and without a 50 sec rinse in saline. A late anaphase cell lysed in detergent (hatched bars) and a late anaphase cell lysed in detergent and further rinsed in saline (solid bars) are shown. Both cells were lysed 30 seconds after injection with biotin-tubulin and microtubule lengths were quantified as described in Methods. The length histograms are the average of 2 (solid bars) and 4 (hatched) repetitions of quantification.

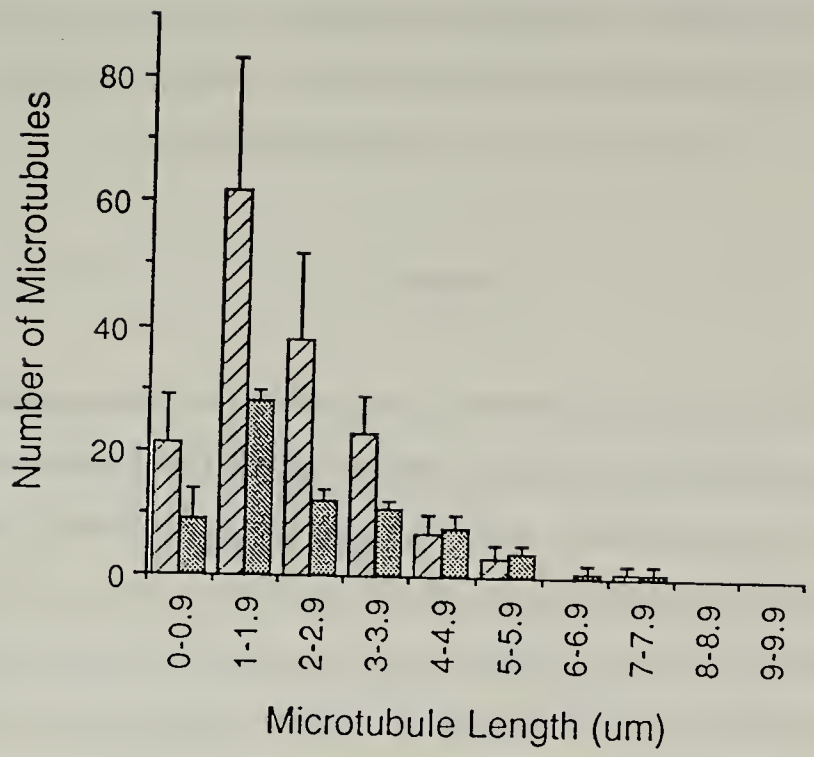
Number of Microtubules
80
60
40
20
0
0-0.9
1-1.9
2-2.9
3-3.9
4-4.9
5-5.9
6-6.9
7-7.9
8-8.9
9-9.9
Microtubule Length (um)

CHAPTER 3

MICROINJECTION OF BIOTIN-TUBULIN INTO ANAPHASE CELLS INDUCES TRANSIENT ELONGATION OF KINETOCHORE MICROTUBULES AND REVERSAL OF CHROMOSOME-TO-POLE MOTION

Abstract

During prometaphase and metaphase of mitosis, tubulin subunit incorporation into kinetochore microtubules occurs proximal to the kinetochore, at the plus-ends of kinetochore microtubules. During anaphase, subunit loss from kinetochore microtubules is also thought to occur mainly from microtubule plus-ends, proximal to the kinetochore. Thus, the kinetochore can mediate both subunit addition and loss while maintaining an attachment to kinetochore microtubules. To examine the relationship between chromosome motion and tubulin subunit assembly in anaphase, anaphase cells have been injected with biotin-labeled tubulin subunits. The pattern of biotin-tubulin incorporation has been revealed using immunoelectron and confocal fluorescence microscopy of cells fixed after injection; chromosome motion has been analyzed using video records of living injected cells. When anaphase cells are examined approximately 30 seconds following injection with biotin-tubulin, bright "tufts" of fluorescence are detected proximal to the kinetochores. Electron microscopic immunocytochemistry further reveals that these tufts of biotin-tubulin containing microtubules are continuous with unlabeled kinetochore fiber microtubules. Biotin-tubulin incorporation proximal to the kinetochore in anaphase cells is detected following injection of 3-30 mg/ml biotin-tubulin, but not in cells injected with 0.3 mg/ml biotin-tubulin. At intermediate concentrations of biotin-tubulin (3-5 mg/ml), incorporation at the kinetochore can be detected within 15 seconds post-injection; by approximately 1 min

post-injection discrete tufts of fluorescence are no longer detected, although some incorporation throughout the kinetochore fiber and into non-kinetochore microtubules is observed. Incorporation of biotin-tubulin proximal to the kinetochore can be detected in cells injected during anaphase A, but not during anaphase B. Analysis of video records of microinjection experiments reveals that kinetochore proximal incorporation of biotin-tubulin is accompanied by a transient reversal of chromosome-to-pole motion. Chromosome motion is not altered following injection of 0.3 mg/ml biotin-tubulin or 5 mg/ml BSA. These results demonstrate that kinetochore microtubules in anaphase cells can elongate in response to the elevation of the tubulin concentration and that kinetochores retain the ability to mediate plus-end dependent assembly of KMTs and plus-end directed chromosome motion after anaphase onset.

Introduction

During mitosis, the motion of chromosomes is mediated by kinetochore microtubules (KMTs), which are attached at their plus, or fast growing, ends to the kinetochore (Euteneuer and McIntosh, 1981). During prometaphase, KMTs must increase in length during motion of the chromosome away from the spindle pole, and shorten during motion toward the spindle pole; during anaphase chromosomes move to the poles as KMTs shorten. In vivo experiments demonstrate that shifting the equilibrium between microtubule assembly and disassembly can induce changes in chromosome motion. For example, microtubule disassembly, induced by the treatment of metaphase cells with microtubule depolymerizing agents such as cold or high hydrostatic pressure (Inoue, 1976; Salmon, 1976), has been shown to cause reversible motion of chromosomes toward an attached spindle pole. Additional experiments on anaphase cells reveal that anaphase chromosome motion can be reversed when microtubule assembly is induced by the addition

of taxol (Bajer et al., 1982). Using these approaches, however, sites of microtubule assembly and disassembly could not be identified and correlated with chromosome motion.

To address this issue, several laboratories have performed experiments in which modified tubulin subunits have been injected into prometaphase and metaphase cells and subsequently localized in fixed cells. The results of these experiments demonstrate that an increase in length of the kinetochore fiber during motion of chromosomes away from the spindle pole occurs by addition of tubulin subunits at the plus-end of the kinetochore fiber microtubules, proximal to the kinetochore (Mitchison et al., 1986; Geuens et al., 1989; Wise et al., 1991). Controversy exists over the site of KMT subunit loss during prometaphase. Some experiments (Wise et al., 1991), indicate that loss of subunits can occur at the kinetochore during prometaphase. In contrast, photoactivation of modified tubulin has provided evidence for subunit loss at the pole or minus-ends of KMTs during metaphase in vivo (Mitchison, 1989). However, the rate of minus-end subunit loss calculated from these photoactivation experiments was significantly slower than the velocity of chromosome oscillations seen in the same cells. Thus, loss of tubulin subunits at the pole cannot fully account for normal oscillatory chromosome motion, and it is likely that both subunit addition and subunit loss can occur at the kinetochore in metaphase.

During anaphase, the motion of mitotic chromosomes is predominantly minus-end directed, although brief, asynchronous oscillations of chromosomes away from the pole during anaphase have been observed in diverse cells (Aist and Bayles, 1988; Bajer, 1982). Experiments conducted in vivo demonstrate that the majority of tubulin subunit loss during KMT shortening in anaphase is at the kinetochore (Gorbsky et al., 1988). Thus, the transition between metaphase and anaphase is accompanied by a change from bi-directional chromosome motion to predominantly minus-end directed motion and from both addition and loss of tubulin subunits to predominantly loss of subunits at the kinetochore.

Despite its importance, the mechanism by which kinetochores remain attached to MTs during KMT length changes remains unknown. Recently, however, in vitro assays of

kinetochore function have begun to examine the interaction between kinetochores and MTs under defined conditions. For example, MTs containing a stable, labeled minus-end have been shown to translocate away from an isolated kinetochore by insertion of tubulin subunits at the microtubule plus-ends, proximal to the kinetochore (Hyman and Mitchison, 1990; Mitchison and Kirschner, 1985(a,b)). Others (Koshland et al., 1988; Hyman and Mitchison, 1990; Coue et al., 1991), have further demonstrated that isolated kinetochores can remain attached to MTs that are induced to shorten by dilution of the tubulin subunit pool. Thus, kinetochores in vitro can provide useful models of in vivo kinetochore function.

In the experiments described here, the assembly of KMTs and the motion of chromosomes in anaphase cells have been examined following microinjection of biotin-labeled tubulin. The results of these experiments demonstrate that the increase in cytosolic tubulin concentration following injection can induce assembly of KMTs at their kinetochore proximal ends and transiently reverse anaphase chromosome-to-pole motion. These experiments demonstrate that kinetochores in anaphase cells retain the ability to mediate chromosome motion away from the spindle pole. Further, these results reveal for the first time that kinetochores do not prevent tubulin subunit addition at KMT plus-ends after anaphase onset. These observations therefore reveal that KMT shortening in vivo is not accomplished simply by the inhibition of KMT polymerization as has been suggested (Hyman and Mitchison, 1990, 1991) and further suggest that tubulin concentration may regulate kinetochore behavior during mitosis.

Materials and Methods

Preparation of Biotin-Tubulin

Biotin-tubulin was prepared as described previously (Mitchison et al., 1986; Wadsworth et al., 1989). Small aliquots were stored at -70^{o}C in injection buffer (20 mM

sodium glutamate, 1 mM EGTA and 0.5 mM $MgSO_4$, pH 7.2). Before use, the protein solution was made 1 mM in GTP and centrifuged for 10 min at maximum speed in an Eppendorf microcentrifuge. The biotin-tubulin concentration was determined by a modification (Schacterle and Pollack, 1973) of the method of Lowry (Lowry et al., 1951).

Cell Culture and Microinjection

PtK_1 cells were grown at 37°C in Ham's F-12 medium supplemented with 10% fetal bovine serum, 10 mM HEPES and antibiotics. Cells were plated on glass coverslips and allowed to grow for 36-48 hours before use. Coverslips were then placed in a laboratory constructed microinjection chamber (Wadsworth et al., 1989), which was mounted on the stage of a Zeiss IM-35 microscope, and microinjected as described previously (Wadsworth et al., 1989). Temperature was maintained at 30° C using an Opti-Quip Red Beam Incubator calibrated with a YSI Telethermister. Cells analyzed for biotin-tubulin incorporation were photographed just after injection and again just after lysis using thirty-five millimeter film. For some experiments, in which cells were incubated longer than thirty seconds, the living cell was photographed after injection and just before lysis to record any change in chromosome position.

Immunofluorescence

Following microinjection, cells were lysed for approximately 50 sec in lysis buffer containing 80 mM PIPES, 5 mM EGTA, 1 mM $MgSO_4$ and 0.5% Triton X-100, pH 6.8 (Cassimeris et al., 1986). Cells were fixed for 25 minutes in 2% paraformaldehyde and 0.1% glutaraldehyde in PBS, pH 7.3 and rinsed in PBS containing 0.1% Tween and 0.02% azide (PBS-Tw-Az) and for 5 min in 1% sodium borohydride. Antibody incubations were performed in humid chambers at room temperature. Cells were incubated first with rabbit anti-biotin antibodies (Enzo Biochemicals, N.Y.) at a dilution of 1:50 in PBS-Tw-Az containing 1% BSA for 30 min, rinsed in PBS-Tw-Az and incubated with

fluorescein goat anti-rabbit and then fluorescein rabbit anti-goat antibodies. Cells were then incubated in a mouse monoclonal anti-tubulin antibody for up to 3 hours, followed by rhodamine goat anti-mouse antibodies. All fluorescent secondary antibodies were purchased from Cappel laboratories and used at a final dilution of 1:50 in PBS-Tw-Az containing 1% BSA, for 30 minutes at room temperature. Stained cells were mounted in 0.1% n-phenyldiamine in glycerol and sealed with nail polish.

Microscopy

For confocal microscopy, a BioRad MRC500 laser scanning head mounted on a Nikon optiphot microscope equipped with a 60X 1.4 NA objective lens was used. The confocal microscope was operated with the pinhole set for a section thickness of approximately 0.9 μm (Shelden and Wadsworth, 1990). Through-focus series of the rhodamine and fluorescein staining patterns were collected independently for each cell. 30 to 50 scans of the specimen were averaged to produce each image. Through-focus series of the rhodamine and fluorescein staining patterns were collected independently for each cell. Images were then digitally rescaled by making the lowest non-zero value black (a value of 0) and the highest pixel value white (a value of 255). This technique (contrast stretching) enhances the appearance of images by using the full range of grey-scale values to display each image. Multiple optical sections obtained from a through focus series were combined by displaying only the highest pixel value in the series at each screen location in the final image.

Pseudocolor Analysis of Images

A computer generated color look-up table was used to examine the changes in staining pattern at short and long times post-injection. The look-up table was generated on a Masscomp computer using locally written software and shows low pixel intensities in purple and blue, intermediate values in green and yellow, and high pixel values in red.

Images were contrast stretched before applying this look-up table. To further reveal changes in immunofluorescent labelling intensity, pixels in some images were vertically displaced to a new location based on intensity value (intensity mapping). Using this technique, regions of different intensities could be easily identified, as brighter pixels were displaced further vertically than less-bright pixels. Linear interpolation was used to fill any spacing which resulted from neighboring pixels being vertically displaced to non-neighboring locations in the new image. Finally, the look-up table described above was applied to these new images.

Electron Microscopy

The procedure used to prepare specimens for immunolocalization of biotin-labeled tubulin has been published previously (Wadsworth et al., 1989). Thin sectioned material was observed on a JEOL TEM100S operated at 60KV.

Video Recording of Injection Experiments

Cells used for video analysis of chromosome motion during injection were held in a Rose chamber (Rose et al., 1958) modified as follows. Coverslips containing PtK_1 cells were placed between two sheets of parafilm in which holes corresponding to the opening of the Rose chamber had been cut. The chamber was filled with medium and placed on a Zeiss IM 35 inverted microscope. Temperature was maintained at 30^{o} C using an Optiquip red beam incubator and a Nickolson Precision Instruments Air Stream Incubator to which flexible hoses were added to allow even heating of the injection chamber (McKenna and Wang, 1989). The red-beam incubator was shut off just before injection and the stage heated only from below using the air stream incubator. This technique reduced evaporation losses from the open injection chamber during the experiment. Temperature was measured using a YSI temperature monitor after injection. No cooling of the injection chamber was detected during these short (2-3 min) injection experiments. Microinjections were made

while observing cells with a Zeiss 63X 1.4 NA oil immersion lens using phase contrast optics. The specimen was illuminated with a Hoffman modulation contrast 0.5 NA (25mm working distance) phase condenser and a 100 watt mercury arc light source. Both heat and interference filters were placed between the illumination source and the cells. Although efforts were made to reduce evaporation losses during the course of observation, cells held in the injection chamber for long periods of time appeared to suffer light and/or heat stress during initial experiments. Only cells which had been found, observed and injected within a few minutes of being placed upon the microscope stage could be used for further analysis. To alleviate these problems, the chamber was subsequently modified by the addition of a cover fashioned from clear acetate. This cover was carefully removed prior to injection and replaced immediately after injection. This technique significantly extended the time over which cells could be observed on the microscope stage. Video sequences were recorded using a Dage MTI Newvicon video camera (model 67M). Images were background subtracted and contrast stretched using a Hughes Aircraft Co. image processor (model 794) before being stored on 3/4 inch video tape using a Sony video recorder (model VO-5800H).

Data Analysis

Video sequences were processed using a three frame running average, contrast enhanced, and digitized in real time using a Masscomp computer. For cells in which a reversal of chromosome-to-pole motion could be detected, rates of chromosome motion were measured before reversal, during the period of reversal, and after recovery of chromosome-to-pole motion. For cells in which no reversal could be detected, rates of chromosome motion were measured before injection, for thirty seconds after injection, and for up to two minutes following this thirty second post-injection interval. Mouse button commands were used to freeze individual frames from the video sequence. The time at which each image was obtained was automatically recorded in a data file. A mouse driven

cursor was placed on the screen and used to mark the kinetochore region of two sister chromatids. The distance in pixel units between these two points was recorded by the computer in the same data file as the time measurements. This procedure was repeated successively for the length of the video sequence. The video sequence was then re-started and the procedure repeated for the next pair of sister chromatids, and so on. Lengths were converted from pixel units to microns using pixel/micron ratios obtained by imaging a slide micrometer. The resulting data sets were graphed with a Macintosh computer. Linear regression analysis of these data was used to determine rates of chromosome motion.

Small changes in the motion of individual chromosomes are under estimated using the technique described above, as chromosome motion is measured as a function of the distance between pairs of chromosomes. In addition, both sister chromatids rarely remained in the plane of focus during the entire observation period, making the accurate localization of more than one chromosome throughout the video sequence extremely difficult. To address these problems, the motion of individual chromosomes was quantified using a second method. For this analysis, images were displayed and recorded as described above. The first point recorded was a reference point chosen to lie both behind the chromosome being analyzed and on a line containing the spindle pole and the kinetochore region. Instead of measuring the distance between separating chromosomes, the location of an individual kinetochore region was then recorded in the data file. A computer program calculated the distance between the original reference point and the position of the kinetochore region. This approach enabled nearly twice as many measurements of chromosome location to be made as the first method, as only one point per image was marked. Furthermore, this method was much more sensitive to small changes in chromosome motion, and could more accurately measure rates of motion for individual chromosomes. Unfortunately, the reference point could not be changed during the course of a video sequence, so only cells in which the spindle did not rotate or change position could be analyzed using this method.

The mitotic stage of injected cells was determined as described previously (Shelden and Wadsworth, 1990). The number of kinetochore proximal tufts of incorporation was determined for cells incubated for 40 seconds or less post-injection by displaying each image of a cell's through focus series on a video monitor. Clear acetate sheets were placed over the video monitor, and the location of any tufts of incorporation were marked on the acetate sheet. The number of tufts/cell for anaphase A (mid and late) and anaphase B cells was counted, and the average number of tufts/cell for each cell stage was then compared using a two-tailed t test.

Results

Incorporation of Biotin-tubulin into Anaphase Cells

When anaphase PtK_1 cells are microinjected with biotin-tubulin (3-5.5 mg/ml in the injection pipette) and immunostained to localize biotin-tubulin and total tubulin, an unexpected biotin-tubulin staining pattern is observed (Figure 3.1). When examined at approximately 30 sec post-injection, bright segments of biotin-tubulin fluorescence are detected proximal to the kinetochore - - presumably the site of subunit loss in anaphase cells (Gorbsky et al., 1988). Comparison of the biotin-tubulin and total tubulin staining patterns (Figure 3.1(a) and (b), respectively) reveals that these "tufts" of anti-biotin stained microtubules co-localize with the plus-ends of KMTs (arrows, Figure 3.1(a)). Anti-biotin stained microtubule segments are also detected in the spindle aster and interzone.

While the immunofluorescent staining pattern reveals that biotin-tubulin can incorporate at the kinetochore proximal end of kinetochore fibers in anaphase, it is not possible, given the resolution limit of the light microscope, to determine if labeled microtubule segments are continuous with pre-existing KMTs, or instead represent new nucleation of MTs at unoccupied sites on the kinetochore plate. To resolve this issue, cells have been injected with 5.5 mg/ml biotin-tubulin and processed for electron microscopic

immunocytochemistry. Examination of injected cells reveals that the biotin-tubulin containing KMT segments are continuous with unlabeled KMT segments (Figure 3.2). Thus, kinetochore proximal incorporation of biotin-tubulin does not occur by nucleation at unoccupied sites at the kinetochore but represents elongation at the plus-ends of existing KMTs.

Immunofluorescent staining of cells injected with biotin-tubulin has been used to further characterize the conditions under which biotin-tubulin incorporates into kinetochore fiber microtubules at their plus-ends during anaphase. First, the incorporation of biotin-tubulin proximal to the kinetochore in mid-anaphase cells has been examined as a function of the concentration of injected biotin-tubulin. When cells are injected with low concentrations of biotin-tubulin (0.3 mg/ml), little or no staining of KMTs is detected at 30 seconds post-injection (Figure 3.3(a)), although dim staining of non-KMTs is occasionally observed (not shown). Higher concentrations of injected biotin-tubulin (3-30 mg/ml) produce prominent kinetochore proximal "tufts" of biotin-tubulin incorporation after similar post-injection intervals (Figure 3.3(b,c)). The intensity of kinetochore proximal staining was somewhat greater in cells injected with biotin-tubulin at concentrations higher than 3 mg/ml (Figure 3.4(c), 30 mg/ml), but, given the limitations of the light microscope, it could not be determined if these higher concentrations of biotin-tubulin induced longer lengths of kinetochore proximal incorporation after similar injection intervals (see Figure 3.7 for longer post-injection intervals). In general, the number of kinetochore proximal tufts/cell and the overall pattern of incorporation were similar in cells injected with 3 or 30 mg/ml biotin-tubulin and examined 20-40 seconds post-injection (for example, compare Figure 3.3(b) and 3.3(c)).

The time course of biotin-tubulin incorporation proximal to the kinetochore has been examined in cells injected with 3.0-5.5 mg/ml of biotin-tubulin. Kinetochore-proximal tufts are detected by approximately 15 sec post-injection (the minimum amount of time required to inject, photograph and lyse a cell) (Figure 3.3(d)), but are less pronounced

than tufts in cells incubated for approximately 30 sec (Figure 3.3(b,e)). With further increases in post-injection incubation time, kinetochore fibers appear uniformly labeled using light microscopy, and increased labeling of non-kinetochore MTs can be detected (Figure 3.3(f)).

To further examine the pattern of incorporation of biotin-tubulin into KMTs at short and long times post-injection, the images shown in Figure 3.3(e) and 3.3(f) have been examined for pixel brightness using pixel mapping (see Methods). Following a 30 second post-injection incubation, anti-biotin staining of the kinetochore fiber is highly non-uniform; a peak in labeling intensity is clearly detected at the plus-end of KMTs, proximal to the kinetochore (Figure 3.4(a,c)). At this time, relatively little incorporation of biotin-tubulin has occurred within the kinetochore fiber or in the spindle asters. When kinetochore fibers are examined following longer post-injection intervals, no peak of anti-biotin labeling at the plus-ends of KMTs is detected (Figure 3.4(b,d)). Rather, label is more evenly distributed along the kinetochore fiber. Further, more biotin-tubulin is detected in the astral region than along the kinetochore fiber at these longer times post-injection. This increase in anti-biotin staining of the astral region presumably reflects the rapid turn-over of non-KMTs (Salmon et al., 1984; Mitchison et al., 1986). Thus, a qualitative difference in the anti-biotin staining pattern is clearly seen when cells are examined after short and long post-injection intervals. It should be noted, however, that these images have been contrast-stretched before this analysis, and therefore no quantitative comparison between cells should be made.

Changes in the pattern of biotin-tubulin incorporation at short and long times post-injection can also be detected at the resolution of the electron microscope. At short time points post-injection, discrete lengths of biotin-labeled microtubules are detected proximal to the kinetochore using immunoelectron microscopy (Figure 3.2). At long time points post-injection, no clearly defined segments of biotin-tubulin incorporation can be seen using immuno-electron microscopy (see Wadsworth et al., 1989). However, incorporation

of biotin-tubulin is detected in a relatively small fraction of KMTs in cells examined at longer times post-injection. This incorporation is detected along the length of the kinetochore fiber, rather than specifically at the kinetochore proximal ends of KMTs. In addition, both labeled and unlabeled MTs can be seen to contact the kinetochore. Thus a distinct change in the pattern of incorporation can be seen between cells incubated for short and long times post-injection using either immunofluorescent or electron microscopic observation.

While cells injected in anaphase A incorporate biotin-tubulin into kinetochore-proximal tufts, few or no tufts of incorporation can be detected when cells are injected after the completion of chromosome-to-pole motion and examined after similar post-injection intervals (compare Figure 3.5(a), mid-anaphase with Figure 3.5(b), late anaphase). To examine further these cell cycle dependent changes in KMT plus-end incorporation of biotin-tubulin, the number of tufts detected in cells injected with 3-5.5 mg/ml biotin-tubulin has been quantified from complete through-focus series obtained using confocal microscopy (see Methods). These data demonstrate that the number of tufts/cell decreases as cells progress through anaphase (Table 3.1). Cells injected during early-mid anaphase A have significantly more tufts than cells injected at the end of anaphase A ($p<0.05$) or during anaphase B ($p<0.01$) (Table 3.1; Shelden and Wadsworth, 1990). Unfortunately, the percent of the total kinetochore fibers labeled in these cells could not be accurately determined for two reasons. First, the cells used for this analysis were not all double labeled for anti-tubulin. Second, not every kinetochore fiber could be unambiguously detected in these cells. It is clear, however, that the number of labeled kinetochore fibers decreases as anaphase progresses. Together, these data strongly suggest that progression through anaphase influences the incorporation of biotin-tubulin proximal to the kinetochore.

Analysis of Chromosome Motion in Injected Cells

In order to determine if incorporation of microinjected biotin-tubulin during anaphase is accompanied by changes in chromosome motion, video records of injection experiments have been analyzed. In the first series of experiments, cells were injected with either 5.5 mg/ml or 0.3 mg/ml of biotin-tubulin or 5 mg/ml BSA. The rate of chromosome motion was measured before injection, for approximately 30 seconds immediately post-injection (see Methods), and following the 30 second post-injection interval (recovery). Measurements of sister chromatid separation in cells injected with 5.5 mg/ml biotin-tubulin revealed that chromosomes paused or transiently reversed direction in 9 of 10 cells examined (data not shown). To more critically examine these changes in chromosome motion, the motion of individual chromosomes was also examined in these cells (see Methods). Because these measurements were made relative to a fixed location on the video monitor, only chromosomes in spindles which were relatively stationary during the experiment could be accurately measured. For nine chromosomes in five cells analyzed using this method, the measured rates of chromosome motion before injection, during motion away from the pole, and after the recovery of chromosome-to-pole motion were 1.0, -0.5, and 0.9 μm/min (Table 3.2, example, see Figure 3.6(a)). These measurements reveal that chromosomes can reverse their direction of motion in cells injected with 5.5 mg/ml biotin-tubulin, and further reveal, since poleward motion resumes at pre-injection rates after the reversal of chromosome-to-pole motion, that this reversal does not result from a permanent alteration to the kinetochore.

While not every chromosome in cells injected with 5.5 mg/ml biotin-tubulin could be observed to reverse its direction of motion following injection, several factors make small changes in chromosome motion difficult to detect. First, small displacements of the kinetochore region cannot be detected unless the microscope is focused directly on the kinetochore of a chromosome under observation. Second, the three-dimensional nature of the spindle also makes accurate measurements of chromosome motion difficult. Motion of

a chromosome which is not in the plane of focus will be only partially detected, and thus the measured rate of chromosome motion will be an underestimate of the actual rate of motion.

Chromosome motion in control cells injected with either low concentrations (0.3 mg/ml) biotin tubulin, or 5.0 mg/ml BSA have also been analyzed using these methods of quantification. Although small changes in the average rates of chromosome motion can be detected following injection in these control experiments, these changes are much more subtle than those seen after injection of higher tubulin concentrations (data not shown). When individual chromosomes were analyzed (example, Figure 3.6(b) (graph) and Table 3.2), no evidence of a reversal of chromosome-to-pole motion could be detected post-injection in these cells.

In these experiments, cells were allowed to recover normal chromosome-to-pole motion following injection, so it was not possible to determine if incorporation of biotin-tubulin at KMT plus-ends had occurred during the reversal of chromosome-to-pole motion. Furthermore, the reversals of chromosome-to-pole motion detected following injection with 5.5 mg/ml biotin-tubulin are small and resemble the normal oscillations of anaphase chromosomes seen in some cells (see discussion). In order to more clearly demonstrate that chromosomes reverse their direction of motion after injection, and that this reversal is accompanied by subunit addition at the plus-ends of attached KMTs, a second series of experiments has been performed. For these experiments, cells were injected with 13 mg/ml biotin-tubulin to increase the ability to detect reversal of chromosome-to-pole motion. Cells were recorded before injection and up to 90 seconds post-injection, when the cells were lysed, fixed and stained to reveal the sites of biotin-tubulin incorporation. In these experiments, chromosome motion away from the pole is clearly observed post-injection (Figure 3.7; panels (b) and (c), also panels (f) and (g)). Further examination of the biotin-tubulin staining pattern (Figure 3.7(d, h)) reveals that the majority of kinetochore fibers have incorporated biotin-tubulin proximal to the kinetochore. In some cases, tufts of

incorporation can be seen at the plus ends of kinetochore MTs attached to chromosomes which were observed to reverse their direction of motion during the injection experiment (Figure 3.7(d)).

Several observations strongly suggest that plus-end dependent assembly of KMTs during anaphase and reversal of anaphase chromosome-to-pole motion are induced by the injection of biotin-tubulin through the action of the same mechanism. First, both can be induced by the injection of high, but not low concentrations of biotin-tubulin. Second, the time-course of KMT plus-end assembly corresponds closely with the time course of the reversal of anaphase chromosome-to-pole motion. Motion of chromosomes away from the pole is initiated immediately following injection of biotin-tubulin, and tufts of incorporation are detected at the earliest time-points that can be assayed. The duration of motion away from the pole occurs over 40±20 seconds, and kinetochore proximal tufts are most pronounced in cells examined after comparable post-injection intervals. Recovery of anaphase chromosome-to-pole motion occurs on average 40 sec. post-injection in cells injected with 5.5 mg/ml biotin-tubulin. Similarly, kinetochore-proximal tufts of incorporation cannot be detected in cells examined for biotin-tubulin incorporation at time-points later than 60 seconds post-injection in cells injected with similar concentrations of tubulin. Finally, the length of kinetochore-proximal biotin-tubulin incorporation detected using EM techniques is similar to the distance of anaphase chromosome-to-pole motion reversal documented using video-microscopy. Together, these results strongly indicate that the assembly of biotin-tubulin at the plus-ends of KMTs is required for the reversal of chromosome-to-pole motion seen in these experiments.

Careful analysis of video records of chromosome reversal in cells injected with 5.5 or 13 mg/ml biotin-tubulin indicate that the reversal of motion seen in these experiments is produced by a force acting directly at the kinetochore. First, stationary phase-dense objects can be seen in cells near chromosomes undergoing motion away from the pole (arrowhead, Figure 3.8). Thus, motion away from the pole is not caused by non-specific relaxation of

the cytoplasmic matrix. Second, motion of chromosomes away from the pole can be detected in half spindles both proximal and distal to the site of injection. Therefore, the reversal of chromosome motion is not caused by the pressure of injection and can in fact occur against any force generated by the injection. Third, the reversal of chromosome motion is of much longer duration than the displacement of the cytoplasm caused by injection. Chromosomes, and other phase-dense objects displaced by the force of injection, returned to their original location within a few seconds post-injection. In contrast, chromosome motion away from the pole occurred over a 40 ± 20 second interval following injection of 5.5 mg/ml biotin-tubulin. Finally, examination of chromosome morphology during the reversal of chromosome-to-pole motion indicates that the force involved is acting directly upon the kinetochore. Chromosomes undergoing a reversal of chromosome-to-pole motion could be seen to change shape as they moved, becoming more flattened at the site of the kinetochore (Figure 3.8). In addition, motion of the chromosome arms can be seen to lag behind the motion of the kinetochore region in some instances (Figure 3.8).

Discussion

In the experiments reported here, the relationship between KMT dynamics and chromosome motion has been examined in living anaphase PtK_1 cells following injection of biotin-labeled tubulin. The results of these experiments demonstrate that tubulin subunit addition can occur at the plus-ends of KMTs in anaphase cells, as has been previously demonstrated in prometaphase and metaphase cells (Mitchison et al., 1986; Wise et al., 1991). Analysis of video records of injection experiments further demonstrates that chromosomes in anaphase can be induced to transiently reverse their direction of motion in response to an elevation of the intracellular tubulin concentration. From these observations it is apparent that the transition from metaphase to anaphase does not irreversibly alter the

interaction between the kinetochore and KMTs with respect to its ability to allow plus-end dependent KMT polymerization.

The results of these experiments demonstrate that reversal of anaphase A chromosome motion and plus-end dependent assembly of KMTs can be induced by an elevation in the concentration of intracellular tubulin. Injection of low concentrations of biotin-tubulin (0.3 mg/ml) did not alter chromosome motion, while injection of concentrations greater or equal to 5.5 mg/ml biotin-tubulin reproducibly induced the transient reversal of chromosome-to-pole motion. Similarly, high, but not low, concentrations of injected tubulin induced assembly at the KMT plus-ends at the majority of kinetochores in mid-anaphase cells. Because a limited number of injection concentrations were tested, the minimum concentration which must be reached to induce KMT plus-end assembly and reversal of motion in anaphase has not been determined. However, concentrations of 3.0 mg/ml biotin-tubulin or greater reproducibly induced the formation of kinetochore proximal tufts of incorporation. If approximately 10% of the cell volume is injected (Saxton et al., 1984; Schulze and Kirschner, 1986; Mitchison et al., 1986; Geuens et al., 1989) and the cellular concentration of tubulin is approximately 2 mg/ml (Pfeffer et al., 1976; Hiller and Weber, 1978) of which roughly 50% is polymerized (Hiller and Weber, 1978), then injection of a solution of 3 mg/ml tubulin will increase the concentration of free subunits by approximately 33%. While these values are only estimates, they suggest that the kinetochore is sensitive to increases of tubulin in the physiological range. Finally, plus-end assembly of KMTs is not detected in cells injected with biotin-tubulin during anaphase B spindle elongation, although incorporation is detected in interzonal MTs during this same period (Shelden and Wadsworth, 1990). Thus, KMT plus-ends in cells which have completed anaphase A apparently do not respond to the elevation in the level of cytosolic tubulin which results from the injection of biotin-tubulin. This observation further indicates that KMT plus-end assembly is not induced indiscriminately in these injection experiments, and, together with the

demonstration that KMT turnover occurs in early but not late anaphase (Wadsworth et al., 1989), suggests that a fundamental change in the attachment of the kinetochore to the KMTs occurs at the completion of anaphase A, the nature of which remains unknown.

Although chromosome motion during anaphase is predominantly directed toward the minus ends of the MTs, at the spindle poles, asynchronous oscillations, both toward and away from the poles, have been detected in diverse cells (Bajer, 1982; Rieder et al., 1986; Aist and Bayles, 1988). Natural oscillations occur with an average velocity which is similar to the value measured here for motion away from the pole induced by injection of 5.5 mg/ml biotin-tubulin (0.9 vs 1.0 μm/min), although the naturally occurring oscillations tend to have a somewhat longer average duration (1.7 vs 0.6 min). During oscillations away from the pole in anaphase, the kinetochore fiber elongates; the results presented here clearly demonstrate that in cells injected with biotin-tubulin, elongation of kinetochore microtubules occurs by subunit incorporation proximal to the kinetochore. It is likely that that incorporation occurs at this site during natural oscillations as well. However, it is unlikely that the incorporation of injected tubulin into KMTs seen here occurs as a result of natural chromosome oscillations. In the experiments reported here, all or nearly all of the kinetochore fibers in mid-anaphase cells incorporate injected biotin-tubulin proximal to the kinetochore. However, natural anaphase oscillations are highly asynchronous, and not all chromosomes reverse simultaneously. Thus, the results of these experiments reveal that the incorporation of biotin-tubulin into the kinetochore fiber, and the reversal of chromosome motion, are induced by the injection of biotin-tubulin.

The observations of chromosome motion reversals reported here indicate that force is applied at or near the kinetochore rather than along the chromosome arms. In the experiments reported here, compression of the kinetochore region is detected during reversal, while little change in the position of the chromosome arms is observed. Some observations of natural oscillations also indicate that movement in the plus-end direction is due to a pushing force at the kinetochore (Bajer, 1981), but in other cases oscillations are

not accompanied by a detectable deformation of the kinetochore region (Bajer, 1982; Rieder et al., 1986; Salmon, 1989; Rieder, 1991) These latter results, and the exclusion from the aster of chromosome fragments which lack a kinetochore, support the view that motion away from the pole results from the pushing of astral MTs along the length of the chromosome (Rieder et al., 1986; Rieder, 1991). In addition, experiments in which anaphase chromosome motion is reversed by taxol also demonstrate that chromosome arms can be pushed back toward the spindle equator (even to the point of breaking) while the kinetochore region remains stretched poleward (Bajer, 1982). Thus, the results of the present study can be distinguished from reversal induced by taxol, and from some instances of natural oscillations, by the differences in chromosome morphology observed during the reversal of chromosome-to-pole motion.

If microtubule polymerization at the kinetochore produces the force responsible for the plus-end directed chromosome motion seen in these experiments, then the force generated by polymerization must either overcome or transiently turn off the minus-end directed force which produces normal chromosome-to-pole motion (Nicklas, 1983). The results obtained in the present study are most simply explained if the force for chromosome-to-pole motion is generated by KMT disassembly alone, as originally proposed by Inoue (Inoue and Sato, 1967; Coue et al., 1991). If this is the case, then a transition from disassembly to assembly of subunits at KMT plus-ends could itself prevent production of minus-end directed forces. Such a transition could be induced by an elevation in the tubulin subunit concentration. The production of force by microtubule polymerization is consistent with both theoretical (Hill, 1981) and experimental evidence that microtubule polymerization can generate pushing forces (Bajer, 1982; Miyamoto and Hotani, 1988).

An alternative explanation for the reversal of motion observed in the experiments reported here is that elongation of the anaphase kinetochore fiber activates plus-end directed microtubule motors located at the kinetochore. For example, a model of kinetochore

organization in which plus-end directed motors are internal to minus-end directed motors has recently been proposed (Huitorel and Kirschner, 1988). In the experiments reported here, the elongation of KMT plus-ends may be sufficient to engage such internal plus-end directed motors. In vitro experiments further reveal that kinetochores contain both plus-end and minus-end directed motor activity and that phosphorylation may regulate the direction and rate of motion (Hyman and Mitchison, 1991). However, movement of MTs relative to the kinetochore in these in vitro experiments is due to lateral interactions between the MTs and the kinetochore. The contribution of plus-end directed motors to the motion of a chromosome which is attached end-on to a bundle of KMTs as in normal anaphase remains unknown.

Finally, the results presented here clearly demonstrate that important cellular events are perturbed by the injection of biotin-tubulin. Alterations in chromosome motion were reproducibly induced following injection of 3.0 mg/ml biotin tubulin. This concentration is within the range (0.15 - 30 mg/ml) of concentrations which have been utilized in a variety of experiments to examine microtubule dynamics (Saxton et al., 1984; Mitchison et al., 1986; Schulze and Kirschner, 1986; Gorbsky et al., 1988; Geuens, et al.,1989; Wadsworth et al., 1989; Shelden and Wadsworth, 1990; Wise et al., 1991). While it is beyond the scope of this paper to evaluate these previous reports, it is noteworthy that cell-cycle dependent changes in microtubule dynamic behavior have been observed using these injection methods (Saxton et al.,1984; Wadsworth et al., 1989; Shelden and Wadsworth, 1990; this report) suggesting that some of the mechanisms which regulate dynamics may function even when the level of tubulin is elevated. Other aspects of microtubule dynamics, such as the rate of microtubule elongation, however, may be more sensitive to perturbation (see Schulze and Kirschner, 1986). Finally, the results of the present study demonstrate that the perturbation resulting from injection is transient; chromosome-to-pole motion resumes shortly after injection. Together these observations indicate that measurement of microtubule dynamics in cells injected with low concentrations of tubulin

analogues or following incubation periods significantly longer than 40 seconds, should accurately reflect endogenous microtubule activity (see Geuens et al., 1989; Wadsworth et al., 1989) but that injection of high concentrations of tubulin and/or examination at short times post-injection should be used with great caution.

Conclusion

In summary, the experiments reported here reveal that kinetochores retain the ability to mediate plus-end dependent assembly of KMTs and the associated motion of chromosomes away from the spindle pole after the onset of anaphase, and that these events can be induced by micro-injection of biotin-labeled tubulin subunits. These results indicate that the transition from metaphase to anaphase chromosome motion is not accomplished through the permanent modification of the kinetochore, especially with respect to its ability to permit subunit incorporation. The reversal of chromosome motion observed here is transient, and is only observed for cells in anaphase A of mitosis. The sensitivity of anaphase chromosome motion to the intracellular tubulin concentration further indicates that the rate and direction of chromosome-to-pole motion may be regulated by the concentration of tubulin subunits at the kinetochore region of an actively moving anaphase chromosome.

Figure 3.1.

Biotin-tubulin incorporates at the plus-ends of KMTs following injection into anaphase cells. A PtK_1 cell injected with 5.5 mg/ml biotin-tubulin and incubated at $30^{o}C$ for 22 seconds post-injection is shown. The cell was stained with (a) anti-biotin; (b) anti-tubulin antibodies. Assembly of biotin-tubulin (arrows Figure 3.1(a)), is detected at the kinetochore proximal or plus-ends of kinetochore fiber microtubules (arrows, Figure 3.1(b)). Phase contrast image was recorded just after injection (inset). Bar, 10 μm.

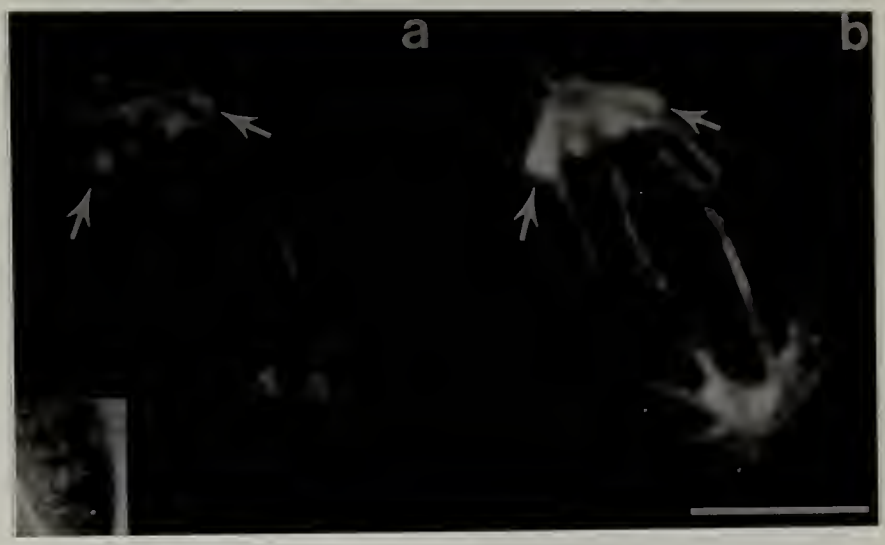
a
b

Figure 3.2.

Anti-biotin staining at the distal or plus-ends of kinetochore fiber microtubules is continuous with unlabeled kinetochore fiber microtubules. Electron microscopic immunocytochemistry of an anaphase cell injected with 5.5 mg/ml biotin-tubulin and incubated for 39 seconds post-injection. The cell was stained with anti-biotin antibodies and 5 nm gold labeled secondary antibodies. Bar, 0.5 μm.

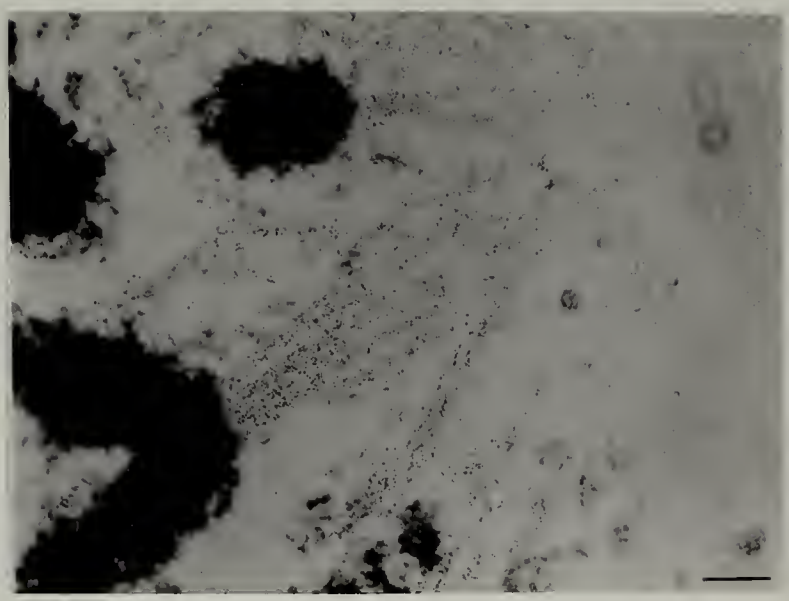

Figure 3.3.

Incorporation of biotin-tubulin into injected anaphase cells is dependent on the concentration of biotin-tubulin and the post-injection interval. Anti-biotin staining is shown in each panel. (a) 0.3 mg/ml biotin-tubulin, 28 sec. post-injection, 2 optical sections; (b) 3.0 mg/ml biotin-tubulin, 28 sec. post-injection, 5 optical sections; (c) 30.0 mg/ml biotin-tubulin, 26 sec. post-injection, 8 optical sections. Plus-end dependent incorporation of injected tubulin into KMTs is seen at high, but not low concentrations of injected biotin-tubulin. (d) 5 mg/ml, 18 sec. post-injection, 4 optical sections; (e) 3.0 mg/ml injected tubulin, 27 sec. post-injection, 2 optical sections; (f) 3 mg/ml, 65 sec. post-injection, 3 optical sections. Plus-end dependent incorporation of biotin-tubulin is more pronounced at 27 sec. post-injection than at 18 sec. post-injection. At 67 sec. post-injection, incorporation is detected throughout the spindle. Bar, 10 μm.

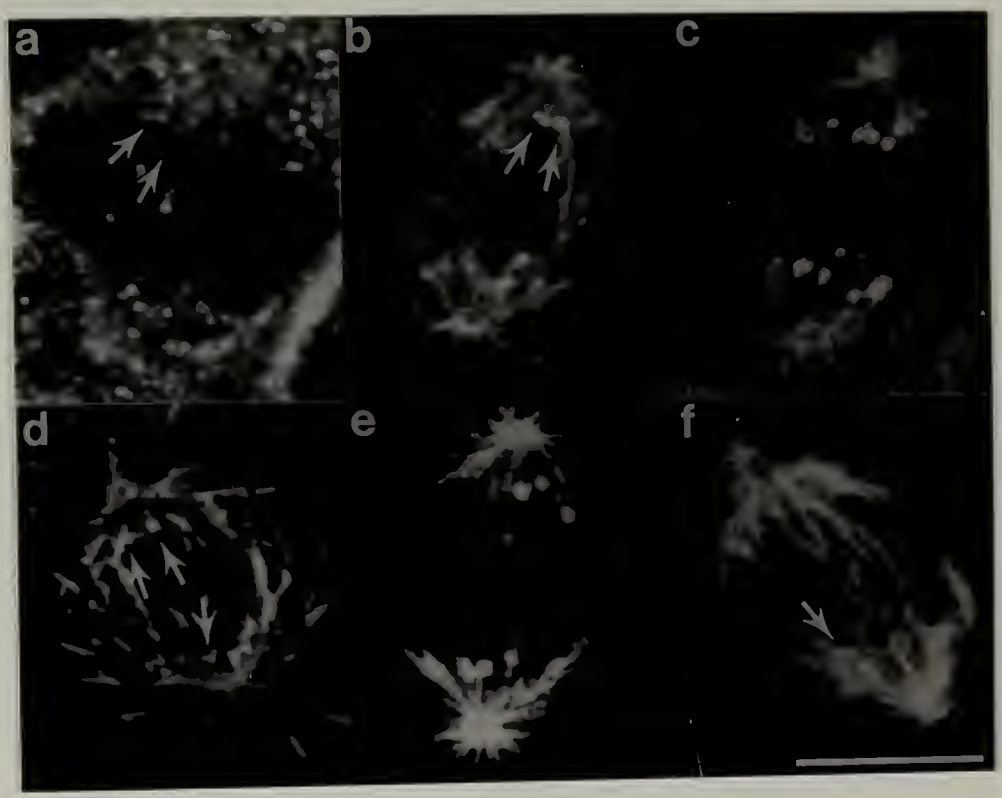
a
b
c
d
e
f

Figure 3.4.

Comparison of anti-biotin tubulin staining patterns for cells incubated for short and long times post-injection. Analysis of the lower half spindle of cells shown in Figure 3.3(e,f). (a) When examined after 27 sec. post-injection incubation, labeling of kinetochore fibers is highly non-uniform, and KMT plus-ends are as bright or brighter than the spindle aster. (b) At 65 sec. post-injection, labeling along KMTs is much more uniform and is less bright than labeling in the spindle aster. (c,d) Pixel mapping of individual kinetochore fibers (arrows, (a) and (b)). The high intensity of staining proximal to the kinetochore (k) seen at short time-points post-injection is not detected at longer time-points; more staining is associated with the spindle aster (A) at long time-points post-injection than at shorter time-points.

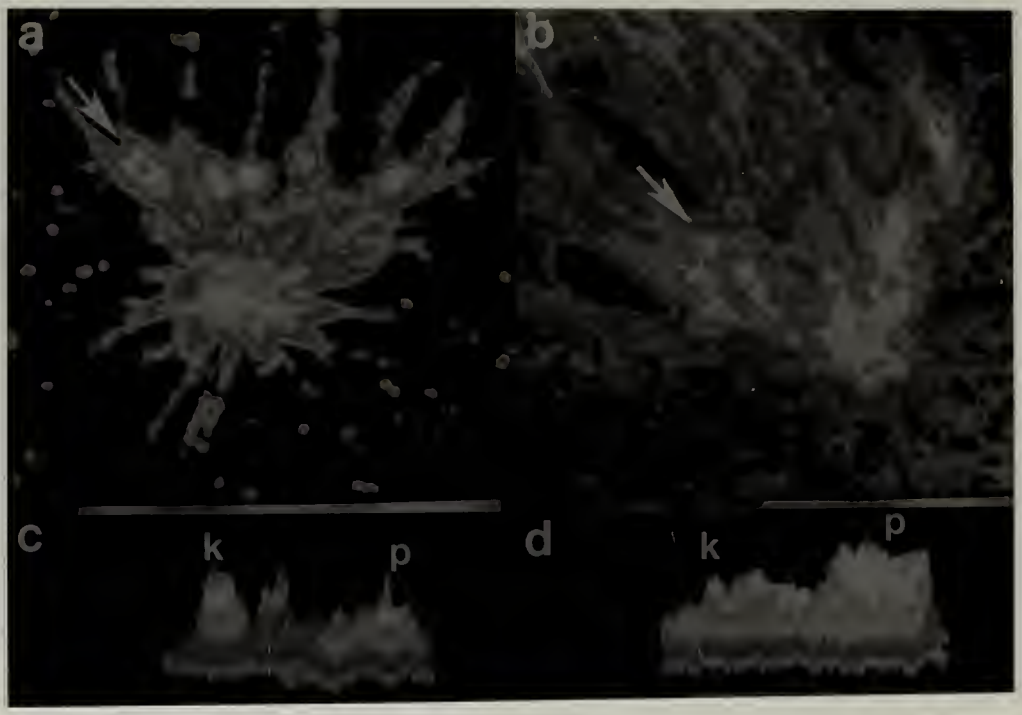
a
b
c
k
p
d
k
p

Figure 3.5.

Incorporation of biotin-tubulin proximal to the kinetochore in anaphase cells occurs during anaphase A, but not anaphase B. (a) Anti-biotin immunofluorescence of a cell injected in mid-anaphase with 3 mg/ml biotin-tubulin and incubated for 24 sec. post-injection. Numerous bright "tufts" of fluorescence are seen proximal to the kinetochores. (b) A cell injected in late anaphase with 3 mg/ml biotin-tubulin and examined 28 sec. post-injection. Astral and interzonal MTs are labeled, but no tufts of biotin-tubulin fluorescence are detected. Phase contrast images of these cells were taken just before (a') and just after (b') lysis. Bar, 10 μm.

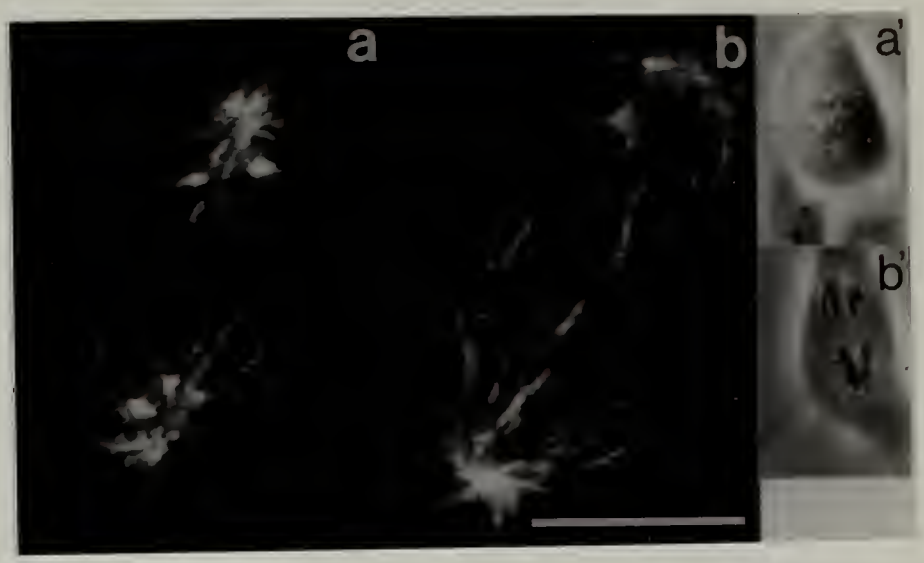
a
b
a'
b'

Figure 3.6.

Analysis of chromosome motion in anaphase cells following injection of 5.5 mg/ml biotin-tubulin (a), or 0.3 mg/ml biotin-tubulin (b). (a) The motion of an individual chromosome in a cell injected with 5.5 mg/ml biotin-tubulin. Transient reversal of chromosome-to-pole motion is clearly seen post-injection. (b) No reversal of chromosome-to-pole motion can be detected in a separate cell following microinjection of 0.5 mg/ml biotin-tubulin. Squares represent points recorded prior to injection, circles represent points recorded for thirty seconds post-injection or until recovery of chromosome-to-pole motion, and diamonds represent points recorded as chromosome-to-pole motion resumed post-injection. The time of injection is designated by an asterisk in each panel.

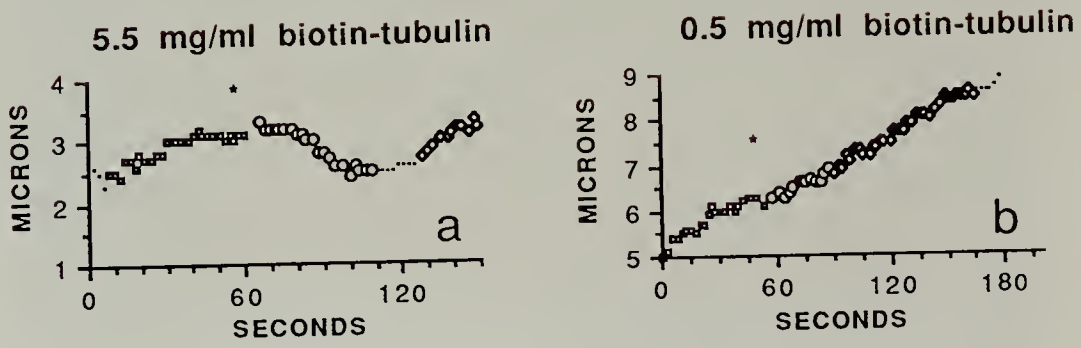
5.5 mg/ml biotin-tubulin
MICRONS
4
3
2
1
0
60
120
SECONDS
a
0.5 mg/ml biotin-tubulin
MICRONS
9
8
7
6
5
0
60
120
180
SECONDS
b

Figure 3.7.

Incorporation of biotin-labeled tubulin accompanies the reversal of chromosome-to-pole motion in injected anaphase cells. A cell is shown approximately one minute before injection (a), immediately after injection (b), and 48 sec. after injection (c). A central pair of chromosomes which reverse their direction of motion are clearly detected (arrows, Figure 3.7(b) and (c)). Anti-biotin immunofluorescent staining reveals that biotin-tubulin has been incorporated into KMTs attached to these and other chromosomes (d). A second cell (Figure 3.7(e-h)) is shown before injection (e), immediately after injection (f), and 55 sec. after injection (g). A slight decrease in the distance between opposing chromosomes can be detected post-injection (asterisks, Figure 3.7(f) and (g)). In this more rounded cell, the increase in chromosome-to-pole distance is expressed as a separation of chromosomes in the same half spindle (asterisks, Figure 3.7(f) and (g)). Biotin-tubulin incorporation is detected proximal to most kinetochores in this cell (Figure 3.7(h)). Bar, 5 μm.

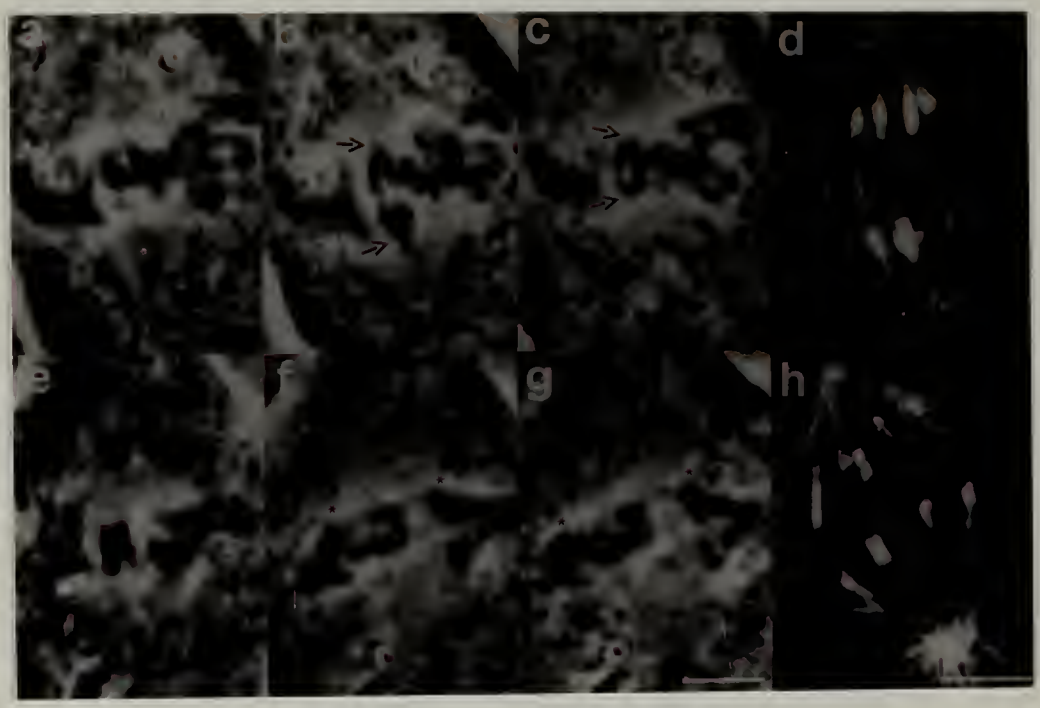
c
d
g
h

Figure 3.8.

Changes in chromosome shape and phase density accompany the reversal of anaphase chromosome-to-pole motion. Phase contrast images of chromosomes (large arrow) taken from video records of injection experiments; photographs were taken at approx. 10 sec. intervals. The cell was injected just prior to the first image. The chromosome shown was located in the half-spindle opposite the site of injection, thus the chromosome moved against the flow from the injection pipette. The kinetochore region of the chromosome becomes more flattened as the reversal of chromosome-to-pole motion occurs. Inspection of the trailing chromosome arms reveals that motion of the kinetochore precedes, and is more extensive than the motion of the arms. A stationary phase-dense organelle is indicated (arrowhead). Bar, 2 μm.

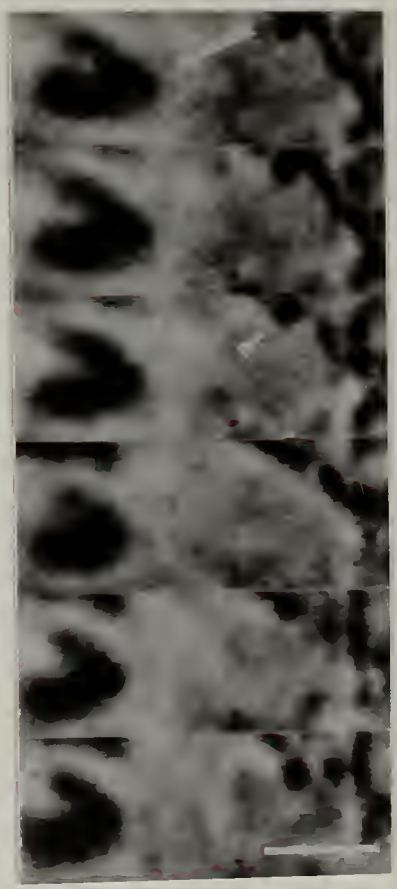

Table 3.1. The number of kinetochore proximal tufts/cell.

mid-Anaphase A	18.3 ± 6.0 (n=11)
late Anaphase A	11.7 ± 3.4 (n=10)
Anaphase B	0.4 ± 1.0 (n=9)

The number of kinetochore proximal tufts were counted from confocal sections of cells stained with antibodies to biotin-tubulin. Cells were injected with 3.0 mg/ml or higher biotin-tubulin and incubated 16 to 41 seconds post-injection.

Table 3.2. The rate of individual chromosome motion in injected cells.

	before inj.	30 s p.inj.	>30 s p.inj.
5.5 mg/ml Tb.	1.0±0.5 n=9	-0.5±0.4 n=9	0.9±0.2 n=9
0.3 mg/ml Tb.	1.4±0.2 n=8	0.9±0.2 n=8	1.2±0.2 n=8
5.0 mg/ml BSA	1.9±0.1 n=2	1.1±0.4 n=4	1.3±0.2 n=4

Measurements were made before injection, for 30 seconds after injection, and at time points greater than 30 seconds post-injection. Rates of chromosome motion are in units of microns/minute. Abbreviations used are Tb: tubulin, BSA: bovine serum albumin, s: seconds, p.inj.: post-injection, n: number of chromosomes analyzed for each group.

CHAPTER 4

OBSERVATION AND QUANTIFICATION OF INDIVIDUAL MICROTUBULE BEHAVIOR IN VIVO: MICROTUBULE DYNAMICS ARE CELL TYPE SPECIFIC

Abstract

Recent experiments have demonstrated that the behavior of the interphase microtubule array is cell type specific: microtubules in epithelial cells are less dynamic than microtubules in fibroblasts (Pepperkok et al., 1990; Wadsworth and McGrail, 1990). In order to determine which parameters of microtubule dynamic instability behavior are responsible for this difference, the behavior of individual microtubules in PtK_1 epithelial and CHO fibroblasts has been examined following injection with rhodamine labeled tubulin subunits. Individual fluorescent microtubules in both cell types were observed to grow, shorten and pause, as expected. The average amount of time microtubules remained within the lamellae of CHO fibroblast, measured from images acquired at 10 second intervals, was significantly shorter than the average amount of time microtubules remained within lamellae of PtK_1 epithelial cells. Further analysis of individual microtubule behavior from images acquired at 2 second intervals reveals that microtubules in PtK_1 cells undergo multiple brief episodes of growth and shortening resulting in little overall change in the microtubule network. In contrast, microtubules in lamellae of CHO fibroblasts are observed to undergo fewer transitions which are of longer average duration, resulting in substantial changes in the microtubule network over time. A small subset of more stable microtubules is also detected in CHO fibroblasts. Quantification of the various parameters of dynamic instability behavior from these sequences demonstrates that the average rates of both growth and shortening are significantly greater for the majority of microtubules in

fibroblasts (19.8±10.8 μm/min and 32.2±17.7 μm/min, respectively) than for microtubules in epithelial cells (11.9±6.5 μm/min and 19.7±8.1 μm/min, respectively). The frequency of catastrophe (1/interval between catastrophe events) is similar in both cell types, but the frequency of rescue (1/ time spent shrinking) is significantly higher in PtK_1 cells. Thus, individual microtubules in PtK_1 lamellae undergo frequent excursions of short duration and extent, while most microtubules in CHO lamellae undergo more extensive excursions often resulting in the appearance or disappearance of microtubules within the field of view. These observations provide the first direct demonstration of cell type specific behavior of individual microtubules in living cells, and indicate that these differences can be brought about by modulation of the frequency of rescue. These results directly support the view that microtubule dynamic instability behavior is regulated in a cell type specific manner.

Introduction

Microtubules are dynamic polymers which alternate stochastically between periods of assembly and rapid disassembly (Cassimeris et al., 1988; Horio and Hotani, 1986; Mitchison and Kirschner, 1984; Sammak and Borisy, 1988a; Schulze and Kirschner, 1988; Walker et al., 1988). This behavior, termed dynamic instability (DI) (Mitchison and Kirschner, 1984), has been directly observed both in living cells (Cassimeris et al., 1988; Sammak and Borisy, 1988a; Schulze and Kirschner, 1988) and in vitro using microtubules nucleated from axonemes or centrosomes (Belmont et al., 1990; Walker et al., 1988). Quantification of the various parameters of DI, however, reveals striking differences between microtubule dynamic behavior in vivo and in vitro. First, microtubules are rarely seen to pause in vitro (Walker et al., 1988), while microtubules in vivo have been observed to remain in a metastable state, during which neither growth or shrinking can be observed, for many minutes (Sammak and Borisy, 1988a; Schulze and Kirschner, 1988). Second,

the average rate of microtubule growth is significantly higher when measured in living cells (Cassimeris et al., 1988) than in vitro (Walker et al., 1988). Finally, the transition from growing to shrinking (catastrophe) and the reverse transition (rescue) occur much more frequently in vivo than in vitro (Walker et al., 1988). These differences are likely to reflect the complex environment found in living cells and further indicate that analysis of microtubules in living cells is necessary to fully understand the mechanisms which cells use to regulate the dynamic behavior of microtubules.

Experiments in which the behavior of the population of microtubules in living cells is measured further reveal that microtubule dynamic behavior is cell type specific. For example, when rhodamine labeled tubulin subunits are injected into living cells and the resulting fluorescent microtubule array photobleached (Pepperkok et al., 1990), fluorescence is recovered in fibroblasts much more quickly than in confluent epithelial cells. Other studies in which microtubules in different cell types are exposed to the microtubule destabilizing drug nocodazole have shown that disassembly of the microtubule population is more rapid in fibroblasts than in epithelial cells (Wadsworth and McGrail, 1990). Interestingly, in both studies two kinetically distinct populations of microtubules are detected in epithelial cells but not in fibroblasts. While these previous studies have demonstrated that microtubule populations in fibroblasts are more labile than those found in epithelial cells, the behavior of individual microtubules was not examined. Therefore, these results do not reveal which aspects of individual microtubule dynamic instability behavior are regulated to generate the observed cell type specific behavior of the microtubule population. Finally, although microtubules have been directly observed in vivo in both epithelial cells and fibroblasts (Cassimeris et al, 1988; Sammak and Borisy, 1988(a); Schulze and Kirschner, 1988) these direct observations have failed to detect cell type specific regulation of microtubule dynamic behavior.

To determine which parameters of individual microtubule dynamic instability behavior are regulated in producing cell type specific differences in microtubule population

behavior, rhodamine labeled tubulin subunits have been injected into PtK_1 epithelial cells and CHO fibroblasts (Wadsworth and McGrail, 1990) and the resulting individual fluorescent microtubules have been examined within thin lamellar regions at intervals of 2 or 10 seconds. Quantitative analysis confirms that individual microtubules in fibroblasts turn over more rapidly than in epithelial cells, as measured by the average amount of time microtubules remain within an approximately equivalent field of view. The average rates of microtubule growth and shortening are also significantly higher in fibroblasts. The frequency of rescue is higher in PtK_1 epithelial cells than CHO fibroblasts, while the frequency of catastrophe is similar in both cell types. In addition, a small number of more stable microtubules are detected in CHO fibroblasts; such meta-stable microtubules have been reported previously from a wide variety of cell sources (Cassimeris et al., 1988; Sammak and Borisy, 1988a; Schulze and Kirschner; 1988). These results provide the first direct demonstration of cell type specific behavior of individual microtubules in vivo, and indicate that differences in interphase microtubule dynamics may be brought about by regulating the frequency of rescue events.

Materials and Methods

Cell Culture and Microinjection

PtK_1 epithelial cells and CHO fibroblasts were cultured as described previously (Wadsworth and McGrail, 1990), plated on glass coverslips, and allowed to grow for a minimum of 48 hours before use. Rhodamine-labeled tubulin was prepared as described by Vigers (Vigers et al., 1988) and injected into cells as described previously (Wadsworth et al., 1989). After microinjection, cells were returned to a 37°C incubator for at least one hour before observation.

Microscopy and Image Acquisition

Cells were held in a Rose chamber (Rose, 1958) modified as described previously (Shelden and Wadsworth, 1992), and examined using a Zeiss IM-35 inverted microscope. All observations were made at 35 to 37°C; temperature was maintained as described previously (Shelden and Wadsworth, 1992). Cells were observed using a Nikon 100x 1.4 NA objective lens, and epifluorescent illumination was provided with a 100 watt mercury arc lamp. To obtain the greatest light transmission, several objective lenses were tested before the lens used in this study was selected. Illumination from the mercury arc lamp was filtered using a narrow bandwidth Zeiss filter cube for rhodamine excitation/emission, and greatly attenuated by defocussing the collector lens and placing neutral density filters in the illumination pathway. Illumination intensity was measured using an IR industries photo-detector (IR Industries Inc., Waltham MA) and locally constructed circuitry, and was typically 0.007 mW/ cm^2. For experiments in which the interval between images was 10 or more seconds, the epifluorescent illumination was shuttered using Uniblitz shutters controlled by a Masscomp computer to further reduce the total amount of illumination received by the cell under observation. A small amount of ascorbic acid (1 mM final concentration) was added to the cell culture medium to increase the resistance of living cells to photodamage (Kochanski and Borisy, 1990). Finally, the field diaphragm of the microscope was reduced to approximately 150 um^2 in order to further reduce the total amount of illumination received by each cell. Images were collected using a DAGE ISIT video camera operated at full gain and sensitivity settings, digitized using the Masscomp computer and stored, along with the time and date, on optical discs using a Panasonic optical memory disc recorder (OMDR). 32 video frames (approx. 2 seconds) were averaged before the final image was written to the OMDR. Unfortunately, the sensitivity of the ISIT camera increases slowly when an image is first placed on the camera faceplate. Thus for observations made at ten second intervals, a short delay (typically 0.3 to 0.5 seconds) between illumination of the specimen and the start of image acquisition was

necessary. For examination at 2 second intervals, cells were observed using continuous illumination for several minutes, and images were collected using a 32 frame running average. After some observation periods, cells were held on the microscope stage without illumination for several minutes, and then subsequently re-examined. No long-term changes in cell morphology or microtubule behavior resulting from the original observation period was detected using these methods (data not shown).

Quantification and Analysis of Microtubule Dynamics

Microtubule dynamic behavior was quantified using data generated from a locally written computer program running on the Masscomp computer and further analyzed using software written in the lab. Microtubules in sequential images were traced using a mouse-driven cursor, and the computer maintained a record of each trace, the interval between sequential images, and any microtubule length changes which occurred between images. During quantification of these image sequences, microtubule traces from a previous image could be overlaid onto the current image in order to facilitate the identification of individual microtubules from one image to the next. Only microtubules which could be clearly distinguished as single microtubules were analyzed in these experiments.

The average amount of time microtubules spent within the area of observation (lifespan) was measured from images obtained at 10 second intervals using intermittent illumination. To minimize the possible effects of photodamage to cells on the quantitative data, and to increase the number of cells which could be analyzed, only the first 3 minutes of each sequence were used for most analyses. Some sequences obtained from epithelial cells were re-analyzed for six minutes in order to determine if stable subsets of microtubules could be detected with these longer periods of observation (see Results).

Microtubule dynamic instability parameters were quantified from image sequences obtained at 2 second intervals. Due to the limit of resolution of the light microscope, and the presence of electronic noise in images generated by the ISIT camera, microtubule length

changes of less than 0.5 μm were considered to be pause events (Sammak and Borisy, 1988a). Because of this limitation, the minimum growth or shrinking rate detectable over a 2 second interval would be 15 μm/minute. In order to detect growth or shrinking events of less than 15 μm/min in rate, sequences were quantified in the following manner. For these experiments, two separate measurements of the microtubule's behavior were obtained as described previously, and the results of these two trials were averaged by the computer to minimize errors in measurement during the tracing of each microtubule. A plot of the average length changes over time obtained from the two measurements (a "life-history" plot) was then placed on a video monitor, and reference lines representing the scale in microns were overlaid onto this graph. This method allowed examination of a microtubule's entire life history and made detection of slow but extended growth and depolymerization events possible. Regions of the graph which represented periods of microtubule elongation, pause or depolymerization were selected using a mouse driven cursor, and the rate, duration and extent of these events were calculated by the computer using appropriate scaling parameters and linear regression techniques. Values for percent time paused were calculated by computing the total time spent paused for all microtubules, and dividing this figure by the total observation time for all microtubules. Rescue frequencies were calculated by taking the inverse of the average amount of time a microtubule spent in a state of depolymerization. Importantly, because many microtubules spent substantial periods of time in a paused state, during which neither growth nor depolymerization was detected, the catastrophe frequency is not simply the inverse of the average duration of a microtubule growth event (Walker et al., 1988). Instead, the frequency of catastrophe events was calculated by taking the inverse of the average interval between catastrophe events. The frequency of transitions per microtubule was calculated by dividing the average number of excursions made per microtubule by the average microtubule lifespan. Finally, statistical comparisons were made using two-tailed t-tests.

Results

When image sequences of fluorescent microtubules are collected at 10 sec intervals and examined, microtubules in lamellar regions of PtK_1 epithelial cells and CHO fibroblasts are observed to grow (g), shrink (s) and pause (p), as expected (Figures 4.1 and 4.2). Careful inspection of microtubule behavior in PtK_1 epithelial cells (Figure 4.1) reveals that microtubules which begin depolymerization frequently stop depolymerization and either pause or resume growing (rescue). Only one of the microtubules visible within the PtK_1 lamella shown in Figure 4.1 can be observed to depolymerize out of the field of view during this 50 second period (asterisk, Figure 4.1) and the overall arrangement of microtubules remains remarkably constant (compare Figure 4.1(a) with (f)). Note that sideways movement of some microtubules can be detected (arrows Figure 4.1). In contrast, much more extensive changes in the microtubule arrangement are observed during similar periods of observation in CHO fibroblasts (Figure 4.2, compare with Figure 4.1). These changes result from microtubules depolymerizing out of (single arrowheads) and entering into (double arrowheads) the field of view during the interval shown (Figure 4.2, compare with Figure 4.1).

Quantitative analysis of these and other image sequences reveals that the average "lifespan" of microtubules in lamellar regions (the average amount of time a microtubule spends within the field of view) is 59±51 seconds for 195 microtubules in 5 CHO cells and 88±57 seconds for 148 microtubules in 5 PtK_1 cells. For this analysis, images of microtubules in living cells were obtained at 10 second intervals, and the first 3 minutes of each sequence were examined. Distributions of the amount of time individual microtubules spent within the field of view further demonstrate that most microtubules remain within the field of view longer in PtK_1 epithelial cells than in CHO fibroblasts (Figure 4.3(a) and (b), respectively). In addition, these distributions reveal that many microtubules in the lamellar region of PtK_1 epithelial cells remain within the field of view for all or nearly all of the 3

minute observation period (Figure 4.3(a)). To determine if these microtubules represent a separate and more stable population of microtubules, image sequences from four PtK_1 epithelial cells have been re-quantified using the first six minutes of each sequence. The average amount of time microtubules remain within the field of view, when measured in this manner, is 125±93 seconds. However, a histogram of the time individual microtubules remain within the field of view during these longer image sequences reveals that only a single population of microtubules can be detected in the lamellae of PtK_1 epithelial cells during this longer observation period (Figure 4.3(c)).

When individual microtubules in the lamellar region of PtK_1 cells are examined at 2 second intervals, multiple, brief episodes of growth and shortening, which are not detected in images obtained at 10 second intervals, are observed (Figures 4.4 and 4.5). For example, the single microtubule near the bottom of each panel in Figure 4.4 grows approximately 1.9 μm (panels a to b), and depolymerizes approximately 1.2 μm (panels b to c). This microtubule therefore appears to grow at a rate of 28 μm/min, and depolymerize at a rate of 17 μm/min. Importantly, if the images of this microtubule had been taken at 8 second intervals, the apparent change in microtubule length between panels a and c would have been 0.7 μm, and the measured growth rate would have been 5.3 μm/min. Furthermore, the depolymerization event detected between panels b and c would not have been detected. The depolymerization event seen in panels b-c is followed by a second growth event (c-d), a pause event of approximately 12 seconds in duration (e-h) and a third growth event (h-j). Therefore, 5 discrete events of growth, shrinking or pause are exhibited by this microtubule in the 36 second interval shown in Figure 4.4.

Similar behavior of microtubules in the lamella of a second PtK_1 epithelial cell is shown in Figure 4.5. In this example, images are shown at 2 second intervals. An individual microtubule is clearly detected in the lower region of each panel, and has been marked in each case with the location of its plus end in the previous image to more clearly demonstrate any changes in microtubule length which occurred between images. Although

the final depolymerization event occurs over the duration of several images (r-t), many growth (a-b, j-k, l-m) and depolymerization (h-i, k-l) events of duration less than or equal to the two second interval between images are detected. Short pauses are detected when the location of the microtubule in a previous image coincides with its present location (a,c,n-p). Thus, microtubules in PtK_1 epithelial cells undergo frequent growth, depolymerization and pause events of short duration.

The behavior of microtubules in PtK_1 lamella has also been examined by plotting the change in microtubule length as a function of time (Figure 4.6) (see Methods). The trace shown in Figure 4.6(a) was obtained from analysis of the microtubule marked by the arrowheads in Figure 4.4, and the interval shown in Figure 4.4 is marked with arrows. Additional representative examples of microtubule "life histories" (Cassimeris et al., 1988) obtained from PtK_1 cells are shown in Figure 4.6 (b,c,d). These life history plots further demonstrate that microtubules in epithelial cells undergo frequent conversions between growth, shortening and pause.

Examination of individual microtubules in CHO cells reveals that the behavior of microtubules in CHO cells is strikingly different from the behavior of microtubules observed in PtK_1 cells. In Figure 4.7, a single microtubule is clearly observed to grow and then shrink across nearly the entire field of view. This microtubule elongates approx 6.8 μm in 20 seconds, or at a rate of 20.4 μm/min between panels a and f. The growth event seen in panels a-f is immediately followed by an episode of rapid shortening (panels f-i), during which the microtubule depolymerizes to its original length in 12 seconds, a rate of 34 μm/min, and subsequently leaves the field of view (not shown). Note that in this particular lamella, many microtubules could not be quantified (upper portion of micrographs). In some cases this results from insufficient clarity in regions where the cell was particularly thick or the microtubules were particularly numerous. In other cases the increased brightness and apparent thickness of fibers suggested that microtubules were laterally associated, or bundled (Sammak and Borisy, 1988b) and thus were not included in

these measurements. Finally, a microtubule fragment is clearly observed in this lamella, and remains relatively stable for the observation period. Such free microtubules were observed infrequently in both cell types; however, the number of fragments did not increase during long observation periods (data not shown) suggesting that they do not result from cellular damage. Microtubule fragments have also been observed in other cells using different methods of observation (Chen and Schliwa, 1990).

The behavior of individual microtubules in CHO cells is further revealed in Figure 4.8. Many microtubules are observed to make long excursions as they polymerize and depolymerize (Figure 4.8). In this example, a "stable" microtubule, which does not grow or shrink during this 44 second sequence, is also detected (arrowhead, Figure 4.8). Finally, although microtubules are observed to bend and to move laterally in PtK_1 epithelial cells (Figure 4.2), CHO lamella are characterized by the straight, almost "stiff" appearance of many microtubules (Figure 4.8).

Life history plots of microtubule behavior in CHO cells are shown in Figure 4.9. A plot of the behavior of the microtubule examined in Figure 4.7 demonstrates that a single growth and a single depolymerization event occurred during the period the microtubule was visible (Figure 4.9(a)). Additional examples, illustrating other typical microtubule behaviors observed in CHO fibroblasts, are shown in Figure 4.9 (b,c,d). A minority of microtubules in these cells are observed to pause for extended periods of time (Figure 4.9(d)). However, regardless of the pause duration, a single depolymerization event frequently results in the complete disappearance of CHO microtubules from the field of view. Thus, the behavior of microtubules in CHO fibroblasts is qualitatively different from the behavior of microtubules seen in PtK_1 epithelial cells.

The various parameters which characterize microtubule dynamic behavior in CHO fibroblasts and PtK_1 epithelial cells have been quantified from images obtained at 2 sec intervals (Table 4.1). Microtubules in PtK_1 epithelial cells are characterized by frequent episodes of growth and shrinking which are of short duration and extent. Although the

average duration of these events measured in PtK_1 cells are both longer than the 2 second interval between observation (Table 4.1) it is possible that some very brief events were not detected using these methods. The average rates of growth and shrinking events (11.9±6.5 and 19.8±10.8 μm/min, respectively) are both substantially higher than rates reported previously for fluorescent microtubules in vivo (Sammak and Borisy, 1988; Schulze and Kirschner, 1988) and are close to the values reported from analysis of microtubule behavior using DIC optics and 0.5 second intervals between observations (Cassimeris et al., 1988). Most noteworthy however, is the observation that most microtubules undergoing depolymerization events in PtK_1 cells are rescued before leaving the field of view, only 11% of the depolymerization events in PtK_1 cells resulted in microtubules leaving the field of view.

In contrast, microtubules in CHO fibroblasts are characterized by longer periods of growth and depolymerization, with relatively infrequent conversions between the two states (Table 4.1). The duration of microtubule growth and depolymerization events for the majority of microtubules in these cells (9.6±7.0 and 7.4±4.2 seconds, respectively) was significantly greater than the duration of these events in PtK_1 epithelial cells ($p \leq 0.01$). In addition, the rates of microtubule growth and depolymerization for these microtubules (19.7±8.1 and 32.0±17.7 μm/min, respectively) are also significantly higher than rates measured here in PtK_1 cells ($p \leq 0.01$). As a result, the proportion of depolymerization events which resulted in a microtubule leaving the field of view (48%) is much higher in these cells than in PtK_1 cells. In addition, although the frequency of catastrophe was similar in both cell types, microtubules in CHO fibroblasts were rescued less frequently than in epithelial cells ($p \leq 0.01$). Finally, the total frequency of growth, shrinking and pause events per microtubule measured in CHO fibroblasts is much lower than the frequency of events per microtubule in PtK_1 cells (Table 4.1). Taken together, these data reveal that individual microtubules in epithelial cells make frequent transitions of short duration resulting in little overall change in the microtubule network. In contrast, most

microtubules in CHO fibroblasts undergo fewer transitions, but the change in microtubule length during these events is much greater than that seen in epithelial cells and results in a more rapid turnover of the microtubule array.

A small number of more stable microtubules is also detected in CHO fibroblasts. Although these microtubules represent only 28% of the individual microtubules examined in CHO cells, these more stable microtubules accounted for 72% of the total time microtubules were observed to pause in these cells. In addition, both the rate of microtubule depolymerization and the frequency of catastrophe events for these microtubules are significantly lower than these values measured for the majority of microtubules in these cells (Table 4.1, $p \leq 0.05$ and $p \leq 0.01$, respectively). However, no other significant differences in the value of microtubule dynamic parameters were detected between these microtubules and the majority of microtubules observed in CHO cells (Table 4.1).

Finally, images of microtubules in PtK_1 epithelial cells obtained at 2 second intervals have been analyzed using only every fifth image. The rates of microtubule growth and depolymerization obtained in this manner are significantly lower than rates obtained by analyzing all images (Table 4.2), and are close to the values obtained by other investigators using images obtained at 10 second intervals (Sammak and Borisy 1988(a), Schulze and Kirschner, 1988). Furthermore, the number of events per microtubule detected using a 10 second observation interval is lower than the number of events detected using 2 second intervals, and the average duration of growth, depolymerization and pause events are significantly greater when measured at 10 rather than 2 second intervals (see Discussion).

Discussion

Microtubule Dynamics are Cell Type Specific

Observations of individual microtubules in CHO fibroblasts and PtK_1 epithelial cells reveal that individual microtubules remain within lamellar regions for longer periods in epithelial cells than in fibroblasts. These observations are consistent with previous studies which demonstrate that the population of interphase microtubules turns over more rapidly in fibroblasts than in epithelial cells (Pepperkok et al., 1990; Wadsworth and McGrail, 1990). To determine which aspects of individual microtubule behavior are involved in generating this cell type specific difference, individual microtubules in small areas of interphase cells have been examined at 2 second intervals. Quantitative analysis reveals that microtubules in CHO fibroblasts polymerize and depolymerize at more rapid rates than those found in PtK_1 epithelial cells. Surprisingly, this analysis further reveals that the total frequency of microtubule transitions is greater in PtK_1 epithelial cells than in CHO fibroblasts. However, microtubules undergoing depolymerization are often rescued in PtK_1 cells, resulting in little overall change in the length of individual microtubules. In contrast, microtubules in CHO fibroblasts are rescued much less frequently than those found in PtK_1 cells; the catastrophe frequency for the majority of microtubules observed in CHO fibroblasts is slightly but not significantly higher than for microtubules in PtK_1 cells. Thus, although the total frequency of microtubule transitions is lower in CHO fibroblasts than in PtK_1 epithelial cells, individual growth and depolymerization events in CHO cells result in extensive microtubule length changes and rapid cahnges in the microtubule array.

Microtubule Sub-Populations are Detected in Some Cells

Previous investigations have demonstrated the presence of 2 kinetically distinct microtubule subpopulations in epithelial cells but not fibroblasts (Pepperkok et al., 1990; Wadsworth and McGrail, 1990), and in both epithelial cells and fibroblasts (Schulze and

Kirschner, 1988). In the present study, populations of more stable microtubules are detected in CHO fibroblasts but not in epithelial cells. The reasons for the apparent absence of microtubule sub-populations in the lamellae of epithelial cells in the present study are not clear, however, it is possible that dynamically distinct microtubule subpopulations could be found within lamellar regions of epithelial cells under different culture conditions (Pepperkok et al., 1990). Alternatively, only a small region of the cell periphery could be examined in the present study, and less dynamic microtubules are often concentrated near the cell center (Schulze and Kirschner, 1986). It is therefore possible that more stable microtubules are present in epithelial cells, but are not detected in the current study due to the limited cell area which can be examined.

The observations presented here do reveal the presence of a small number of dynamically distinct microtubules in CHO fibroblasts. These microtubules spent longer periods of time in a paused state, during which neither growth nor depolymerization could be detected, than the majority of microtubules observed in these cells. The functional significance of these metastable microtubules has not been determined. Quantitative analysis of the behavior of these more stable microtubules reveals that the frequency of catastrophe events and the rate of microtubule depolymerization are significantly lower than for the majority of microtubules in CHO cells. A decrease in microtubule depolymerization rates for metastable microtubules has also been reported for individual microtubules in PtK_1 and BSC cells (Schulze and Kirschner, 1988). Finally, recent <u>in vitro</u> experiments have shown that both the rate of microtubule polymerization and the frequency of rescue are increased by MAP binding (Bre and Karsenti, 1990; Pryer, 1989). However, the results of the present study reveal that the more stable microtubules detected in CHO cells do not differ significantly from the majority of microtubules found in CHO cells with respect to either of these parameters. These findings therefore indicate that the behavior of these less dynamic microtubules in CHO fibroblasts may be regulated by a different mechanism.

Regulation of Interphase Microtubule Dynamics

Regulation of catastrophe and rescue frequencies has been postulated to play a role in the organization and behavior of diverse microtubule arrays in interphase cells. For example, it has been suggested that reducing the frequency of microtubule transitions is involved in the polarization of cultured epithelial cells (Bre et al., 1990; Pepperkok et al., 1990), and that increasing the number of rescue events may contribute to the formation of stable axonal microtubule arrays during axon outgrowth (Tanaka and Kirschner, 1991). Here, a lower frequency of rescue has been demonstrated for microtubules in fibroblasts, which are actively ruffling and capable of locomotion, than for microtubules in stationary epithelia. In addition, although values obtained for rescue and catastrophe frequency from amphibian epithelial and neuronal cells (Table 4.3) are lower than and more similar to each other than values obtained from mammalian tissue culture cells (this report), examination of the reported values reveals greater differences in the frequency of rescue than catastrophe among interphase cells of both groups (Table 4.3). For example, the values reported for catastrophe frequency in newt lung epithelial cells (Cassimeris et al., 1988) are similar to values reported for catastrophe in Xenopus nerve growth-cones (Tanaka and Kirschner, 1991), while rescue frequency in newt lung epithelial cells is higher than the rescue frequency calculated for microtubules in nerve growth cones (Table 4.3). These results suggest that variation in microtubule behavior among interphase cells involves cell type specific regulation of microtubule rescue frequencies, regardless of cell origin.

Although the transition from interphase to mitosis also involves changes in microtubule dynamic instability behavior, it is not clear if the frequency of rescue events is regulated during this transition. For example, in Xenopus oocyte extracts, the frequency of catastrophe measured for microtubules in mitotic extracts is approximately 6 fold higher than for microtubules in interphase extracts (Belmont et al., 1990); the frequency of rescue was also increased slightly in the mitotic extracts (approximately two-fold). However, the measured frequency of rescue events in both types of extracts (Belmont et al., 1990) is

much lower that values obtained from living interphase cells (Cassimeris et al., 1988; Tanaka and Kirschner, 1991; present study). The low value of microtubule rescue frequency measured from interphase Xenopus oocyte extracts may indicate that interphase conditions present in undifferentiated oocytes are not directly comparable to interphase conditions in non-embryonic cells. Alternatively, the low values for interphase rescue frequency may reflect the difficulties in reproducing in vivo conditions in in vitro extracts. It should be noted that a decrease in the frequency of rescue events has also been postulated to occur as cells enter mitosis (Cassimeris et al., 1988). Direct observation of the behavior of microtubules in living cells as they progress into mitosis may be necessary to resolve this issue.

Imaging Techniques Affect the Measurement of Microtubule Dynamic Behavior

The results presented here directly demonstrate that the interval between successive observations greatly affects the values obtained for the parameters of dynamic instability behavior. The rate, duration and extent of microtubule growth and shortening events, as well as the number of detected events per microtubule, are all significantly affected by the observation interval (Table 4.2). For example, the average rates of microtubule growth and shrinking are significantly greater when measured at 2 second, rather than 10 second intervals. These rates of microtubule growth and shortening are also much greater than growth and shortening rates measured in vitro (Walker et al., 1988), in vivo at longer observation intervals (Sammak and Borisy, 1988(a); Schulze and Kirschner, 1988), or from immunolocalization of tubulin analogues after microinjection and fixation (Schulze and Kirschner, 1986; Bre et al., 1990). Thus these latter methods may seriously underestimate the in vivo rates of microtubule growth and shrinking. In addition, fewer catastrophe and rescue events are detected in PtK_1 epithelial cells from images taken at 10 second rather than 2 second intervals (present study). Thus, both the number of events

which can be detected and the rates of growth and shrinking are significantly affected by the interval between observations.

Acquisition of images at 2 second intervals (using the imaging system available for these experiments) requires continuous, although greatly attenuated, illumination of the cell area under observation. Although efforts were made to minimize any adverse effects of illumination on the cells (see Methods), it has been demonstrated previously that fluorescent microtubules in vitro can be damaged and may break at certain levels of illumination (Vigers et al., 1988). However, several observations strongly suggest that the experimental conditions used in the present study do not affect microtubule behavior in vivo. First, when sequences collected at 2 sec are analyzed at 10 sec, the results are similar to values reported by other investigators using 10 second observation intervals and intermittent illumination (Schulze and Kirschner, 1988). Second, damage to fluorescent microtubules under illumination in vitro is accompanied by photobleaching (Vigers et al., 1988), and loss of microtubule fluorescence during the observation periods used here is not detected. Third, microtubules were never observed to break during the sequences used for this study, although microtubule fragments were occasionally detected. Rather, microtubule turnover occurs as a consequence of individual microtubules entering and leaving the cell area under observation. Finally, photo-damage of microtubules in vivo is accompanied by diminished microtubule dynamic behavior (Schulze and Kirschner, 1988), and both high rates of microtubule growth and depolymerization and high rescue and catastrophe frequencies are obtained in the present study. Together, these observations strongly indicate that limited exposure to low levels of continuous illumination over small areas of the cell, used in conjunction with low doses of ascorbic acid, do not result in detectable alterations of microtubule behavior in vivo, and that the differences in results obtained from observations made at 2 and 10 second intervals reflect the greater temporal resolution of measurements made at 2 second intervals.

While the observations of microtubules at 2 second intervals represent the greatest temporal resolution thus far reported for images of fluorescent microtubules in living cells, only a limited area of the cell could be examined during these experiments. It is important to consider the effect of this limitation on the quantification of microtubule dynamic instability parameters. For example, microtubule growth and shrinking events resulting in a microtubule entering or leaving the field of view are only partially detected in these experiments, and the measured duration of such an event therefore underestimates its actual duration. Because the duration of growth and depolymerization events is used to calculate the frequency of catastrophe and rescue events, these latter values may in turn be overestimated. In PtK_1 cells, only a small minority of microtubule growth and depolymerization events result in a microtubule entering or leaving the field of view. Thus, the degree to which the behavior of the total population of microtubules in these lamellae could be misrepresented is small. In contrast, half of the observed microtubule depolymerization events and over one third of the observed growth events in CHO fibroblasts result in a microtubule leaving or entering the field of view (see Results). Thus, the analytical methods used in the present study may underestimate the extent and duration of microtubule growth and shortening events in CHO fibroblasts, and overestimate the frequency of rescue and catastrophe events in these cells. Therefore, the differences between microtubule behavior in CHO fibroblasts and PtK_1 epithelial cells may actually be greater than indicated by the results obtained in this study.

Microtubule Dynamics and Intracellular Tubulin Concentration May Be Interrelated

The results presented here indicate that microtubules in PtK_1 epithelial cells have an increased frequency of rescue and a decreased rate and duration of microtubule growth and depolymerization events than the majority of microtubules in CHO fibroblasts; no significant difference in the frequency of microtubule catastrophe events is detected. It is of interest to consider the manner in which these observed differences in microtubule behavior

may arise. Kinetic analysis of microtubule assembly in vitro has shown MAP binding increases both the rate and extent of microtubule polymerization and the resistance of microtubules to various microtubule destabilizing drugs (Herzog and Weber, 1978; Sloboda et al., 1976; Yen et al., 1988). Analysis of individual microtubules in vitro further reveal that MAPs increase the frequency of rescue events; the rate of microtubule depolymerization may also be decreased (Bre and Karsenti, 1990; Pryer, 1989). Microinjection of tau protein into living cells has also been shown to increase both microtubule stability and the amount of microtubule polymer, however, the increase in microtubule polymer in living cells is limited by the free tubulin concentration (Drubin and Kirschner, 1986). Thus, in living cells, an increase in total microtubule polymer may result in a decrease in the intracellular tubulin concentration. Finally, decreasing the concentration of free tubulin in vitro has been shown to both decrease the rate of microtubule polymerization and increase the frequency of catastrophe events (Walker et al., 1988).

The results described above suggest that the binding of MAPs to microtubules in a PtK_1 cell containing limited free tubulin could result in an increase in the number of microtubule transitions and thus a decrease in the extent and duration of microtubule growth and depolymerization events in these cells. In addition, although the binding of MAPs to microtubules has been shown to increase the rate of microtubule polymerization, in a living cell the resulting decrease in the concentration of free tubulin may eventually reduce the rate of microtubule growth. Thus, although no difference in the frequency of catastrophe is detected between the two cell types, many of the differences in microtubule behavior observed between PtK_1 cells and CHO fibroblasts may none the less be explained by cell type specific expression of MAPs in PtK_1 cells. It is therefore possible that PtK_1 epithelial cells contain higher concentrations of MAPs than CHO fibroblasts or a unique type of MAP not found in CHO fibroblasts and that the concentration of free tubulin in PtK_1 epithelial cells is lower than that found in CHO fibroblasts.

Such a model, in which the behavior of microtubules and the intracellular concentration of free tubulin are interdependent, is supported by several lines of evidence. First, the concentration of free tubulin in living cells is known to be autoregulated at the level of tubulin mRNA translation (Yen et al., 1987), suggesting that the concentration of free tubulin is of physiological importance. Second, transient increases in the concentration of free tubulin by microinjection of tubulin subunits have been shown to result in an increased rate of microtubule growth (Schulze and Kirschner, 1986) and the plus-end dependant elongation of kinetochore microtubules in anaphase (Shelden and Wadsworth, 1992). These experiments demonstrate that important aspects of microtubule behavior may be regulated by the concentration of free tubulin in vivo.

Conclusion

In summary, the results of this study provide direct evidence of cell type specific microtubule behavior. The average amount of time individual microtubules under observation remain within lamellar protrusions is significantly higher in epithelial cells than in fibroblasts. Observation of microtubules at 2 second intervals reveals that microtubules in the lamellae of epithelial cells are less dynamic than the majority of microtubules found in CHO fibroblasts due to a higher frequency of rescue and a lower rate of microtubule growth and depolymerization; the frequency of catastrophe for these microtubule populations is not significantly different.

Figure 4.1.

Individual microtubule dynamic behavior in PtK_1 cells examined at 10 second intervals. Individual microtubules are clearly observed to grow (g), shrink (s) and pause (p) in the lamella of this PtK_1 cell during the 50 second interval shown. A microtubule which moves sideways (laterally) is also observed within this lamella (arrows points to the microtubule and the original location of its plus end). Only one of the microtubules present in the first panel leaves the field of view during the interval shown (asterisk). Bar 4 μm.

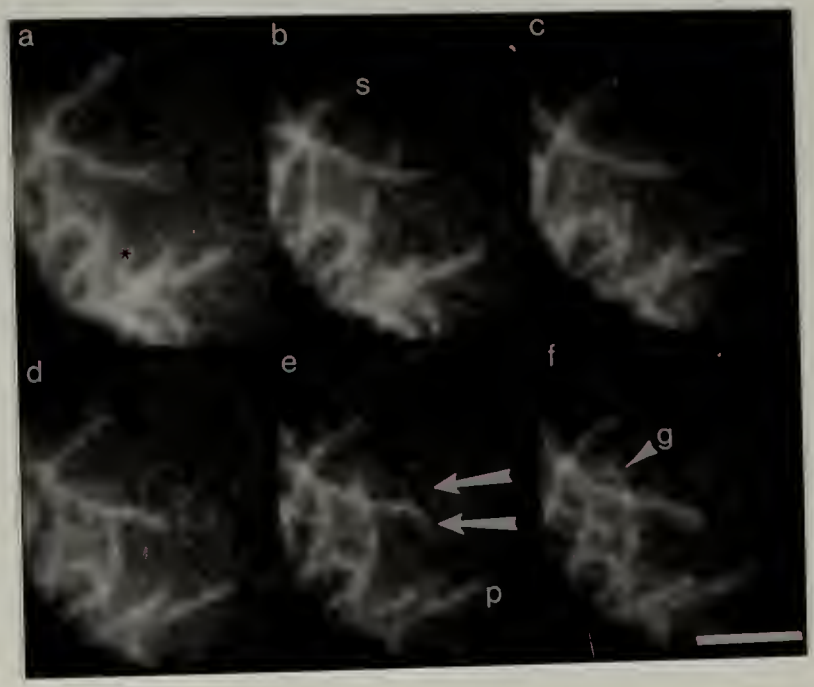
a
b
c
s
*
d
e
f
g
p

Figure 4.2.

Individual microtubule dynamic behavior in a CHO lamella examined at 10 second intervals. Many of the individual microtubules detected in this lamella leave the field of view during the 50 second interval shown (single arrowheads). In addition, several new microtubules are observed to enter the field of view during this interval (double arrowheads). Many microtubules completely appear and disappear during the 10 second interval between two images. Bar 4 μm.

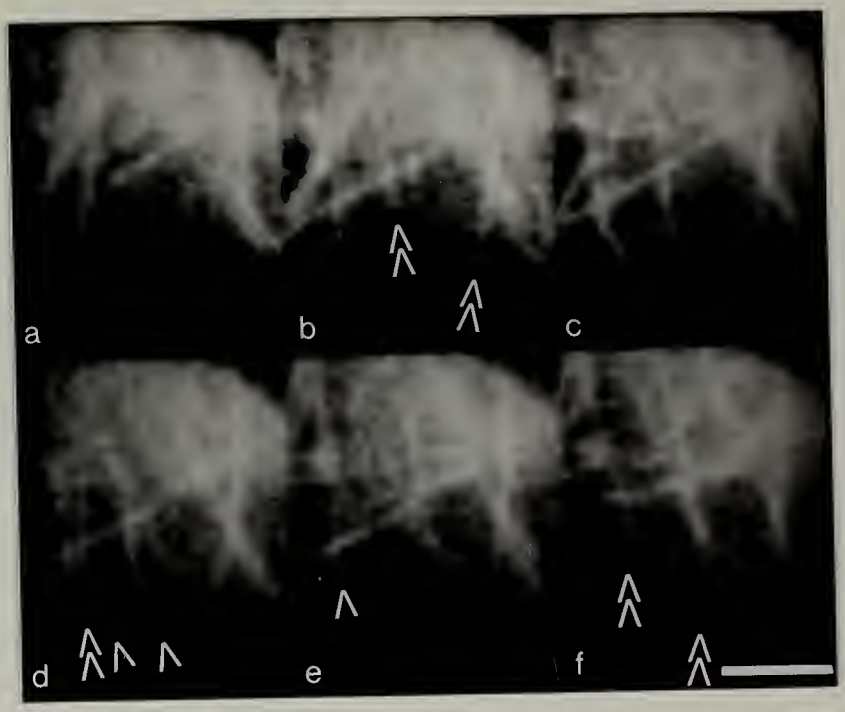
a
b
c
d
e
f

Figure 4.3.

Distributions of microtubule lifespans in PtK_1 epithelial cells and CHO fibroblasts. Most microtubules in PtK_1 epithelial cells remain within the field of view longer than microtubules in CHO fibroblasts. Microtubule lifespans were obtained from images acquired at 10 second intervals. Most microtubules in PtK_1 epithelial cells (A) spend more time within the field of view than microtubules in CHO fibroblasts (B) when the first 3 minutes of each sequence is examined. Many microtubules in PtK_1 cells remain within the field of view for the entire 3 minute sequence (A), however, analysis of the first 6 minutes of these sequence (C) demonstrates that only a single distribution of microtubules is detected in PtK_1 epithelial cells using these methods.

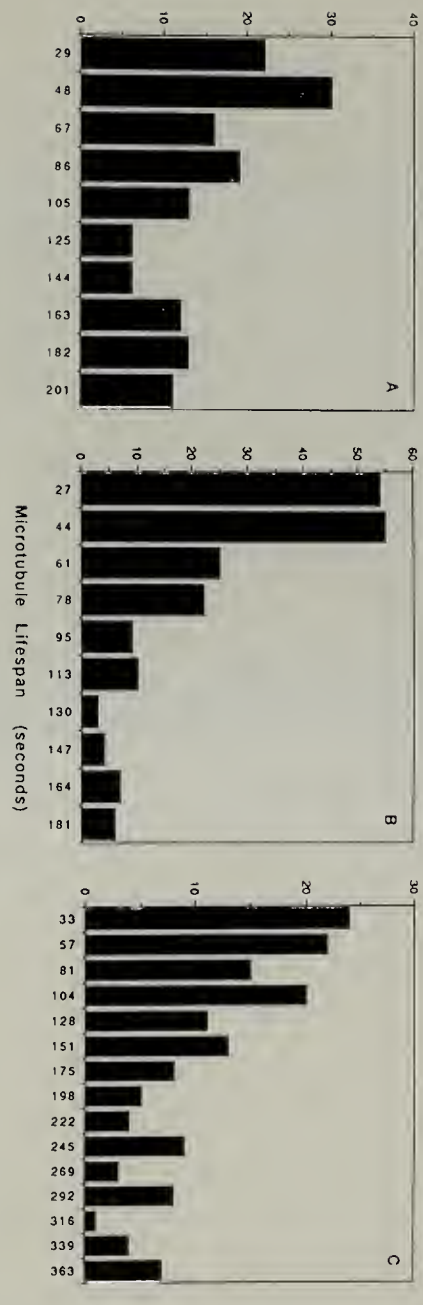
Microtubule Lifespan (seconds)
A
B
C

Figure 4.4.

Individual microtubules are observed to undergo frequent episodes of growth, shortening and pause when images of microtubules in PtK_1 cells are obtained at 2 second intervals. The interval between displayed images is 4 seconds. An individual microtubule can be observed to undergo three growth events (a-b, c-d, h-j), a depolymerization event (b-c) and a pause event (e-h) during the 36 second interval shown (see also Figure 4.6(a)). The arrowhead marks the starting location of this microtubule's plus end, and a second arrowhead marks its plus end in panels b and f. Other microtubules can be observed to enter or leave this lamellar region during the interval shown. Bar 4 μm.

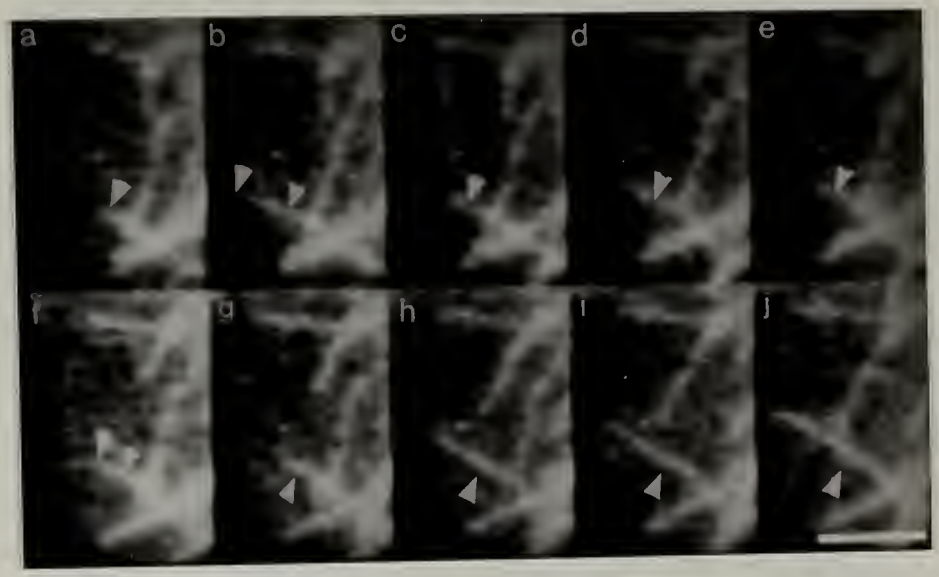
a
b
c
d
e
f
g
h
i
j

Figure 4.5.

Some microtubule growth and shrinking events observed in PtK_1 epithelial cells are less than or equal to 2 seconds in duration. Images of individual microtubules in a PtK_1 cell obtained at 2 second intervals are shown. An individual microtubule is clearly detected in the lower region of each panel, and has been marked in each case with the location of its plus-end obtained from the previous panel. Small growth events (a-b, j-k, l-m) and depolymerization events (h-i, k-l) of less than or equal to 2 seconds in duration are observed. Bar 4 μm.

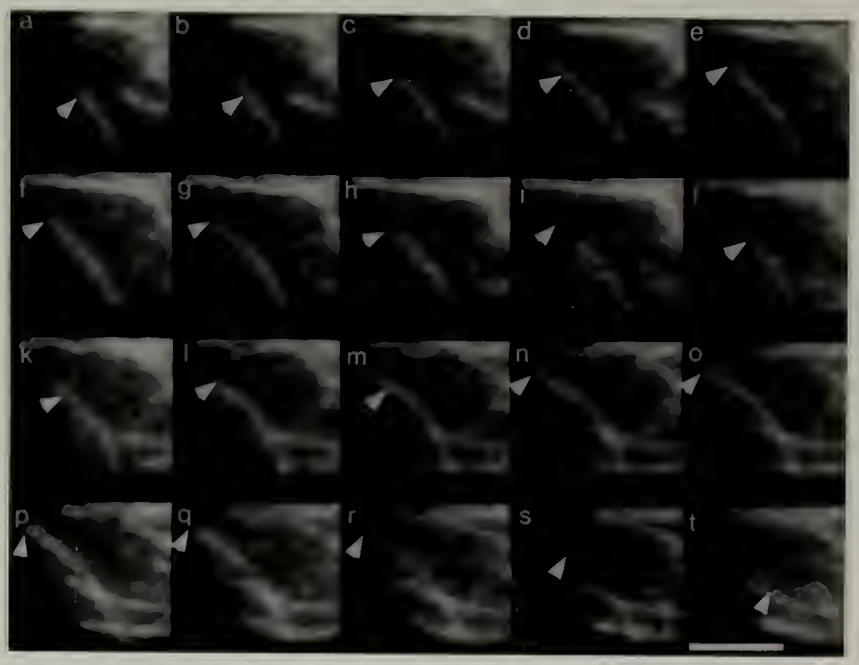
a
b
c
d
e
f
g
h
i
j
k
l
m
n
o
p
q
r
s
t

Figure 4.6.

Life history plots obtained from individual microtubules in PtK_1 cells. Microtubules in these cells undergo frequent length changes of short duration and extent. A life history plot obtained from the microtubule shown in Figure 4.4 is shown in panel (a). The interval shown in Figure 4.4 is marked with arrows (a). Numerous growth and shrinking events occur during the observation periods shown for this microtubule (a) and for other representative microtubules (b,c,d). The axes are marked in microns (vertical) and seconds (horizontal).

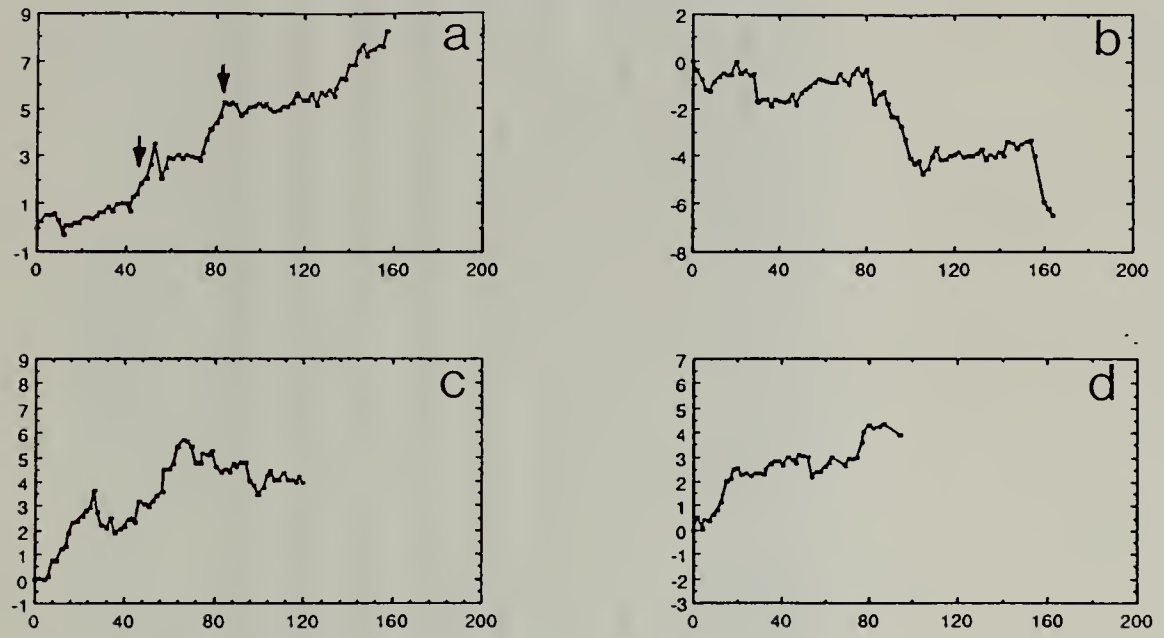
a
b
c
d

Figure 4.7.

Individual microtubules in CHO fibroblasts undergo growth and depolymerization events which result in extensive microtubule length changes. A series of images from a sequence obtained at 2 second intervals is shown, the interval between displayed images is 4 seconds. An individual microtubule is clearly detected in the lower portion of each image and has been marked with the location of its plus-end in the first image. The microtubule grows rapidly across the region of the cell under observation (a-e) and then depolymerizes back to its starting location (f-i). It subsequently leaves the field of view (not shown). Other microtubules which either grow into (g) or shrink out of (s) the field of view are also detected. Bar 4 μm.

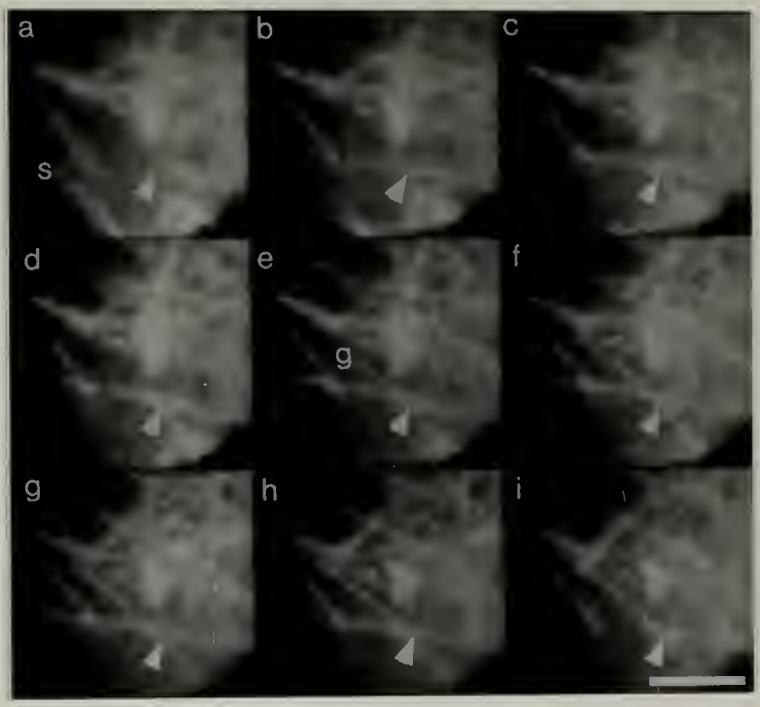
a
b
c
s
d
e
f
g
g
h
i

Figure 4.8.

Dynamic and stable microtubules are detected in CHO fibroblasts. Images obtained at 2 second intervals are shown, the interval between displayed images is 4 seconds. Numerous microtubules can be observed to grow (g) or shrink (s) rapidly across this region of a CHO fibroblast. A single microtubule which does not appear to grow or shrink during the 44 second interval shown is also detected (arrowhead). Bar 4 μm.

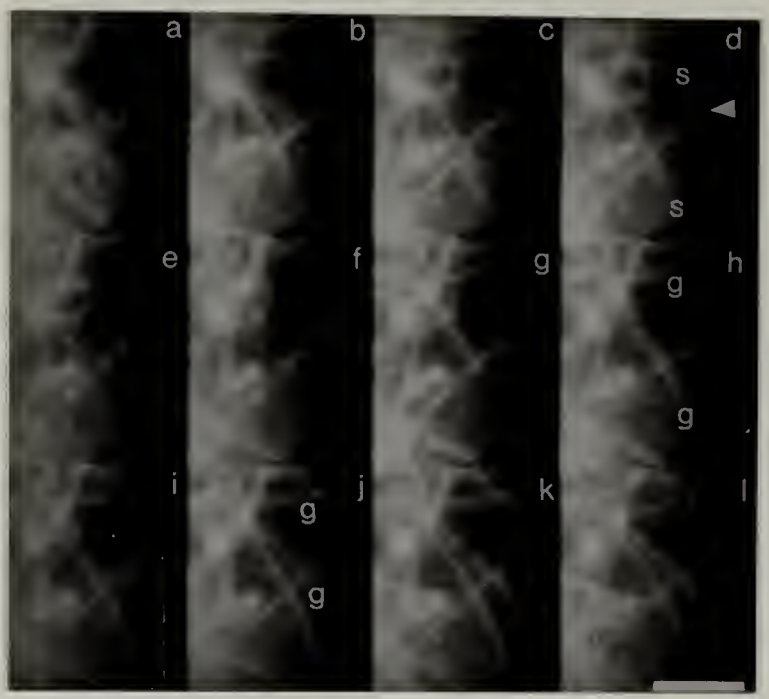
a
b
c
d
s
s
e
f
g
h
g
g
i
j
g
k
l
g

Figure 4.9.

Life history plots of microtubules in CHO fibroblasts demonstrate that most microtubules in these cells undergo long periods of growth and depolymerization with infrequent conversions. A life history plot obtained from the microtubule indicated in Figure 4.7 is shown (a). Only a single growth and depolymerization event occurs during the period this microtubule remains visible. (b-c) Additional examples of typical microtubule behavior in CHO fibroblasts; single growth or depolymerization events result in extensive changes in microtubule length. A minority of microtubules in these cells appear to remain in a paused state for some period of time (d). However, these microtubules do undergo growth and depolymerization excursions before and after pausing (d). The axes are marked in microns (vertical) and seconds (horizontal).

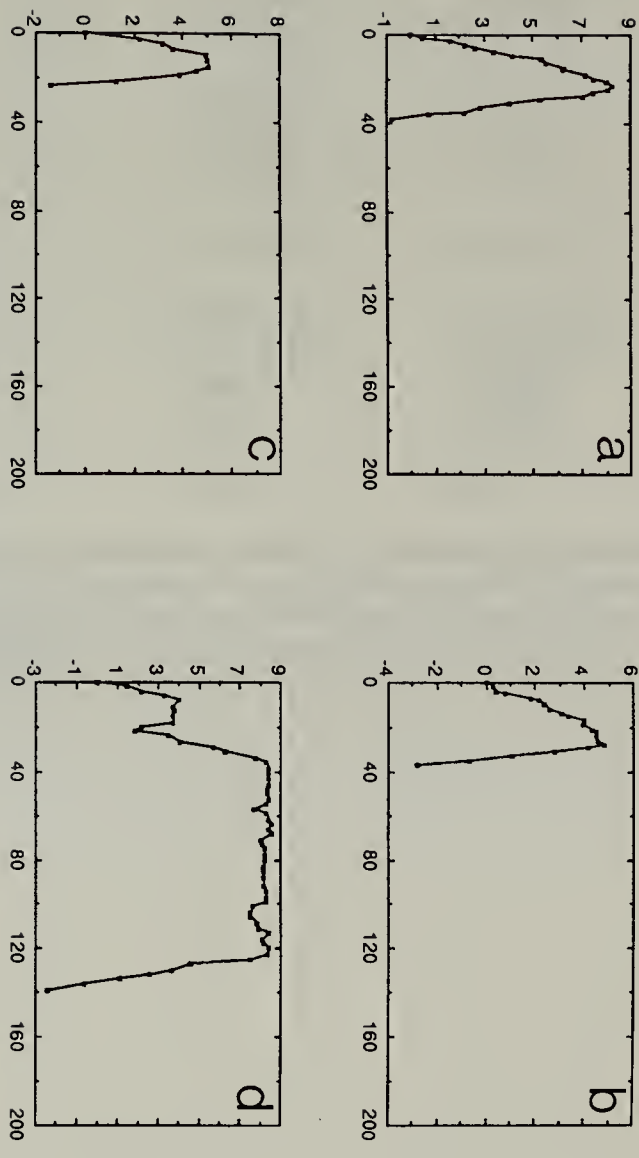
a
b
c
d

Table 4.1. Microtubule dynamic parameters measured in PtK_1 and CHO cells at 2 second intervals.

	PtK(19)	CHO(18)	CHO(st)(7)
gr rate*	11.9 ± 6.5	19.7 ± 8.1	21.2 ± 11.7
gr length$^+$	1.3 ± 0.9	3.2 ± 2.5	2.6 ± 2.3
gr time@	7.9 ± 6.6	9.6 ± 7.0	7.6 ± 5.3
sh rate*	19.8 ± 10.8	32.2 ± 17.7	21.1 ± 11.5
sh length$^+$	1.6 ±1.4	4.3 ± 3.3	3.2 ± 3.2
sh time@	5.1 ± 3.8	7.4 ± 4.2	7.4 ± 4.6
ps time@	8.5 ± 5.5	8.0 ± 4.6	26.6 ± 19.9
1/c s^{-1}	18.5 ± 15.0	16.5 ± 10.1	31.3 ± 26.5
1/r s^{-1}	5.1 ± 3.8	7.7 ± 3.9	7.3 ± 4.9
c s^{-1}	.0541	.0606	.0319
r s^{-1}	.1961	.1299	.1370
events/MT/min	7.3	4.0	4.0

The value of microtubule dynamic instability parameters measured from images obtained at 2 second intervals. The numbers in parenthesis represent the number of individual microtubules analyzed for each group. Units are: * microns/minute; + microns; @ seconds; abbreviations used are gr: growth; sh: depolymerization; ps: pause c: catastrophe; r: rescue, MT: microtubule, st: stable, s: seconds.

Table 4.2. Comparison of microtubule dynamic parameters in PtK_1 cells measured at 2 and 10 sec intervals.

	2 sec(19)	10 sec(10)
gr.rate*	11.4±6.2	5.15±2.8
gr.time@	6.7±6.1	18.9±10.8
gr.length+	1.0±0.85	1.4±0.86
N_{gr}	113	31
sh.rate*	17.2±10.3	13.8±14.1
sh.time@	4.4±3.5	11.4±4.5
sh.length+	1.3±1.3	2.0±1.2
N_{sh}	72	21
c s^{-1}	.054	.0217
r s^{-1}	.225	.0735
ps time@	8.5±5.4	15.8±9.9
%ps time@	46.3	27.6
#ps /MT	4.5	2.0
#gr /MT	5.9	3.1
#sr /MT	3.8	2.1

Comparison of the values of microtubule dynamic instability parameters measured using 2 or 10 second intervals between observations from images collected at 2 second intervals. The numbers in parenthesis represent the number of individual microtubules analyzed for each group. Units are: * microns/minute; + microns; @ seconds; abbreviations used are gr: growth; sh: depolymerization; ps: pause c: catastrophe; r: rescue, MT: microtubule, sec: seconds, s: seconds, N_{gr},N_{sh}: the number of observed growth and shrinking events.

Table 4.3. Comparison of microtubule dynamic parameters reported from cells and cell extracts.

Source	catastrophe/sec	rescue/sec
PtK1*	0.054	0.196
CHO*	0.061	0.130
Newt Lung@	0.014	0.044
Xenopus Neuron+	0.012	0.029
Xenopus Interphase Extracts#	0.018	0.011
Xenopus Mitotic Extracts#	0.116	0.027

*PtK_1,CHO; present study
@Newt lung epithelial cells; Cassimeris et al., 1988
+Xenopus neuron; Tanaka and Kirschner; 1991
#Xenopus extracts; Belmont et al., 1991

REFERENCES

Aist, J.R. and Berns, M.W. 1981. Mechanics of chromosome separation during mitosis in Fusarium (*Fungi Imperfecti*): New evidence from ultrastructural and laser microbeam experiments. J. Cell Biol. 91:446-458.

Aist, J.R. and C.J. Bayles. 1988. Video motion analysis of mitotic events in living cells of the fungus *Fusarium solani*. Cell Motil. 9:325-336.

Aist, J. R., C. J. Bayles, W. Tao and M. W. Berns. 1992. Direct experimental evidence for the existence, structural basis and finction of astral forces during anaphase B in vivo. J. Cell Sci. 100:279-288.

Allen, C. and G. G. Borisy. 1974. Structural polarity and directional growth of microtubules of *Chlamydomonas* flagella. J. Mol. Biol. 90:381-402

Amos, L. A. and A. Klug. 1974. Arrangement of subunits in flagellar microtubules. J. Cell Sci. 14:523-549.

Amos, L. A., R. W. Linck and A. Klug. 1976. Molecular structure of flagellar microtubules. In Cell Motility. Cold Spring Harbor Conferences on Cell Proliferation, Vol. 3. R. Goldman, T. Pollard and J. Rosenbaum, editors. Cold Spring Harbor Laboratory, Cold Spring Harbor, N. Y. pp. 847-867.

Bajer, A. S. 1982. Functional autonomy of monopolar spindle and evidence for oscillatory movement in mitosis. J. Cell Biol. 93:33-48.

Bajer, A. S., C. Cypher, J. Mole-Bajer and H. M. Howard. 1982. Taxol induced anaphase reversal: Evidence that elongating microtubules can exert a pushing force in live cells. Proc. Natl. Acad. Sci. USA 79:6569-6573.

Bayley, P. M. 1990. What makes microtubules dynamic? J. Cell Sci. 95:33-48.

Belmont, L. D., A. A. Hyman, K. E. Sawin and T. J. Mitchison. 1990. Real-time visualization of cell cycle-dependent changes in microtubule dynamics in cytoplasmic extracts. Cell. 62:579-589.

Bergen, L. G. and G. G. Borisy. 1980. Head-to-tail polymerization of microtubules in vitro. J. Cell Biol. 84: 141-150.

Bergen, L. G. and G. G. Borisy. 1983. Tubulin-colchicine complex inhibits microtubule elongation at both plus and minus ends. J. Biol. Chem. 258:4190-4194.

Bergen, L. G., R. Kuriyama and G. G. Borisey. 1980. Polarity of microtubules nucleated by centrosomes and chromosomes of chinese hamster ovary cells in vitro. J. Cell Biol. 84: 151-159.

Berns, M., and M. S. Richardson. 1977. Continuation of mitosis after laser microbeam irradation of the centriolar region. J. Cell Biol. 75:977-982.

Binder, L. I. and J. L. Rosenbaum. 1978. The in vitro assembly of flagellar outer doublet tubulin. J. Cell Biol. 79:500-515.

Black, M. M. and P. Keyser. 1987. Acetylation of alpha-tubulin in cultured neurons and the induction of tubulin acetylation in PC12 cells by treatment with nerve growth factor. J. Neurosci. 7:1815-1833.

Bloom, G. S. and R. B. Vallee. 1989. Microtubule-associated proteins in the sea-urchin egg mitotic spindle. In Mitosis molecules and mechanisms; ed. J.S. Hyams and B.R. Brinkley, Academic Press,SanDiego, Ca. pp.183-201.

Bre, M.-H. and E. Karsenti. 1990. Effects of brain microtubule-associated proteins on microtubule dynamics and nucleation activity of centrosomes. Cell Motil. Cytoskeleton 15:88-98.

Bre, M.-H., R. Pepperkok, A. M. Hill, N. Levilliers, W. Ansorge, E. H. K. Stelzer and E. Karsenti. 1990. Regulation of microtubule dynamics and nucleation during polarization in MDCK II cells. J. Cell Biol. 111:3013-3021.

Brinkley, B. R. M. M. Valdivia, A. Tousson, and R. D. Balczon. 1989. The kinetochore: Structure and molecular organization. In: Mitosis molecules and mechanisms; ed. J.S. Hyams and B.R. Brinkley, Academic Press, San Diego, Ca. pp. 77-118.

Brinkley, B.R. and J. Cartwright. 1971. Ultrastructural analysis of mitotic spindle elongation in mammalian cells *in vitro*. Direct microtubule counts. J. Cell Biol. 50:416-431.

Bryan, J. 1972. Vinblastin and microtubules. II. Characterization of two protein subunits from the isolated crystals. J. Mol Biol. 66:157.

Burton, P. R. and R. H. Himes. 1978. Electron microscope studies of pH effects on assembly of tubulin free of associated proteins. J. Cell Biol. 77:120-133.

Cambray-Deakin, M. A. and R. D. Burgoyne. 1987. Posttranslational modification of alpha-tubulin: Acetylated and deacetylated forms in axons of rat cerebellum. J. Cell Biol. 104:1569-1574.

Cande, W. Z. 1981. Physiology of chromosome movement in lysed cell models. In International Cell Biology 1980-1981. H. G. Schweiger, editor. Springer Verlag, Berlin. 382-391.

Cande, W.Z. and K.L. McDonald. 1985. In vitro reactivation of anaphase spindle elongation using isolated diatom spindles. Nature 316:168-170.

Cande, W. Z., T. Baskin, C. Hogan, K. L. McDonald, H. Masuda and L. Wordeman. 1989. In vitro analysis of anaphase spindle elongation. In Cell Movement, Volume 2: Kinesin, Dynein and Microtubule Dynamics. F. D. Warner, J. R. McIntosh, editors. Alan R. Liss Inc., New York, N. Y. pp. 441-452.

Carlier, M. F. 1982. Guanosine-5'-triphosphate hydrolysis and tubulin polymerization. Mol. Cell Biochem. 47:97-113.

Carlier, M. F. and D. Panteloni. 1981. Kinetic analysis of guanosine 5'-triphosphate hydrolysis associated with tubulin polymerization. Biochemistry 20:1918-1924.

Cassimeris, L. U., P. Wadsworth and E. D. Salmon. 1986. Dynamics of microtubule depolymerization in monocytes. J. Cell Biol. 102:2023-2032.

Cassimeris, L. U., N. K. Pryer and E. D. Salmon. 1988. Real-time observations of microtubule dynamic instability in living cells. J. Cell Biol. 107:2223-2231.

Cassimeris, L. U., C. L. Rieder, G. Rupp and E. D. Salmon. 1990. Stability of microtubule attachment to the metaphase kinetochores in PtK_1 cells. J. Cell Sci. 96:9-15.

Chen, Y. T. and M. Schliwa. 1990. Direct observation of microtubules dynamics in *Reticulomyxa*: Unusually rapid length changes and microtubule sliding. Cell Motil. Cytoskeleton. 17:214-226.

Cleveland, D. W., S.-Y. Hwo and M. W. Kirschner. 1977. Physical and chemical properties of purified tau factor and the role of tau in microtubule assembly. J. Mol. Biol. 116:227-247.

Coue, M., V.A. Lombillo and J.R. McIntosh. 1991. Microtubule depolymerization promotes particle and chromosome movement in vitro. J. Cell Biol. 112:1165-1175.

De Mey, J., M. Moeremans, G. Geuens, R. Nuydens, H. Van Belle and M. DeBrabander. 1980. Immunocytochemical evidence for the association of calmodulin with microtubules of the mitotic apparatus. In M. DeBrabander and J. DeMay (eds): Microtubules and Microtubule Inhibitors. Amsterdam: Elsevier/North Holland Biomedical, pp. 227-241.

Dentler, W. L., Witman, G. B. and J. L. Rosenbaum. 1974. Directionality of brain microtubule assembly in vitro. Proc. Natl. Acad. Sci. USA 71:1710-1714.

Drubin, D. G. and M. W. Kirschner. 1986. Tau protein function in living cells. J. Cell Biol. 103:2739-2746.

Dustin, P. 1984. Microtubules, 2nd ed. Berlin-Heidelberg-New York-Tokyo:Springer.

Dye, R. B. and R. C. Williams, Jr. 1991. Stability and subunit exchange in microtubules structurally capped at both ends. J. Cell Biol. 115:118a.

Euteneuer, U. and M. Schliwa. 1984. Persistant directional motility of cells and cytoplasmic fragments in the absence of microtubules. Nature 310:58-61.

Euteneuer, U. and J.R. McIntosh. 1980. Polarity of midbody and phrogmoplast microtubules. J. Cell Biol. 87:509-515.

Euteneuer, U. and J.R. McIntosh. 1981. Structural polarity of kinetochore microtubules. J. Cell Biol. 89:338-345.

Farrell, K.W., M.A. Jordan, H.P. Miller and L. Wilson. (1987). Phase dynamics at microtubule ends: the coexistence of microtubule length changes and treadmilling. J. Cell Biol. 107:1035-1046.

Gard, D. L. and M. W. Kirschner. 1985. A polymer-dependent increase in phosphorylation of beta-tubulin accompanies differentiation of a mouse neuroblastoma cell line. J. Cell Biol. 100:764-774.

Geuens, G., A. M. Hill, N. Levillers, A. Adoutte and M. DeBrabender. 1989. Microtubule dynamics investigated by microinjection of Paramecium axonemal tubulin: lack of nucleation but proximal assembly of microtubules at the kinetochore during prometaphase. J. Cell Biol. 108:939-954.

Geuens, G., G. G. Gunderson, R. Nuydens, F. Cornelissen, J. C. Bulinski and M. DeBrabander. 1986. Ultrastructural colocalization of tyrosinated and detyrosinated alpha-tubulinn in interphase and mitotic cells. J. Cell Biol. 103:1883-1893.

Gibbons, I. R. 1975. The molecular basis of flagellar motility in sea urchin spermatazoa. In S. Inoue and R. E. Stephens (eds): Molecules and Cell Movement. New York: Raven Press, pp. 207-232.

Gorbsky, G. J., and G. G. Borisy. 1989. Microtubules of the kinetochore fiber turnover in metaphase but not anaphase. J. Cell Biol. 109:653-662.

Gorbsky, G.J., P.J. Sammak and G.G. Borisy. 1988. Microtubule dynamics and chromosome motion visualized in living anaphase cells. J. Cell Biol. 106:1185-1192.

Gotlieb, A. I., M. L. McBurnie, L. Subrahmanyan and V. I. Kalnins. 1981. Distribution of microtubule organizing centers in migrating sheets of epithelial cells. J. Cell Biol. 91:589-594.

Gould, R. R. and G. G. Borisy. 1977. The pericentriolar material in Chinese hamster cells nucleates microtubule formation. J. Cell Biol. 73:601-615.

Gould, R. R. and G. G. Borisy. 1978. Quantitiative initiation of microtubule assembly by chromosomes from chinese hamster ovary cells. Exp. Cell Re. 113:369-374.

Greer, K. and J. L. Rosenbaum. 1989. Post-translational modifications of tubulin. In Cell Movement, Volume 2: Kinesin, Dynein and Microtubule Dynamics. F. D. Warner, J. R. McIntosh, editors. Alan R. Liss Inc., New York, N. Y. pp. 47-66.

Gunderson , G. G. and J. C. Bulinski. 1986a. Microtubule arrays in differentiated cells contain elevated levels of a post-translationally modified form of tubulin. Eur. J. Cell Biol. 42:288-294.

Gunderson, G. G. and J. C. Bulinski. 1986b. Distribution of tyrosinated and nontyrosinated alpha-tubulin during mitosis. J. Cell Biol. 102:1118-1126.

Gunderson, G. G. and J. C. Bulinski. 1988. Selective stabilization of microtubules oriented toward the direction of cell migration. Proc. Natl. Acad. Sci. U.S.A. 85:5946-5950.

Gunderson, G. G., M. H. Kalnoski, and J. C. Bulinski. 1984. Distinct populations of microtubules: Tyrosinated and nontyrosinated alpha-tubulin are distributed differently in vivo. Cell 38:779-789.

Haimo, L. T., B. R. Telzer and J. L. Rosenbaum. 1979. Dynein binds to and crossbridges microtubules. Proc. Natl. Acad. Sci. USA 76:5759-5763.

Hamaguchi, M. S. and Y. Hiramoto. 1986. Analysis of the role of astral rays in pronuclear migration in sand dollar eggs by the colcemid-UV method. Dev. Growth and Differ. 28:143-156.

Hays, T. S., D. Wise, and E. D. Salmon. 1982. Traction force on a kinetochore at metaphase acts as a linear function of kinetochore fiber length. J. Cell Biol. 93:374-382.

Heidemann, S. R. and J. R. McIntosh. 1980. Visualization of the structural polarity of microtubules. Nature 286:517-519.

Hepler, P. K. 1980. Membranes in the mitotic apparatus of barley cells. J. Cell Biol. 86:490-499.

Hepler, P. K. 1989. Membranes in the mitotic apparatus. in: Mitosis Molecules and Mechanisms; ed. J.S. Hyams and B.R. Brinkley, Academic Press, San Diego, Ca. pp. 241-271.

Hepler, P. K. and D. A. Callaham. 1987. Free calcium increases during anaphase in stamen hair cells of *Tradescantia*. J. Cell Biol. 105:2137-2143.

Herzog, W. and K. Weber. 1978. Fractionation of brain microtubule-associated proteins. Isolation of two different proteins which stimulate microtubule polymerization *in vitro*. Eur. J. Biochem. 92:1-8.

Hill, T. L., 1981. Microfilament or microtubule assembly or disassembly against a force. Proc. Natl. Acad. Sci. USA 78:5613-5617.

Hiller, G. and K. Weber. 1978. Radioimmune assay for tubulin: A quantitative comparison of the tubulin content of different established tissue culture cells and tissues. Cell. 14:795-804.

Horio, T. and H. Hotani. 1986. Visualization of the dynamic instability of individual microtubules by dark-field microscopy. Nature 321:605-607.

Huitorel, P. and M.W. Kirschner. 1988. The polarity and stability of microtubule capture by the kinetochore. J. Cell Biol. 106:151-159.

Hyman, A. A. and T.J. Mitchison. 1990. Modulation of microtubule stability by kinetochores *in vitro*. J. Cell Biol. 110:1607-1616.

Hyman, A. A. and T. J. Mitchison. 1991. Two different microtubule-based motor activities with opposite polarities in kinetochores. Nature. 351:206-211.

Inoue, S. 1964. Organization and function of the mitotic spindle. In Primitive motile systems in cell biology. S. Inoue and R. E. Stephens, editors. Raven Press, New York. pp 119-141.

Inoue, S. 1976. Chromosome movement by reversible assembly of microtubules. In Cell Motility. Cold Spring Harbor Conferences on Cell Proliferation, Vol. 3., R. Goldman, T. Pollard and J. Rosenbaum, editors. Cold Spring Harbor Laboratory, Cold Spring Harbor, N. Y. 1317-1328.

Inoue, S. and H. Sato. 1967. Cell motility by labile association of molecules. The nature of mitotic spindle fibers and their role in chromosome movement. J. Gen. Physiol. 50:259-292.

Izant, J. G. 1983. The role of calcium ions during mitosis. Calcium participated in the anaphase trigger. Chromosoma 88:1-10.

Jameson, L. and M. Caplow. 1981. Modification of microtubule steady-state dynamics by phosphorylation of the microtubule-associated proteins. Proc. Natl. Acad. Sci. USA 78:3413-3417.

Jordan, M. A., R. L. Margolis, R. H. Himes and L. Wilson. 1986. Identification of a distinct class of vinblastin binding sites on microtubules. J. Mol. Biol. 187:61-73.

Joshi, H. C. , M. J. Palacios, L. McNamara and D. W. Cleveland. 1992. Gamma-tubulin is a centrosomal protein required for cell cycle dependent microtubule nucleation. Nature 356:80-82.

Kiehart, D. P. 1981. Studies on the in vivo sensitivity of spindle microtubules to calcium ions and evidence for a vescicular calcium-sequestering system. J. Cell Biol. 88:6704-617.

Kochanski, R. S. and G. G. Borisy, 1990. Centriole visualization and tracking in living cells. J. Cell Biol. 111 (5 pt. 2) 180a.

Koonce, M. P., R. A. Cloney and M. W. Berns. 1984. Laser irradiation of centrosomes in newt eosinophils: Evidence of centriole role in motility. J. Cell Biol. 98:1999-2010.

Koshland, D. E., T. J. Mitchison and M.W. Kirschner. 1988. Poleward chromosome movement driven by microtubule depolymerization *in vitro*. Nature 331:499-504.

Kronebusch, P.J. and G.G. Borisy. 1981. Anaphase pole movements after central spindle disruption in PtK_1 cells. J. Cell Biol. 91:319a.

Kuriyama, R. and G. G. Borisy.1981. Microtubule-nucleating activity of centrosomes in chinese hamster ovary cells is independent of the centriole cycle but coupled to the mitotic cycle. J. Cell Biol. 91:822-826.

Lee, Y. C. and J. Wolff. 1984. Calmodulin binds to both microtubule associated protein 2 and tau proteins. J. Biol. Chem. 259:1226-1230.

Lowry, O.H., N.J. Rosebrough, A.L. Farr and R.J. Randall. 1951. Protein measurement with the folin phenol reagent. J. Biol. Chem. 193:265-275.

Luduena, R. F., E. M. Shooter and L. Wilson. 1977. Structure of the tubulin dimer. J. Biol. Chem. 252:7006-7014.

Mabuchi, I. 1986. Biochemical aspects of cytokinesis. Int. Rev. Cytol. 101:175-214.

Mandelkow, E and E.-M. Mandelkow. 1989. Tubulin, microtubules and oligomers: Molecular structure and implications for assembly. In Cell Movement, Volume 2: Kinesin, Dynein and Microtubule Dynamics. F. D. Warner, J. R. McIntosh, editors. Alan R. Liss Inc., New York, N. Y. pp. 23-45.

Mandelkow, E.-M., E. Mandelkow, and R. A. Milligan. 1991. Microtubule dynamics and microtubule caps: a time resolved cryo-electron microscopy study. J. Cell Biol. 114:977-991.

Margolis, R. L., and L. Wilson. 1977. Addition of colchicine-tubulin complex to microtubule ends: The mechanism of substoichiometric colchicine poisoning. Proc. Natl. Acad. Sci. U.S.A. 74:3466-3470.

Margolis, R. L., and L. Wilson. 1978. Opposite end assembly and disassembly of microtubules at steady state in vitro. Cell 13:1-8.

Maruta, H., K. Greer and J. L. Rosenbaum. 1986. The acetylation of alpha-tubulin and its relationship to assembly and disassembly of microtubules. J. Cell Biol. 103:571-579.

Masuda, H. and W. Z. Cande. 1987. The role of tubulin polymerization during spindle elongation *in vitro*. Cell 49:193-202.

Masuda, H. and W. Z. Cande. 1988. The mechanism of anaphase spindle elongation: Uncoupling of tubulin incorporation and microtubule sliding during *in vitro* spindle reactivation. J. Cell Biol. 107:623-633.

McBeath, E. and K. Fujiwara. 1990. Microtubule detachment from the microtubule-organizing center as a key event in the complete turnover of microtubules in cells. Eur. J. Cell Biol. 52:1-16.

McDonald, K. 1989. Mitotic spindle ultrastructure and design. In Mitosis molecules and mechanisms; ed. J.S. Hyams and B.R. Brinkley, Academic Press,SanDiego, Ca. pp. 1-38.

McIntosh, J.R. 1985. Spindle structure and mechanisms of chromosome movement. In Aneuploidy: Etiology and Mechanisms. V.L. Delarco, P.E. Voytec and A. Hollaender, editors. Plenum Publishing Corp. New York, 197-229.

McIntosh, J.R., K.L. McDonald, M.K. Edwards and B.M. Ross. 1979. Three dimensional structure of the central mitotic spindle of *Diatoma vulgare*. J. Cell Biol. 83:428-442.

McIntosh, J.R., U.-P. Roos, B. Neighbors and K.L. McDonald. 1985. Architecture of the microtubule component of mitotic spindles from *Dictyostelium discoideum*. J. Cell Sci. 75:93-129.

McIntosh, J.R., W.Z. Cande and J.A. Snyder. 1975. Structure and physiology of the mammalian mitotic spindle. In: Molecules and Cell Movement. Ed: S. Inoue and R.E. Stephens, Raven Press, N.Y. pp. 31-76.

McIntosh, J. R., G. P. A. Vigers, and T. S. Hays. 1989. Dynamic behavior of mitotic microtubules. In Cell Movement, Volume 2: Kinesin, Dynein and Microtubule Dynamics. F. D. Warner, J. R. McIntosh, editors. Alan R. Liss Inc., New York, N. Y. pp. 371-382.

McKenna, N. M. and Y. L. Wang. 1989. Culturing cells on the microscope stage. In Methods in Cell Biology, Vol. 29(a) pp. 195-205.

Mitchison, T. J. 1988. Microtubule dynamics and kinetochore function in mitosis. Annu. Rev. Cell Biol. 4:527-549.

Mitchison, T. J. 1989a. Poleward microtubule flux in the mitotic spindle: Evidence from photoactivation of fluorescence. J. Cell Biol. 109:637-652.

Mitchison, T. J. 1989b. Chromosome alignment at mitotic metaphase: Balanced forces or smart kinetochores? In Cell Movement Vol. 2: Kinesin, Dynein and Microtubule Dynamics. F. D. Warner and J. R. McIntosh, editors. 421-430.

Mitchison, T. J. and K. E. Sawin. 1990. Tubulin flux in the mitotic spindle: Where does it come from, where is it going? Cell Motil. Cytoskeleton 16:93-98.

Mitchison, T. J. and M. W. Kirschner. 1984a. Dynamic instability of microtubule growth. Nature. 312:237-242.

Mitchison, T. J., and M. W. Kirschner. 1984b. Microtubule assembly nucleated by isolated centrosomes. Nature 312:232-237.

Mitchison, T. J. and M. W. Kirschner. 1985a. Properties of the kinetochore in vitro. I. Microtubule nucleation and tubulin binding. J. Cell Biol. 101:755-765.

Mitchison, T. J. and M. W. Kirschner. 1985b. Properties of the kinetochore in vitro. II. Microtubule capture and ATP dependent translocation. J. Cell Biol. 101: 766-777.

Mitchison, T. J., L. Evans, E. Schultz and M. Kirschner. 1986. Sites of microtuble assembly and disassembly in the mitotic spindle. Cell 45:515-527.

Miyamoto, H. and H. Hotani. 1988. Polymerization of microtubules in liposomes produces morphological changes of shape. Proc. Tanaguichi Internat. Symp. 14:220-242.

Murphy, A. S. and M. Flavin. 1983. Microtubule assembly using the microtubule associated protein MAP-2 prepared in defined states of phosphorylation with protein kinase and phosphatase. Eur. J. Biochem. 137:37-46.

Nicklas, R. B. 1983. Measurements of the force produced by the mitotic spindle in anaphase. J. Cell Biol. 97:542-548.

Nicklas, R. B. 1987a. Chromosomes and kinetochores do more in mitosis than previously thought. In Chromosome structure and function: The impact of new concepts. Eds J. P. Gustafson, R. Apels, and R. J. Kaufman. Plenum, N. Y.

Nicklas, R. B. 1987b. Chromosomes move on truncated spindles. J. Cell Biol. 105:176a.

Nicklas, R. B. 1989. The motor for poleward chromosome movement in anaphase is at or near the kinetochore. J. Cell Biol. 109:2245-2255.

Olmsted, J. B. 1986. Microtubule-associated proteins. Annu. Rev. Cell Biol. 2:421-457.

Olmsted, J. B. and G. G. Borisy. 1973. Microtubules. Annu. Rev. Biochem. 42:507.

Osborn, M., R. E. Webster and K. Weber. 1978. Individual microtubules viewed by immunofluorescence and electron microscopy in the same PtK2 cell. J. Cell Biol. 78:27-34.

Paschal, B. M., and R. B. Vallee. 1987. Retrograde transport by microtubule-associated protein MAP 1C. Nature (London) 330:181-183.

Pepperkok, R., M. H. Bre, J. Davoust and T. E. Kreis. 1990. Microtubules are stabilized in confluent epithelial cells but not fibroblasts. J. Cell Biol. 111:3003-3012.

Petzelt, C. 1984. Localization of an intracellular membrane bound Ca^{++}-ATPase in PtK-cells using immunofluorescence techniques. Eur. J. Cell Biol. 33:55-59.

Pfarr, C. M., M. Coue, P. M. Grissom, T. S. Hays, M. E. Porter and J. R. McIntosh. 1990. Cytoplasmic dynein is localized to kinetochores during mitosis. Nature 345:263-265.

Pfeffer, T.A., C.F. Asnes and L. Wilson. 1976. Properties of tubulin in unfertilized sea urchin eggs. Quantitation and characterization by the colchicine binding reaction. J. Cell Biol. 69:599-607.

Pickett-Heaps, J. D. 1969. The evolution of the mitotic apparatus: an attempt at comparative cytology in dividing plant cells. Cytobios 1:257-280.

Pickett-Heaps, J. D. 1991. Cell division in diatoms. Int. Rev. Cytol. 128:63-108.

Poenie, M., J. Alderton, R. Steinhardt and R. Tsein. 1986. Calcium rises abruptly and briefly throughout the cell at the onset of anaphase. Science 233:886-888.

Pryer, N. K. 1989. Individual microtubule dynamics observed by video microscopy. PhD Thesis, University of N. Carolina, Chapel Hill.

Purich, D. L. and D. Kristofferson. 1984. Microtubule assembly: A review of principles and perspectives. Adv. Protein Chem. 36:133-212.

Rappaport, R. 1986. Establishment of the mechanism of cytokinesis in animal cells. Int. Rev. Cytol. 101:245-281.

Ratan, R. R., M. L. Shelanski, and F. R. Maxfield. 1986. Transition from metaphase to anaphase is accompanied by local changes in cytoplasmic free calcium in PtK2 kidney epithelial cells. Proc. Natl. Acad. Sci. 83:5136-5140.

Raybin, D. and Flavin, M. 1977. Enzyme which specifically adds tyrosine to the alpha-chain of tubulin. Biochemistry 16:2189-2194.

Rieder, C.L. 1982. The formation, sturcture and compostion of the mammalian kinetochore and kinetochore fiber. Int. Rev. Cytol. 79:1-58.

Rieder, C.L. 1991. Mitosis: towards a molecular understanding of chromosome behavior. Current Opinion in Cell Biol. 3:59-66.

Rieder, C. L. and S. P. Alexander. 1990. Kinetochores are transported poleward along a single astral microtubule during chromosome attachment to the spindle in newt lung cells. J. Cell Biol. 110:81-95.

Rieder, C. L., E. A. Davison, L. C. W. Jensen, L. Cassimeris and E.D. Salmon. 1986. Oscillatory movements of monooriented chromosomes and their position relative to the spindle pole result from the ejection properties of the aster and half-spindle. J. Cell Biol. 103:581-591.

Roos, U. P. 1973. Light and electron microscopy of rat kangaroo cells in mitosis. II. Kinetochore structure and function. Chromosoma 41: 195-220.

Rose, G. G., C. M. Pomerat, T. O. Shindler and J. B. Trunnell. 1958. A cellophane strip technique for culturing tissue in multipurpose culture chambers. J. Biophys. and Biochem. Cytol. 4:761-764.

Salmon E. D. and R. R. Segall. 1980. Calcium-labile mitotic spindles isolated from sea urchin eggs (Lytechinus variegatus). J. Cell Biol. 86:355-365.

Salmon, E. D. 1976. Pressure-induced depolymerization of spindle microtubules: Production and regulation of chromosome movement. In Cell Motility. Cold Spring Harbor Conferences on Cell Proliferation, Vol. 3. R. Goldman, T. Pollard and J. Rosenbaum, editors. Cold Spring Harbor Laboratory, Cold Spring Harbor, N. Y. 1329-1342.

Salmon, E.D. 1989. Microtubule dynamics and chromosome movement. In Mitosis molecules and mechanisms; ed. J.S. Hyams and B.R. Brinkley, Academic Press,SanDiego, Ca. pp. 119-181.

Salmon, E.D., R.J. Leslie, W.M. Saxton, M.L. Karow and J.R. McIntosh. 1984. Spindle microtubule dynamics in sea urchin embryos: analysis using a fluorescein-labelled tubulin and measurements of fluorescence redistribution after laser photobleaching. J. Cell Biol. 99:1066-1075.

Sammak, P. J. and G. G. Borisy. 1988a. Direct observation of microtubule dynamics in living cells. Nature 332:724-726.

Sammak, P.J. and G.G. Borisy. 1988b. Detection of single fluorescent microtubules and methods for determining their dynamics in living cells. Cell Motil. and Cytosk. 10:237-245.

Saxton, W.M. and J.R. McIntosh. 1987. Interzone microtubule behavior in late anaphase and telophase spindles. J. Cell Biol. 105:875-886.

Saxton, W.M., D.L. Stemple, R.J. Leslie, E.D. Salmon, M. Zavortink and J.R. McIntosh. 1984. Tubulin dynamics in cultured mammalian cells. J. Cell Biol. 99:2175-2186.

Schacterile, G.R. and R.L. Pollack. 1973. A simplified method for the quantitative assay of small amounts of protein in biologic material. Anal. Biochem. 51:654-660.

Schatten, G. 1981. Sperm incorporation, the pronuclear migrations and their relation to the establishment of the first embryonic axis: Time-lapse video microscopy of the movements during fertilization of the sea urchin *Lytechinus variegatus*. Dev. Biol. 86:426-437.

Schiff, P. B. and S. B. Horowitz. 1980. Taxol stabilizes microtubles in mouse fibroblast cells. Proc. Natl. Acad. Sci. U.S.A. 77:1561-1565.

Schliwa, M. 1986. The Cytoskeleton. An Introductory Survey. In Cell Biology Monographs. Volume 13. M Alfert, W. Beermann, L. Goldstein and K. R. Porter editors. Springer-Verlag, Wein. pp. 64-66.

Schneider, A., T. Sherwin, R. Sasse, D. G. Russell, K. Gull and T. Seebeck. 1987. Subpellicular and flagellar microtubles of *Trypanosoma brucei brucei* contain the same alpha-tubulin isoforms, J. Cell Biol. 104:431-438.

Scholey, J. M., M. E. Porter, P. M. Grissom, and J. R. McIntosh. 1985. Identification of kinesin in sea urchin eggs and evidence for its localization in the mitotic spindle. Nature 318:483-486.

Schulze, E., D. Asai, J. C. Bulinski, and M. W. Kirschner. 1987. Post-translational modification and microtubule stability. J. Cell Biol. 105:2167-2177.

Schulze, E. and M. Kirschner. 1986. Microtubule dynamics in interphase cells. J. Cell Biol. 102:1020-1031.

Schulze, E. and M. Kirschner. 1988. New features of microtubule behavior observed *in vivo*. Nature 334:356-359.

Shelden, E. and P. Wadsworth 1990. Interzonal microtubules are dynamic during spindle elongation. J. Cell Sci. 97:273-281.

Shelden, E. and P. Wadsworth 1992. Injection of biotin-tubulin into anaphase cells induces transient elongation of kinetochore microtubules and reversal of chromosome-to-pole motion. J. Cell Biol. 116:1409-1420.

Sherwin, T., A. Schneider, R. Sasse, T. Seebeck and K. Gull. 1987. Distinct localization and cell cycle dependence of COOH terminally tyrosylated alpha-tubulin in microtubules of *Trypanosoma brucei brucei*. J. Cell Biol. 104:439-446.

Sloboda, R. D. and J. L. Rosenbaum. 1979. Decoration and stabilization of intact, smooth walled microtubules with microtubule-associated proteins. Biochemistry 18:48-55.

Sloboda, R. D., S. A. Rudolph, J. L. Rosenbaum and P. Greengard. 1975. Cyclic AMP-dependent endogenous phosphorylation of a microtubule associated protein. Proc. Natl. Acad. Sci. USA 72:177-181.

Sloboda, R. D., W. L. Dentler and J. L. Rosenbaum. 1976. Microtubule-associated proteins and the stimulation of tubulin assembly *in vitro*. Biochem. 15: 4497-4505.

Snyder, J. A., B. T. Hamilton and J. M. Mullins. 1982. Loss of mitotic centrosomal microtubule initiation capacity at the metaphase-anaphase transition. Eur. J. Cell Biol. 27:191-199.

Snyder, J. A. and J. R. McIntosh. 1975. Initiation and growth of microtubules from mitotic centers in lysed mammalian cells. J. Cell Biol. 67:744-760.

Steuer, E. R., L. Wordeman, T. A. Schroer, and M. P. Sheetz. 1990. Localization of cytoplasmic dynien to mitotic spindles and kinetochores. Nature 345:266-268.

Summers K. and M. W. Kirschner. 1979. Characteristics of the polar assembly and disassembly of microtubules observed in vitro by darkfield light microscopy. J. Cell Biol. 83:205-217.

Tanaka, E. M. and M. W. Kirschner. 1991. Microtubule behavior in the growth cones of living neurons during axon elongation. J. Cell Biol. 115:345-363.

Vale, R. D. 1991. Severing of stable microtubules by a mitotically activated protein in *Xenopus* egg extract. Cell 64:827-839.

Vale, R. D., B. J. Schnapp, T. Mitchison, E. Steuer, T. S. Reese, and M. P. Sheetz. 1985a. Different axoplasmic proteins generate movement in opposite directions along microtubules in vitro. Cell 43: 623-632.

Vale, R. D., T. S. Reese and M. P. Sheetz. 1985b. Identification of a novel force-generating protein, kinesin, involved in microtubule-based motility. Cell 42:39-50.

Vallee, R. B. 1982. A taxol-dependent procedure for the isolation of microtubule-associated proteins (MAPs). J. Cell Biol. 92:435-442.

Vasiliev, J. M. and I. M. Gelfand. 1976. Effects of colcemid on morphogenetic processes and locomotion in fibroblasts. In Cell Motility. Cold Spring Harbor Conferences on Cell Proliferation, Vol. 1. R. Goldman, T. Pollard and J. Rosenbaum, editors. Cold Spring Harbor Laboratory, Cold Spring Harbor, N. Y. pp. 279-304.

Verde, F., J.-C. Labbe, M. Doree and E. Karsenti. 1990. Regulation of microtubule dynamics by cdc2 protein kinase in cell-free extracts of *Xenopus* eggs. Nature 343:233-238.

Verde, F. H.-M. Berrez, C. Antony and E. Karsenti. 1991. Taxol-induced microtubule asters in mitotic extracts of *Xenopus* eggs: Requirement for phosphorylated factors and cytoplasmic dynein. J. Cell Biol. 112:1177-1187.

Vigers, G. P. A., M. Coue and J. R. McIntosh. 1988. Fluorescent microtubules break up under illumination. J. Cell Biol. 107:1011-1024.

Wadsworth, P. and M. McGrail. 1990. Interphase microtubule dynamics are cell type-specific. J. Cell Sci. 95:23-32.

Wadsworth, P., E. Shelden, G. Rupp and C.L. Rieder. 1989. Biotin tubulin incorporates into kinetochore fiber microtubules during early but not late anaphase. J. Cell Biol. 109: 2257-2266.

Walker, R. A., E. T. O'Brien, N. K. Pryer, M. F. Soboeiro, W. A. Voter, H. P. Erickson and E. D. Salmon. 1988. Dynamic instability of individual microtubules analyzed by video light microscopy: Rate constants and transition frequencies. J. Cell Biol. 107:1437-1448.

Walker, R. A., N. K. Pryer and E. D. Salmon. 1991. Dilution of individual microtubules observed in real time in vitro: evidence that cap size is small and independent of elongation rate.

Webster, D. R., Wehland, J., Weber, K., and Borisy, G. G. 1990. Detyrosination of alpha tubulin does not stabilize microtubules in vivo. J. Cell Biol. 111:113-122.

Wehland, J. and K. Weber. 1987. Turnover of the carboxy-terminal tyrosine of alpha-tubuln and means of reaching elevated levels of detyrosination in living cells. J. Cell Sci. 88:185-203.

Weisenberg, R. C. 1972. Microtubules formation in vitro in solutions containing low calcium concentrations. Science 177:1104-1105.

Weisenberg, R. C., G. G. Borisy and E. W. Taylor. 1968. The cholchicine binding protein of mammalian brain and its relationship to microtubules. Biochemistry 7:4466-4479.

Welsh, M. J., J. R. Dedman, B. R. Brinkley and A. R. Means. 1978. Calcium dependent regulator protein localization in the mitotic apparatus of eukaryotic cells. Proc. Natl. Acad. Sci. USA 75:18647-1871.

White, J.G., W.B. Amos and M. Fordham. 1987. An evaluation of confocal versus conventional imaging of biological structures by fluorescence light microscopy. J. Cell Biol. 105:41-48.

Wiche, G., C. Oberkanins and A. Himmler. 1991. Molecular structure and function of microtubule-associated proteins. Int. Rev. Cytol. 124:217-273.

Wise, D., L. Cassimeris, C. L. Rieder, P. Wadsworth and E. D. Salmon. 1991. Chromosome fiber dynamics and congression oscillations in metaphase PtK_1 cells. Cell Motil. Cytoskel. 18:131-142.

Wordeman, L., E. R. Steuer, M. P. Sheetz and T. Mitchison. 1991. Chemical subdomains within the kinetochore domain of isolated CHO mitotic chromosomes. J. Cell Biol. 114:285-294.

Yen, T. J., P. S. Machlin and D. W. Cleveland. 1988. Autoregulated instability of ß tubulin mRNAs by recognition of the nascent amino terminus of ß tubulin. Nature 334: 580-586.

Zeeberg, B. and M. Caplow. 1979. Determination of free and bound microtubule proteins and gaunine nucleotide under equilibrium conditions. Biochemistry. 18:3880-3886.

Zhang, D. H., D. A. Callaham, and P. K. Hepler. 1990. Regulation of chromosome motion in Tradescantia stamen hair cells by calcium and related signalling agents. J. Cell Biol. 111:171-182.

Zhang, D. H., P. Wadsworth and P. K. Hepler. 1992. Modulation of anaphase spindle microtubule structure in stamen hair cells of *Tradescantia* by calcium and related agents. J. Cell Sci. 102:79-89.